University of Alberta

Analysis and Intracellular Uptake of β-Cyclodextrin and a β-Cyclodextrin Complex

By

HAI WEI

A thesis submitted to the Faculty of Graduate Studies and Research in partial fulfillment of the requirements for the degree of Master of Science

In

Pharmaceutical Sciences

Faculty of Pharmacy and Pharmaceutical Sciences

Edmonton, Alberta

Spring 2000

National Library of Canada
Acquisitions and Bibliographic Services
395 Wellington Street
Ottawa ON K1A 0N4
Canada

Bibliothèque nationale du Canada
Acquisitions et services bibliographiques
395, rue Wellington
Ottawa ON K1A 0N4
Canada

Your file Votre référence

Our file Notre référence

The author has granted a non-exclusive licence allowing the National Library of Canada to reproduce, loan, distribute or sell copies of this thesis in microform, paper or electronic formats.

L'auteur a accordé une licence non exclusive permettant à la Bibliothèque nationale du Canada de reproduire, prêter, distribuer ou vendre des copies de cette thèse sous la forme de microfiche/film, de reproduction sur papier ou sur format électronique.

The author retains ownership of the copyright in this thesis. Neither the thesis nor substantial extracts from it may be printed or otherwise reproduced without the author's permission.

L'auteur conserve la propriété du droit d'auteur qui protège cette thèse. Ni la thèse ni des extraits substantiels de celle-ci ne doivent être imprimés ou autrement reproduits sans son autorisation.

0-612-60194-3

Canada

UNIVERSITY OF ALBERTA

LIBRARY RELEASE FORM

NAME OF AUTHOR:	**HAI WEI**
TITLE OF THESIS:	**Analysis and Intracellular Uptake of β-Cyclodextrin and a β-Cyclodextrin Complex**
DEGREE:	**Master of Science**
YEAR THIS DEGREE GRANTED:	**2000**

Permission is hereby granted to the University of Alberta Library to reproduce single copies of this thesis and to lend or sell such copies for private, scholarly or scientific research purposes only.

The author reserves all other publication and other rights in association with the copyright in the thesis, and except as hereinbefore provided, neither the thesis nor any substantial portion thereof may be printed or otherwise reproduced in any material form whatever without the author's prior written permission.

2137 D/P Building
Faculty of Pharmacy and Pharmaceutical Sciences
University of Alberta
Edmonton, Alberta, Canada, T6G 2N8

Date: March 22, 2000

University of Alberta

Faculty of Graduate Studies and Research

The undersigned certify that they have read, and recommend to the Faculty of Graduate Studies and Research for acceptance, a thesis entitled **Analysis and Intracellular Uptake of β-Cyclodextrin and a β-Cyclodextrin Complex** submitted by **Hai Wei** in partial fulfillment of the requirements for the degree of Master of Science in Pharmaceutical Sciences.

Dr. Leonard I. Wiebe (Supervisor)

Dr. James M. Diakur (Co-supervisor)

Dr. Gerald G. Miller

Dr. Tapan K. Basu (External Examiner)

Date: 17 March 2000

ABSTRACT

The goal involves the analysis and characterization of cyclodextrin (CyD)/drug complexes. The fluorescent derivative of β-CyD (NBD-β-CyD) was successfully prepared. The intracellular uptake of NBD-β-CyD was studied in two cell lines (HepG2 and SK-MEL-24) using confocal laser scanning microscopy (CLSM). Electrospray mass spectrometry (ES-MS) was applied for the analysis of a non-covalent complex of β-CyD with amantidine. In addition, a group of nitro-functionalized compounds was also selected for analysis by ES-MS.

The studies showed that NBD-β-CyD entered cells by a mechanism that was temperature-dependent. The serum proteins had no significant effect on the intracellular uptake. No significant difference of intracellular uptake between NBD-β-CyD and its amantidine complex was observed. The nitro-functionalized compounds investigated were readily detected in either the positive or negative ionization mode of ES-MS. ES-MS can detect the β-CyD complex, and can be potentially employed as a general technique to analyze these non-covalent complexes in biological matrices.

To my beloved mom and dad: Shudong Dong and Yongji Wei.

ACKNOWLEDGEMENTS

I would like to express my deepest gratitude to Dr. L. I. Wiebe and Dr. James M. Diakur for their excellent supervision, guidance, mentoring, encouragement and enthusiasm throughout the duration of my studies. Their enthusiastic support made this project possible.

I wish also to express my deepest appreciation to Dr. Gerald G. Miller for his advice and guidance in this project.

I would like to thank Dr. Vera Chlumecky for CLSM training, Dr. A. Morales for providing the mass spectra, Dr. V. Somayaji and Dr. Hassan Monzavi for providing the NMR spectra, Dr. Piyush Kumar and Dr. Elena Atrazheva for synthesizing IAZA, Don Whyte for his expert technical assistance, Dr. Zuping Xia, Dr. Joan Z. Zuo, Mrs. Weili Duan and Dr. Keykavous Parang for many helpful discussions during this work.

I am also indebted to my mother, Shudong Dong and my father, Yunji Wei, for their love, encouragement, support, advice and understanding over my entire life, and particularly over the course of my studies.

Table of Contents

Chapter 1 OVERVIEW 1

Chapter 2 INTRACELLULAR UPTAKE OF FLUORESCENT LABELED β-CYCLODEXTRIN AND ITS AMANTIDINE INCLUSION COMPLEX 4

1. Introduction 4

1.1. Cyclodextrin 4

1.1.1. Background 4

1.1.1.1. History 5

1.1.1.2. Cyclodextrin Inclusion Complexes 9

1.1.2. Pharmacokinetics and Metabolism of CyDs 10

1.1.2.1. Stability 11

1.1.2.2. Parenteral Administration 12

1.1.2.3. Oral Administration 13

1.1.3. Interaction of CyDs with Lipophiles and Biological Membranes 16

1.1.3.1. Cellular Cholesterol Efflux Mediated by CyDs or High Density Lipoprotein (HDL) 16

1.1.3.2. Interaction of CyDs with Cell Membranes 18

1.1.3.3. Cyclodextrins Permeate Biological Membranes 19

1.2. Confocal Laser Scanning Microscopy 23

1.3. Chemistry of Fluorescent Derivatives of β-Cyclodextrin and a Guest Drug 27

1.3.1. Fluorescent Dyes 27

1.3.2. Applications of NBD Derivatives 28

1.3.3. Fluorescent Cyclodextrin Derivatives 30

2. Hypothesis and Objectives 33

3. Experimental 34

3.1. General Materials and Methods 34

3.2. Synthesis of Fluorescent Labeled β-Cyclodextrin 35

3.3. Study of NBD-β-CyD and its Amantidine Complexes by Fluorescence Spectrofluorometry 38

3.4. Stability of NBD-β-CyD in MEM and RPMI-1640 Media 38

3.5. Fluorescent Labeled Amantidine 39

3.6. Intracellular Uptake of NBD-β-CyD and its Amantidine Inclusion Complexes ... 41

3.7. Data Statistical Analysis 44

4. Results and Discussion 44

4.1. Synthesis of Fluorescent Labeled β-CyD 45

4.2. Study of NBD-β-CyD and its Amantidine Complex by Spectrofluorometry 48

4.3. Stability of NBD-β-CyD in MEM and RPMI-1640 Media 52

4.4. Fluorescent Labeled Amantidine (NBD-Amantidine, **6**) 53

4.5. Rhodamine B Isothiocyanate Labeled Amantidine (**8, 9**) 54

4.6. Intracellular Uptake of NBD-β-CyD and its Amantidine Inclusion Complex 55

4.6.1. Intracellular Distribution of NBD-β-CyD 55

4.6.2. Effect of Temperature on Intracellular Uptake 59

4.6.3. Effect of Serum Proteins on Intracellular Uptake 65

4.6.4. Intracellular Uptake Kinetics Study 69

5. Conclusion and Future Work 77

Chapter 3 ELECTROSPRAY MASS SPECTROMETRY STUDIES OF NITRO-FUNCTIONALIZED DRUGS AND CYCLODEXTRIN DRUG COMPLEXES 79

1. Introduction 79

1.1. Background 79

1.2. Electrospray Mass 80

1.3. The Overall Mechanism of the Ionization Process of ES-MS 81

1.4. Application of ES-MS 83

1.5. Investigation of Nitro-Functionalized Drugs Using ES-MS 86

2. Hypothesis and Objectives 89

3. Experimental 90

3.1. General Materials and Methods 90

3.2. ES-MS Studies of Nitro-Functionalized Compounds 91

3.3. Characterization of β-CyD Complexes with ES-MS 93

4. Results and Discussion 95

4.1. ES-MS Studies of Niro-Functionalized Drugs 95

4.2. ES-MS Detection Limits of Four Nitro-Functionalized Drugs 102

4.3. Characterization of β-CyD Complexes using ES-MS 105

5. Conclusions 111

Chapter 4 GENERAL DISCUSSION AND CONCLUSIONS 112

REFERENCES 114

List of Figures

Chapter 2. Figure 1.1.1.1 Cyclodextrins 5

Chapter 2. Figure 1.1.1.2. Structure of amantidine (adamantanamine hydrochloride) 10

Chapter 2. Figure 1.1.3 Two metabolic routes of starch 22

Chapter 2. Fig. 1.2.1 The essential feature of confocal microscopy 23

Chapter 2. Fig. 1.2.2 Simplified Optics of a CLSM 26

Chapter 2. Fig.1.3.1 Structure of (a) Rhodamine B Isothiocyanate (b) NBD-Cl 28

Chapter 2. Fig. 4.2.1 Fluorescence spectra of NBD-β-CyD a) emission spectrum b) excitation spectrum (0.2mg/mL) 50

Chapter 2. Fig. 4.2.2 Fluorescence spectra of NBD-β-CyD complex with amantidine a) emission spectrum b) excitation spectrum (0.2 mg/mL) 51

Chapter 2. Fig. 4.6.1 Selected areas for semi-quantification of fluorescence intensity (SK-MEL-24 with NBD-β-CyD incubated 30 min in RPMI-1640 medium) 57

Chapter 2. Fig. 4.6.2 Confocal microscopic images of NBD-β-CyD in a) HepG2 cells in monolayer culture b) SK-MEL-24 cells in monolayer culture 58

Chapter 2. Fig. 4.6.3 Temperature-dependence of intracellular fluorescence intensity after incubation with NBD-β-CyD and NBD-β-CyD/amantidine complex (HepG2, 30 min in normal medium) 63

Chapter 2. Fig. 4.6.4 Temperature-dependence of intracellular fluorescence intensity after incubation with NBD-β-CyD and NBD-β-CyD/amantidine complex (SK-MEL-24, 30 min in normal medium) 64

Chapter 2. Fig. 4.6.5 Effect of serum proteins on cell uptake of intracellular fluorescence intensity after incubation with NBD-β-CyD and NBD-β-CyD/amantidine complex (HepG2, 30 min) 67

Chapter 2. Fig. 4.6.6 Effect of serum proteins on cell uptake of intracellular fluorescence intensity after incubation with NBD-β-CyD and NBD-β-CyD/amantidine complex (SK-MEL-24, 30 min) 68

Chapter 2. Fig. 4.6.7 Kinetics study of cell uptake of intracellular fluorescence intensity after incubation with NBD-β-CyD and NBD-β-CyD/amantidine complex (HepG2, Fluorescence in mitochondria) 73

Chapter 2. Fig. 4.6.8 Kinetics study of cell uptake of intracellular fluorescence intensity after incubation with NBD-β-CyD and NBD-β-CyD/amantidine complex (HepG2, Fluorescence in cytoplasm) 74

Chapter 2. Fig. 4.6.9 Kinetics study of cell uptake of intracellular fluorescence intensity after incubation with NBD-β-CyD and NBD-β-CyD/amantidine complex (SK-MEL-24, Fluorescence in mitochondria) 75

Chapter 2. Fig. 4.6.10 Kinetics study of cell uptake of intracellular fluorescence intensity after incubation with NBD-β-CyD and NBD-β-CyD/amantidine complex (SK-MEL-24, Fluorescence in cytoplasm) 76

Chapter 3. Figure 1.3 (a) Schematic diagram of an electrospray inlet/ion source (b) Ion formation 82

Chapter 3. Fig. 4.1.1 Structures of nitro-functionalized compounds (part I) 96

Chapter 3. Fig. 4.1.1 Structures of nitro-functionalized compounds (part II) 97

Chapter 3. Fig. 4.1.1 Structures of nitro-functionalized compounds (part III) 98

Chapter 3. Fig. 4.1.2 Possible ionization mechanisms for IAZA (a) IAZA in positive ionization mode (b) IAZA in negative ionization mode 100

Chapter 3. Fig. 4.1.3 The spectra of IAZA a) in positive ionization mode b) in negative ionization mode 101

Chapter 3. Fig. 4.2.1 The spectra of serial dilution of IAZA in the negative ionization mode a) 31.2 μg/mL (*m/z*: 353.9) b) 1.95 μg/mL (*m/z*: 353.6) 104

Chapter 3. Fig. 4.3.1 The spectra of two complexes a) complex between β-CD and amantidine (5 mg/mL) b) NBD-β-CyD with amantidine (1 mg/mL)..... 108

Chapter 3. Fig. 4.3.2 The effect of dilution on the formation of CyD/amantidiine complex a) 5 mg/mL b) 0.625 mg/mL 109

Chapter 3. Fig. 4.3.3 The effect of high cone voltage on the formation of CyD/amantidine complex a) cone voltage 35 V b) cone voltage 70 V 110

List of Tables

Chapter 2. Table 1.1.1 Commonly used CyD derivatives.....8

Chapter 2. Table 4.2 The fluorescence intensities of NBD-β-CyD and its complex in water.....49

Chapter 2. Table 4.6.1 The regression data of kinetic studies of intracellular fluorescence intensity after incubation with NBD-β-CyD and NBD-β-CyD/amantidine complex.....70

Chapter 3. Table 4.1.1 ES-MS spectra (either positive (ES^+) or negative (ES^-) ionization mode) of the thirteen compounds in Figure 4.1.1.....99

Chapter 3. Table 4.2.1 Limit of detection (LOD) in ES-MS negative ionization mode.....102

List of Schemes

Chapter 2. Scheme 4.1 Synthesis of NBD-β-CyD.....47

Chapter 2. Scheme 4.4 Synthesis of fluorescently labeled amantidine.....53

Chapter 2. Scheme 4.5 Reaction of a primary amine with an isothiocyanate.....55

ABBREVIATIONS

Amantidine	Adamantanamine hydrochloride
ATP	Adenosine triphosphate
AUC	Area under the curve from the time of dose administration to time x
CGTases	Cyclodextrin glucosyltransferase
CI	Chemical ionization
CLSM	Confocal laser scanning microscopy
CM-β-CyD	Carboxymethyl-β-cyclodextrin
CME-β-CyD	Carboxymethyl-ethyl-β-cyclodextrin
CyDs	Cyclodextrins
cym	A group of *cgt* genes coding for cyclodextrin glycosyltransferase
β-CyDN_3	Mono-6-deoxy-6-azido-β-cyclodextrin
β-CyDNH_2	Mono-6-deoxy-6-amino-β-cyclodextrin
β-CyDOTs	Mono-6-deoxy-6-(*p*-toluenesulfonyl)-β-cyclodextrin
DCI	Direct chemical ionization
DE-β-CyD	Diethyl-β-cyclodextrin
DM-β-CyD	Dimethyl-β-cyclodextrin
DMAB	*p*-(Dimethylamino)benzoyl
DMF	*N, N*-Dimethylformamide
Dy-FAB	Dynamic Fast Atom Bombardment
EI	Electron ionization
ER	Endoplasmic reticulum
ES^+	Positive ionization mode
ES^-	Negative ionization mode
ES-MS	Electrospray mass spectrometry
FBS	Fetal bovine serum
FI	Field ionization

FITC	Fluorescein isothiocyanate
G_1-β-CyD	Glucosyl-β-cyclodextrin
G_2-β-CyD	Maltosyl-β-cyclodextrin
Glut-2	One member of a family of Na^+-independent glucose transporters
Gly	Glycine
HCl	Hydrochloride
HDL	High density lipoprotein
HE-β-CyD	Hydroxyethyl-β-cyclodextrin
HP-β-CyD	2-Hydroxypropyl-β-CyD
HPLC	High performance liquid chromatography
IAZA	Iodoazomycin arabinoside
i.v.	Intravenous
JD1-199L	2 (*p*-Nitrophenyl)ethyl-*O*-(β-*D*-galactopyranosyl)-(1→4)-β-D-glucopyranoside
$K_{1:1}$	Binding constant
KP	Short-pass excitation filter
Lamb	Maltoporin
LCAT	Lecitin cholesterol acyltransferase
LC-MS	Liquid chromatography-mass spectrometry
LD_{50}	Lethal dose at 50% concentration
LDL	Low density lipoprotein
LOD	Limit of detection
LP	Long-pass filter
MalE	Maltodextrin-binding proteins
MalF and MalG	Cytoplasmatic membrane proteins
MalP	Maltodextrin phosphorylase (MalP)
MalQ	Amylomaltase
MalZ	Maltodextrin glucosidase
M-β-CyD	Methyl-β-cyclodextrin
MALDI	Matrix-assisted laser desorption/ionization
NBD-amantidine	4-(1-*N*-Adamantanamino)-7-nitrobenzofuran

NBD-Cl	4-Chloro-7-nitrobenzofurazan
2-NBDG	2-(*N*-(7-Nitrobenz-2-oxa-1,3-diazol-4-yl)amino)-2-deoxyglucose
6-NBDG	6-(*N*-(7-Nitrobenz-2-oxa-1,3-diazol-4-yl)amino)-6-deoxyglucose
12-NBD stearate	12-(*N*-Methyl)-*N*-[(7-nitrobenz-2-oxa-1,3-diaxol-4-yl)amino]octadecanoic acid
NBD-β-CyD	4-(*N*-Mono-6-deoxy-6-amino-β-cyclodextrin)-7-nitrobenzofuran
PBS	Phosphate buffer saline
Phe	Phenylalanine
PMT	Photomultiplier
PSP	Plasmaspray
R_f	Retardation factor (rate of flow)
RAMEM	Random methyl-β-cyclodextrin
rpm	Revolutions per minute
SBE-β-CyD	Sulfobutyl ether-β-cyclodextrin
SD	Standard deviation
TFA	Trifluoroacetic acid
THF	Tetrahydrofuran
TK	Dichroic beam splitting mirror position
Trp	Tryptophane
TSP	Thermospray
V_{dss}	Steady-state volumes of distribution

Chapter 1

OVERVIEW

Cyclodextrins (CyDs) are cyclic α-(1,4)-linked oligosaccharides of α-D-glucopyranose containing a relatively hydrophobic central cavity and hydrophilic outer surface. The most common CyDs are α-, β- and γ-CyD, which consist of six, seven and eight glucopyranose units, respectively (Loftsson *et al.* 1996). The central cavity of the CyD molecule is lined with skeletal carbons and ethereal oxygens of the glucose residues and is lipophilic. The central cavity provides a lipophilic microenvironment into which suitably sized drug molecules may enter and be included. No covalent bonds are formed or broken during the formation of the inclusion complex, and in aqueous solution, the process is in equilibrium. The unique feature of CyDs, the formation of inclusion complexes with many suitable drugs, makes them useful for many applications in the pharmaceutical field, such as increasing bioavailability, enhancing stability, reducing side effects, increasing solubility and potentially being drug carriers.

The cavity of CyD is suitable for the inclusion of hydrophobic therapeutic agents of appropriate dimensions. In theory, a CyD carrier is typically suitable for solubilization and delivery of only one equivalent of therapeutic agent. CyD, as an intravenous (*i.v.*) delivery vehicle, could be used to define the administered amount of highly toxic and highly unstable agents which should be accurately controlled their doses. Before CyDs are applied as drug carriers in the pharmaceutical field, their own pharmacokinetics, metabolism and toxicity should be thoroughly studied. Many research groups have studied the pharmacokinetics, metabolism and cellular interactions of CyDs with cell

membranes. Few studies have been carried out on the permeation of CyDs across biological membranes, and there is not convincing evidence to prove that CyDs can pass across cell membranes. One reason for this lack of information is that there are only limited methods (radiolabelling, etc.) for the microanalysis of CyDs in biological matrices, due in large part to the absence of chromophoric group on the CyDs which prevents direct spectrophotometric detection.

Confocal laser scanning microscopy (CLSM) is a powerful technique to observe the permeation of fluorescent derivatives across biological membranes. The major advantage of CLSM over conventional fluorescence microscopy is the reduction of out-of-focus fluorescence resulting in improved resolution and contrast. Another important feature of CLSM is dual channel scanning, which can differentiate two different fluorescence signals in the sample simultaneously.

For the application of CyD as drug carriers *in vivo*, the ability to detect and characterize CyD complexes at low concentrations is critical to their development for this purpose. Electrospray Mass Spectrometry (ES-MS) has recently emerged as a powerful tool for studying non-covalent complexes (Vincenti *et al.* 1995). Soft ionization techniques such as ES-MS have proven valuable for the detection of molecular ions of multiply charged molecules, and little or no fragmentation is usually observed. This technique relies on analyte ions being already present in solution prior to introduction to the mass spectrometer. These ions can be generated by proton transfer (positive ion formation) or abstraction (negative ion formation).

In the first part of this thesis, CLSM was selected as a detection method to study the intracellular uptake and distribution of a fluorescent CyD derivative and its inclusion

complex. A fluorescently labeled derivative of β-CyD and a guest drug (amantidine) were the focus of the work reported here. Ideally, two different fluorescent probes would be incorporated into β-CyD and amantidine, respectively. The two selected fluorescent reagents were 4-chloro-7-nitrobenzofurazan (NBD-Cl) and rhodamine B isothiocyanate. A fluorescent derivative of β-CyD and its amantidine complex were used to study the intracellular uptake and distribution in two cell lines (HepG2 and SK-MEL-24) using CLSM.

In the second part of this thesis, ES-MS was applied to characterize CyD/drug complexes. In order to become familiar with this technique and to test whether it is directly applicable to our MS studies of NBD-labeled CyD, thirteen nitro-functionalized compounds were studied using ES-MS. Four of these selected drugs as well as a CyD host-guest complex were studied in greater detail. Of the thirteen compounds, four (nifedipine, hydroxyflutamide, flutamide, and iodoazomycin arabinoside (IAZA)) are drugs used in either clinical or experimental diagnostic medicine. This experience was then applied to host-guest complexes (complexation of β-CyD and amantidine), and to an assessment of the applicability of this technique (ES-MS) for analysis of CyD host/guest complexes.

Chapter 2

INTRACELLULAR UPTAKE OF FLUORESCENT LABELED β-CYCLODEXTRIN AND ITS AMANTIDINE INCLUSION COMPLEX

1. Introduction

1.1. Cyclodextrin

1.1.1. Background

Cyclodextrins (CyDs) are a homologous family of cyclic oligosaccharides composed of α-(1,4)-linked glucopyranose units (Loftsson *et al.* 1996). The three major CyDs consist of six (α-CyD), seven (β-CyD) and eight (γ-CyD) glucopyranose units, and in terms of molecular architecture, can be viewed as toroidal baskets with cavity diameters of 4.9, 6.2 and 7.9 Å, respectively (Figure 1.1.1.1, Diakur *et al.* 1999). CyDs have an overall geometric shape of a torus or truncated cone containing a relatively hydrophobic central cavity and hydrophilic outer surface. Their interior cavity is formed by C-H bonds and ether-oxygen linkages and is distinctly hydrophobic, thus allowing for the inclusion of low molecular weight lipophilic drugs. The exterior surface of CyDs is populated with hydroxyl groups and is hydrophilic. Primary and secondary hydroxyl groups are located on both faces of the truncated cone. The primary hydroxyl groups at carbon 6 are on the narrow "open" side (primary face) and two secondary hydroxyl groups at carbons 2 and 3 are on the opposite wide side (secondary face)(Diakur *et al.* 1999).

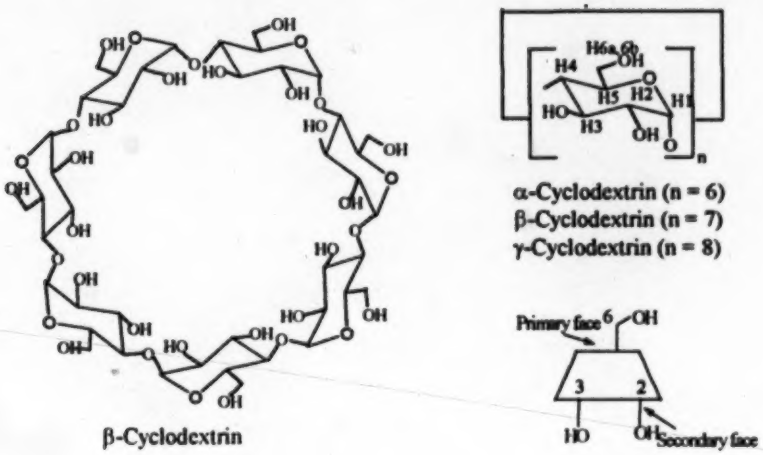

Figure 1.1.1.1 Cyclodextrins

1.1.1.1. History

Cyclodextrins (CyDs) were first isolated by Villiers in 1891 (Wenz, 1994). Schardinger characterized CyDs as cyclic oligosaccharides in 1904 (Cramer, 1981). The structure of the Schardinger dextrins was identified by Freudenberg in 1938 (Saenger 1980). Between 1911 and 1935, Pringsheim showed that CyD could form stable aqueous complexes with many compounds (Straighten, 1990). The first patent on CyDs and their complexes was registered in 1953 (Loftsson *et al.* 1996). Before the mid-1970s, most CyD research was based on the unmodified parent CyDs. Several factors which prevented CyDs from widespread applications in pharmaceutical formulations were: production limit (only a small amount of unmodified α-, β-, γ-CyD could be produced at that time), high production costs, and nephrotoxicity of the β-CyD (Rajewski *et al.* 1996; Loftsson *et al.* 1996). By the middle of the 1970's, CyDs had been structurally and

chemically characterized. From then on, the properties of CyDs have been investigated in detail. As a result of these extensive investigations along with biotechnological advances, the production of CyDs has been dramatically improved. CyDs are now produced in industrial-scale. Widespread utilization of CyDs is focused in pharmaceutical, food, chemical, cosmetics and other industries (Szejtli, 1985).

For a number of reasons such as price, availability, approval status and cavity dimensions, β-cyclodextrin (β-CyD) is the most widely used, accounting for at least 95% of all produced CyDs. Most of the CyD producing enzymes known produce predominantly β-CyD (Flaschel *et al.* 1981). β-CyD can easily form inclusion complexes with many drugs because its cavity diameter (6.2 Å) is suitable for accommodating aromatic groups possessed by many drug molecules. The cavity of α-CyD is too small for a favorable fit because of its cavity diameter (4.9 Å), which can accommodate only aliphatic chains. γ-CyD can also form inclusion complexes with many drugs, but its cavity diameter (7.9 Å) is too wide for many drug molecules such as prostaglandin E_1, and results in a loose fit (Rajewski *et al.* 1996; Szejtli, 1994).

Due to the poor aqueous solubility of β-CyD (18 g/L) and the low solubility of some of its complexes, such as its insoluble complex formed with cholesterol, many chemically modified CyDs have been synthesized to increase their hydrophilic activity and minimize renal toxicity. Now many CyD derivatives can be industrially produced on the hundred ton level. The available CyD derivatives include: dimethyl-β-CyD (DM-β-CyD), random methyl-β-CyD (RM-β-CyD), 2-hydroxypropyl-β-CyD (HP-β-CyD), sulfobutyl ether-β-CyD (SBE-β-CyD), and maltosyl and glucosyl β-CyD (Table 1.1.1)

(Rajewski *et al.* 1996; Szejtli, 1994). At the same time, CyD-utilizing technologies are continuously developing.

Table 1.1.1 Commonly used CyD derivatives

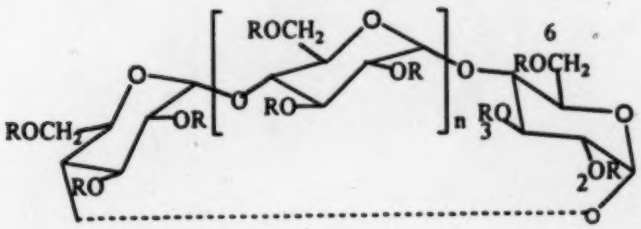

Cyclodextrin	Abbreviation	R	N
Carboxymethyl-β-cyclodextrin	CM-β-CyD	CH_2CO_2H or H	5
Carboxymethyl-ethyl-β-cyclodextrin	CME-β-CyD	CH_2CO_2H,CH_2CH_3 or H	5
Diethyl-β-cyclodextrin	DE-β-CyD	CH_2CH_3 or H	5
Dimethyl-β-cyclodextrin	DM-β-CyD	CH_3 or H	5
Methyl-β-cyclodextrin	M-β-CyD	CH_3 or H	5
Random methyl-β-cyclodextrin	RM-β-CyD	CH_3 or H	5
Glucosyl-β-cyclodextrin	G_1-β-CyD	Glucosyl or H	5
Maltosyl-β-cyclodextrin	G_2-β-CyD	Maltosyl or H	5
Hydroxyethyl-β-cyclodextrin	HE-β-CyD	CH_2CH_2OH or H	5
Hydroxypropyl-β-cyclodextrin	HP-β-CyD	$CH_2CHOHCH_3$ or H	5
Sulfobutylether-β-cyclodextrin	SBE-β-CyD	$(CH_2)_4SO_3Na$ or H	5

Derivatives may have different degrees of substitution on the 2, 3 and 6 positions (Rajewski *et al.* 1996)

1.1.1.2. Cyclodextrin Inclusion Complexes

Inclusion complexes are entities comprising of two or more molecules, in which one of the molecules, the "host", includes totally or in part only by physical forces, a "guest" molecule (Szejtli, 1994). The CyDs are naturally occurring cyclic oligosaccharides known to function as hosts in the formation of host-guest inclusion complexes. CyDs can be considered as "empty" capsules of molecular size. They can form inclusion complexes with a great variety of "guest" molecules having the size of one or two benzene rings, or even larger molecules that have a side chain of comparable size (Szejtli, 1994). Many drug molecules or functional groups match these requirements and can be introduced into the cavity of CyDs in the presence of water.

In aqueous solution, the slightly apolar cavity of CyDs is filled by water molecules which are energetically unfavored (polar-apolar interaction) and are therefore readily substituted by appropriate "guest molecules" which are less polar than water. The driving forces involved in the inclusion complex formation are van der Waals interactions (Nashijo *et al.* 1991), hydrogen bonding (Tong *et al.* 1991; Jones *et al.* 1984), hydrophobic interaction (Nashijo *et al.* 1991; Tabushi *et al.* 1978), release of ring strain in the CyD molecule (Jones *et al.* 1984), and change in the solvent-surface tension (Orstan *et al.* 1987).

The cavity of CyD is suitable for complexing a variety of small drug molecules. It is more useful to extend the range of therapeutic agents that can be accommodated by the introduction of predicted binding. The diameter of the β-CyD cavity is 6.2 Å, and molecular modeling has revealed that the adamantane skeleton (diameter ~ 5.15 Å) is a

perfect fit. This has been confirmed by determination of the association constant for the complexation of β-CyD with amantidine ($4.2x10^4$ M^{-1}) (Eftink *et al.* 1989).

Amantidine has recently been applied to the prophylactic and therapeutic treatment of influenza A virus infections (Diakur *et al.* 1999). Figure 1.1.1.2 shows the structure of amantidine. This rigid structure readily forms an inclusion complex with β-CyD. The complex formation with equimolar amounts of β-CyD is rapid and the resulting host-guest complex is easily dissolved in water (Diakur *et al.* 1999). The complex formed between amantidine and β-CyD was studied in this project.

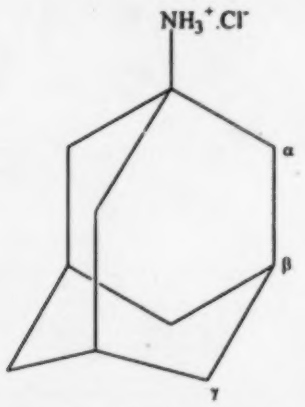

Figure 1.1.1.2. Structure of amantidine (adamantanamine hydrochloride)

1.1.2. Pharmacokinetics and Metabolism of CyDs

As a result of intensive research (industrial-scale production, toxicity, *etc.*) during the past decade, CyDs have been applied to pharmaceutical, foods, cosmetics, and other industry. Actually, almost all of the current applications of CyDs involve complexation. The following discussion will focus on the application of CyDs in the pharmaceutical field.

Pharmaceutical applications of CyDs include complexation of drugs, ingredients in drug formulation (as vehicle in tableting), direct therapeutic use (in intraperitoneal dialysis etc.) and nontherapeutic uses (in diagnostics etc.). The most common application of CyDs in the pharmaceutical industry is that CyDs form complex with a great variety of drugs. The potential advantages in using the parent CyDs and their chemically modified derivatives in medicine have been extensively studied (Irie *et al.* 1997). By forming inclusion complexes with CyDs, certain properties of drugs, such as solubility, stability and bioavailability can be improved. The enhancement of drug activity and reduction of local side effects can also be achieved. CyDs can therefore be used as drug carriers to formulate and deliver many size-suitable drugs. They are especially useful for solubilizing poorly soluble drugs into aqueous injectable solutions (PROSTAVASIN®: the molar ratio of prostaglandin E_1 to α-CyD is 1:11) (Szejtli, 1994). Although CyDs as potential drug carriers have many advantages for developing new dosage forms, before they can be used practically, pharmacokinetics, toxicity and metabolism of CyDs should be thoroughly understood.

1.1.2.1. Stability

The cyclic nature of CyDs renders these oligosaccharides stable in alkaline medium. They can however, be hydrolyzed to series of linear maltosaccharides by strong acids such as 1 N HCl solution at 60 ^{0}C (Szejtli, 1988). The ring-opening hydrolysis rate of CyDs is much lower than that of corresponding hydrolysis of linear oligosaccharides, and depends on the size of the macrocycle and on its conformation. For example, the rate of acid-catalyzed hydrolysis increases in the following order: α-CyD < β-CyD < γ-CyD

(Miyazawa *et al.* 1995). In living systems, glycosidic bonds of CyDs are cleaved by specific enzymes. Since the cyclic nature of CyDs make them less susceptible to attack by enzymes such as α-amylase, the rate of hydrolysis is much slower than that of linear sugars (Szejtli, 1988). When substituents are introduced on the hydroxyl groups, the enzymatic hydrolysis of CyDs is slowed down even further because the affinity of CyDs to enzymes decreases (Irie *et al.* 1997). For example, maltosyl-β-CyD (G_2-β-CyD) is a good substrate for glucoamylase and pullulanase, and is hydrolyzed at a very slow rate by α-amylase because of the steric hindrance of the branched sugar (Hirayama *et al.* 1992). Many bacterial strains isolated from the human colon are able to degrade CyDs, using them as their sole carbon source. This characteristic of CyDs may be useful for site-specific delivery of drugs to the colon (Irie *et al.* 1997).

1.1.2.2. Parenteral Administration

After CyDs are intravenously administrated, they disappear rapidly from systemic circulation and are excreted mainly via the kidney. Intact β-CyD and gluocosyl-β-CyD were recovered in urine in over 90% of each dose within 10 h after intravenous administration (50 mg/kg), respectively to rats. Their concentration in plasma fell to below 0.3 μg/mL within 3 h (Kubota *et al.* 1996). The pharmacokinetic behavior of most CyDs, including parent CyDs and their chemically modified derivatives, were similar after intravenous administration. The steady-state volumes of distribution (V_{dss}) for β-CyD and HP-β-CyD in rats, rabbits, dogs, and humans corresponds well with the extracellular fluid volumes of each species, assuming that no deep compartments of storage in pools are involved. Elimination of CyDs occurred through glomerular

filtration. When a dose of 200 mg/kg β-CyD was intravenously administered in rats, the elimination rate was decreased, probably as a result of nephrotoxicity of the β-CyD/cholesterol complex (Frijlink *et al.* 1990).

The most critical toxic effects of parent CyDs for parenteral use are on kidneys. Kidneys are the main organs for clearance of CyDs from systemic circulation. CyDs are concentrated in the proximal convoluted tubule after glomerular filtration (Irie *et al.* 1997). Parent CyDs, especially β-CyD, can form insoluble cholesterol complexes in the form of crystals in the kidneys, which results in nephrotoxicity. In order to avoid the nephrotoxicity, numerous chemically modified CyDs have been made. Due to their heterogeneity and hydrophilic properties, these CyD derivatives can not be crystallized and do not form crystalline cholesterol complexes, thus their renal toxicity is expected to be lower than the parent CyDs (Szejtli, 1994; Irie *et al.* 1997). HP-β-CyD has been most extensively studied with regard to the parenteral safety in several types of animals and in humans (Irie *et al.* 1997). HP-β-CyD can form soluble complexes with cholesterol in tissues and circulation of rabbit and humans and be excreted to urine via kidneys (Irie *et al.* 1992). HP-β-CyD has very low toxicity when intravenously administrated even at high doses (Irie *et al.* 1997).

1.1.2.3. Oral Administration

Gastrointestinal absorption of CyDs in intact form is limited due to their bulky and hydrophilic nature. Generally, drug carrying CyDs deliver drug molecules through an aqueous milieu to absorption sites on the intestinal epithelium. Andersen *et al.* (1963) administered ^{14}C-labeled potato-starch and α- and β-CyD orally to rats, and measured the

radioactivity of respiratory carbon dioxide in the function of time. The radioactivity in urine, intestinal contents and various organs was also determined. The results showed that the metabolism of starch was much faster than CyD. This conclusion was proven by Szejtli (Szejtli *et al.* 1980). In his experiment, ^{14}C-labelled β-CyD and glucose were orally administered to rats and the blood radioactivity was measured. The maximum radioactivity of orally administered ^{14}C-labelled glucose in the blood appeared within 10 min, while the maximum radioactivity of orally administered ^{14}C-labelled β-CyD in the blood appeared within 6 h. The authors suggested that rats metabolized CyD, but metabolism by the intestinal flora has not yet been ruled out in this case. The absorption, distribution, excretion and metabolism of orally administered ^{14}C-labelled β-CyD and glucose were compared (Gerloczy *et al.* 1985). In this study no specific accumulation was observed in various organs after ^{14}C-labeled β-CyD was orally administered to rats. It is assumed that β-CyD is metabolized in rat at a much slower rate than glucose. All of the results (above) suggest that CyDs are enzymatically hydrolyzed to open-chain dextrin, and thereafter, are rapidly hydrolyzed to maltose and glucose. Radiolabelling alone cannot differentiate between the intact β-CyD molecule and its metabolites which enter the blood after oral administration. Kubota (Kubota *et al.* 1996) studied the absorption, distribution and excretion of β-CyD and glucosyl-β-CyD administered orally in rats, using HPLC equipped with amperometric detection. The maximum plasma concentrations of both CyDs were below 5 μg/mL at an oral dose of 500 mg/kg. The $AUC_{0\text{-}2h}$ of β-CyD and glucosyl-β-CyD were 6.57±0.15 and 1.59±0.13 μg.h/mL, respectively. Only an insignificant amount (below 0.002% of dose) of both CyDs was detected in the urine. The conclusion was that only an insignificant amount of intact β-

CyD and glucosyl-β-CyD was absorbed from the gastrointestinal tract in rats. The fate of the parent CyDs in the gastrointestinal tract depends on their resistance to hydrolysis and enzymatic degradation. Both α- and β-CyD are resistant to stomach acid, salivary and pancreatic amylases. They are however, hydrolyzed in the colon. Studies on healthy volunteers and ileostomy patients have shown that β-CyD and glucosyl-β-CyD were poorly digested in the human small intestine but they were readily fermented by the colonic flora (Flourie *et al.* 1993). The transit time through the human colon is ~ 40 h, which is long enough for bacterial enzymes to completely hydrolyze the parent CyDs. The chemically modified CyDs such as glucosyl-β-CyD are more resistant to the intestinal hydrolases than the parent CyDs. The absorption of these modified CyDs however, is lower than the absorption of the parent CyDs when orally administered. Most of the administered CyD is excreted in the feces in the intact form. Kubota (Kubota *et al.* 1996) reported that the $AUC_{0\text{-}2h}$ value of β-CyD obtained from the oral administration of β-CyD was about 4 times higher than that of glucosyl-β-CyD. The cumulative urinary excretion of β-CyD was about twice that of glucosyl-β-CyD during a 5 day period after administration.

Toxicity studies have shown that orally administered CyDs are practically nontoxic because only insignificant amounts of CyDs are absorbed in the gastrointestinal tract (Gergely *et al.* 1981). These authors reported that β-CyD administered orally to rats and dogs did not cause any toxic effect over the long-term toxicity studies. Szejtli reported in 1982 (Zuo, 1998) that the LD_{50} value of β-CyD was 12,500 mg/kg for mice, and 12,000 mg/kg for rat. The acute LD_{50} values were estimated after a single oral administration.

1.1.3. Interaction of CyDs with Lipophiles and Biological Membranes

1.1.3.1. Cellular Cholesterol Efflux Mediated by CyDs or High Density Lipoprotein (HDL)

CyDs and their derivatives are usually applied in the pharmaceutical industry for the improvement of drug solubility, delivery and bioavailability (Szejtli, 1994). Recent studies have additionally shown that CyDs can interact with lipid and cholesterol in biological membranes and the systemic circulation of the body (Grosse *et al.* 1998). The parent CyDs and their modified derivatives can form inclusion complexes with lipophiles. The acyl chain of a phospholipid fits tightly into the hydrophobic cavity of α-CyD and more loosely into the larger cavities of β- and γ-CyDs. The side chain of cholesterol fits into the cavity of β-CyD (Irie *et al.* 1997). CyDs can interact with serum lipoproteins because CyDs can form inclusion complexes with accessible hydrophobic regions of the lipoproteins, leading to precipitation (Irie *et al.* 1997). Based on these observations, it has been suggested that CyDs can act as artificial lipid carriers that can functionally supplement the natural circulatory lipid carriers such as lipoproteins and serum albumin (Irie *et al.* 1992). These authors have also reported that intravenous administration of HP-β-CyD to rats has led to a transient decrease in plasma cholesterol levels. This is due to the fact that HP-β-CyD forms complexes with cholesterol in circulation and subsequently delivers cholesterol from intravascular to extravascular compartments.

Cholesterol is an integral membrane component that is essential for normal cellular function. In mammalian cells, this sterol is derived either from low density lipoprotein (LDL) following receptor-mediated endocytosis and subsequent hydrolysis in

lysosomes, or via *de novo* biosynthesis in the endoplasmic reticulum (ER) (Neufeld *et al.* 1996). The transport of cholesterol from cells to serum or interstitial fluid plays an important role in the maintenance of cellular cholesterol homeostasis and is also the first step in the transport of peripheral tissue cholesterol back to the liver for excretion (Atger *et al.* 1997). This first step, known as reverse cholesterol transport, is the efflux of cellular cholesterol to a suitable acceptor. The process is mediated primarily by high density lipoprotein (HDL) or specific HDL subclasses which are physiological cholesterol acceptors (Kilsdonk *et al.* 1995) that couple with serum enzymes such as cholesteryl ester transfer protein and lecitin cholesterol acyltransferase (LCAT) (Smith *et al.* 1978; Atger *et al.* 1997). The mechanism of the transport of cholesterol molecules from the cell plasma membranes to acceptor lipoproteins involves aqueous diffusion. It is thought that the cholesterol molecule desorbs from the membrane and is incorporated into the acceptor after traversing the intervening aqueous phase. This movement is a function of a cholesterol gradient established between the plasma membrane and the phospholipid in the lipoprotein acceptors. Since serum lipoproteins contain unesterified cholesterol that exchanges between cells and lipoproteins, the movement of cholesterol is a bidirectional process (influx and efflux), and net movement of cholesterol mass is determined by the relative contribution of both influx and efflux.

Water-soluble CyDs can readily form inclusion complexes with cholesterol, and thus dramatically enhance their solubility in aqueous solution. Recently CyDs were shown to stimulate efflux of cholesterol from cultured cells with high efficiency (Neufeld *et al.* 1996). Additional studies have compared cellular cholesterol efflux mediated by either CyDs, including parent CyDs (β-CyD), chemically modified CyDs (HP-β-CyD,

M-β-CyD, etc.) and HDL (Kilsdonk *et al.* 1995; Neufeld *et al.* 1996; Atger *et al.* 1997). The results obtained showed that the major efflux portion of the cholesterol from mouse L-cell fibroblasts mediated by β-CyD was released from cells within 2 hours, Under the same conditions, HDL released cholesterol at a constant rate over 8 hours. Thus, the kinetics for the efflux of cellular cholesterol mediated by CyDs and HDL are not the same (Kilsdonk *et al.* 1995; Neufeld *et al.* 1996). In the experiment above, several cell lines such as normal and NP-C fibroblasts, Fu5AK rat hepatoma and GM3468A human skin fibroblasts, were selected. The efflux of cellular cholesterol induced by CyDs was not cell specific, and the kinetic profiles of cholesterol efflux varied only slightly. Other recent studies supported the fact that CyDs were efficient lipid carriers or modulators of cholesterol. This was especially true for the methyl-β-CyD-induced efflux of cholesterol in Hep-2 and Hela cell lines (Rodal *et al.* 1999) and in mouse sperm (Chio *et al.* 1998).

1.1.3.2. Interaction of CyDs with Cell Membranes

The intrinsic cytotoxicity of a potential drug carrier is one of the most essential characteristics to be considered for drug delivery. The ideal drug carrier should have no cytotoxicity. As mentioned previously, CyDs can extract cholesterol from biological membranes, thereby altering the cell membrane (Grosse *et al.* 1998). These changes modify the membrane's fluidity and permeability and therefore, enable drug passing across the biological membrane (Masson *et al.* 1999). On the other hand, the interaction between CyDs and cholesterol can lead to cytotoxicity. The interaction of CyDs with the cell membrane is thought to be the first step of cell damage (Irie *et al.* 1997). CyDs can affect membrane invagination on human erythrocytes and even cause lysis (Irie *et al.*

1982; Ohtani *et al.* 1989). The hemolytic activity of parent CyDs is in the order β-CyD >α-CyD> γ-CyD (Irie *et al*, 1982).

It has been shown (Ohtani *et al.* 1989) that the process of extraction of membrane components (cholesterol) from erythrocytes occurs without entry of CyD into the membrane. When ^{14}C-labelled β-CyD in PBS solution was added to erythrocytes and incubated at 37 ^{0}C for 30 min, most of the^{14}C-labelled β-CyD remained free in solution and only a negligibly small amount of ^{14}C-labelled β-CyD was associated with erythrocytes, indicating that CyD extracted the membrane cholesterol into the aqueous phase. This removal of membrane components led to enhanced fluidity and permeability of the cell membrane, and loss of these components induced shape changes of membrane invagination, and consequently caused cytolysis. Studies on the interaction of CyD with different types of cells including human skin fibroblasts, intestinal cells, and *E. coli* bacterial cells were also performed (Irie *et al.* 1997). The results obtained suggest that the mechanisms involved in CyD-induced cytotoxicity are not specific to the cell type and are mainly dependent on a loss of vital cellular components (cholesterol) which are extracted by CyDs.

1.1.3.3. Cyclodextrins Permeate Biological Membranes

CyD molecules are relatively large (molecular weight ranging from 1000 to over 1500) and poorly permeate biological membranes, such as mucosal membranes (Matsubara *et al.* 1995; Masson *et al.* 1999). As described previously, CyDs as drug carriers and absorption enhancers keep drug molecules in solution and deliver them to the surface of the biological membrane, such as mucosa or the eye cornea. The drugs can

partition into the membranes. At high concentration, CyDs could facilitate their own absorption (Irie *et al.* 1997). Matsubara *et al.* (1995) reported that when 80 mM DM-β-CyD was administered nasally to rats, a considerable amount of DM-β-CyD (15.8 ± 3.7% of each dose) was recovered in intact form in the urine within 3 h. Marques *et al.* (1991) detected the pulmonary absorption of CyDs. They concluded that HP-β-CyD has the best potential as a drug carrier for improving the pulmonary delivery of drugs. When β-CyD, DM-β-CyD and HP-β-CyD were administered intratracheally in rabbits, their absorption rates were considerably higher than those observed for oral, rectal and nasal routes of administration. For example, the bioavailability of β-CyD, DM-β-CyD and HP-β-CyD after intratracheal instillation were 65.9 ± 12.8, 73.9 ± 13.2 and 79.8 ± 12%, respectively (Marques *et al.* 1991; Irie *et al.* 1997). The information above suggests that the mechanism of CyD transport across the biological epithelium was paracellular, however, the mechanism of the absorption process is not yet clear. One of the goals of this project is to determine whether or not the endocytotic uptake of fluorescently labeled CyDs also occurs during the absorption of CyDs.

Recently some reports (Fielder *et al.* 1996; Pajatsch *et al.* 1998) have shown that CyD can be transported into the cytoplasm of *Klebsiella oxytoca* (*K.oxytoca*) via a specific binding-protein dependent uptake system. This sugar is then metabolized in the cytoplasm. *K.oxytoca* can be grown in the presence of starch as the sole carbon and energy source via two metabolic routes (Fig. 1.1.3). The first route involves the conversion of starch into linear isomaltodextrins by hydrolysis of the α-1,6-glycosidic bonds via the cell surface-associated pullulanase. Cleavage of the α-1,4-glycosidic linkages is then carried out by extracellular α-CyD-glucosyltransferases (CGTases), a

subgroup of the α-amylase class of enzymes (Bender, 1977). *Klebsiella pneumoniae* and *Escherichia coli* can then take up these linear maltodextrins (maltose to maltoheptaose) via a binding protein-dependent transporter consisting of maltoporin (LamB), the maltodextrin-binding proteins (MalE), and the cytoplasmic membrane proteins (MalF and MalG). These linear maltodextrins would be intracellularly metabolized into glucose and glucose-1-phosphate by enzymes such as amylomaltase (MalQ), and the maltodextrin phosphorylase (MalP). A second route was only found in *K.oxytoca* (Pajatsch *et al.* 1998). Starch can be degraded extracellularly into CyDs (α-, β-CyDs) by the cyclization activity of the α-CGTase produced by *Klebsiella oxytoca* M5a1. *K.oxytoca* is grown in the presence of CyD as its sole carbon and energy source and takes up the CyDs via the *cym* gene system. The Cym gene system consists of ten genes that can produce a group of specific binding proteins for the transport of CyDs. CyDs are linearized by a cyclodextrinase (CymH) into linear maltooligosaccharides in the cytoplasm, and then degraded into glucose as in the first route (Feederle *et al.* 1996). The information above suggests endocytotic uptake of CyDs can occur.

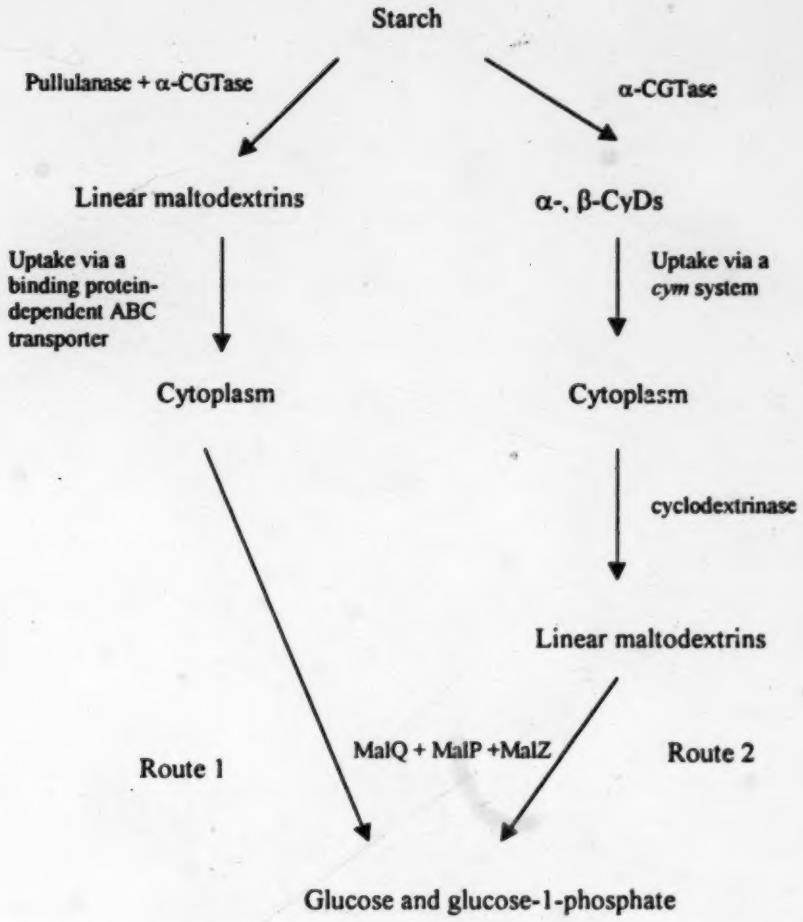

Figure 1.1.3 Two metabolic routes of starch

1.2. Confocal Laser Scanning Microscopy

In order to study the permeation pathways of CyD across cell membranes, a highly sensitive detection method is required. The most widely used methods for this purpose include radiometry and conventional fluorescence microscopy. Confocal laser scanning microscopy (CLSM) has been established as a more advantageous technique in this area (Ladic, 1999; Jaffe, 1999). CLSM can be used to study permeation routes of fluorescent compounds across cell layers *in vitro* without any physical damage to a specimen at a subcellular level (Jaehde *et al.* 1994). Measurement of fluorescence requires little biological material for study and can be used to measure solute uptake by individual cells rather than the average uptake rate of a heterogeneous population of cells as is done with isotopic uptake (Rauchman *et al.* 1992).

Generally, CLSM allows the researcher to "optically section" a fluorescently labeled specimen. The advantage of CLSM over conventional fluorescence microscopy is the restriction of fluorescence to a narrow focal depth, resulting in improved resolution and contrast of the image, and the ability of this technique to make clearly resolved optical sections of the tissue (Marttin *et al.* 1997).

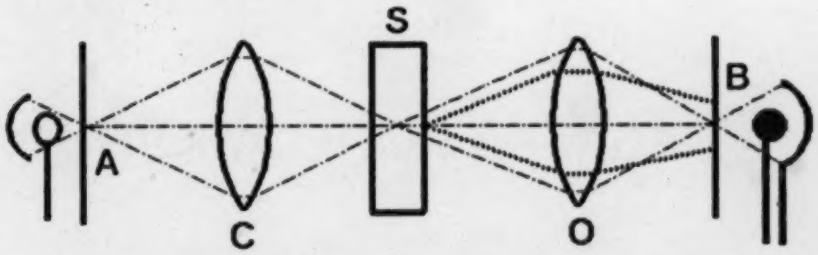

Fig. 1.2.1 The essential feature of confocal microscopy (Jaffe, 1999)

Figure 1.2.1 shows that the essential feature of confocal microscopy is the reduction of out-of-focus light. Illumination is admitted through pinhole A (left) such that the point of light is focused via the condenser (C) onto the specimen (S). There is a point of focus within the specimen. The point of the transmitted light will be scanned along the specimen in both the X and Y directions to create an image comprised of an optical section through the specimen. This point of light is then magnified by the objective (O) whose image is aligned so that the image passes through a second pinhole B to the detector (right). Light from above and below the focal plane (dotted line) is not in focus and thus will not pass through pinhole B to the detector (Jaffe, 1999).

Figure 1.2.2 shows a simplified scheme of a confocal laser scanning microscope. Excitation light, of predetermined wavelength, is reflected by a dichroic mirror (beam splitter) and is then focussed by an objective lens to a small point on a fluorescently labeled specimen. The mixture of reflected light and emitted fluorescent light is captured by the same objective lens and is then focussed onto a photodetector (photomultiplier) by the same dichroic mirror. Only the emitted fluorescent light can pass to the photodetector and the reflected light (low wavelength) is deflected by the dichroic mirror. The dichroic mirror reflects light below a predetermined wavelength (e.g. 420 nm) and allows light above the same wavelength to pass through the dichroic mirror. The fluorescent light emitted from the specimen will be at longer wavelength than the excitation beam, and pass on to the detector. A confocal aperture (pinhole) is located in front of the photodetector. The fluorescent light focussed from the specimen that is not within the focal plane (out-of-focus light) will be mainly blocked by the pinhole, so the

contaminating optical information from both above and below the focal plane is largely decreased (Ladic, 1999; Jaffe, 1999).

CLSM can be applied to visualize the transport pathways of fluorescently labeled compounds across biological membranes, and can also be used for studying cell morphology (Marttin *et al.* 1999). The transport pathways of fluorescein isothiocyanate (FITC)-labeled dextrans across rat nasal epithelium *in vivo* were studied by using CLSM. The results obtained suggested that the major transport pathway of the high molecular weight compound (FITC-labeled dextran, average MW: 3000) was paracellular. The intracellular uptake of this macromolecular compound was observed. Visualization of (FITC)-labeled dextrans intracellularly in foci was due to endocytotic uptake of the dextran molecules. The effect of randomly methylated β-CyDs as absorption enhancers on the rat nasal epithelium was also studied by CLSM. The results proved that randomly methylated β-CyDs increased the paracellular permeability of the nasal epithelium when co-administered (Marttin *et al.* 1997; Marttin *et al.* 1999). Optical "thin sections" in monolayer cell culture can be used to determine the intracellular distribution of fluorescently labeled compounds. The semiquantitative nature of CLSM can be used to study intracellular uptake kinetics and subcellular distribution of fluorescent substances (Miller *et al.* 1995; Miller *et al.* 1997). In CLSM, dual channel sequential scanning can be employed to distinguish between two different fluorescent dyes and therefore two different fluorescent derivatives can be studied simultaneously. This feature is especially suitable for studying the CyD inclusion complexes. Both CyD and a guest can be labeled with different fluorescent dyes. The movement across biological membranes of the host and guest molecules labeled with two different fluorescent dyes can be therefore studied

at same time. The resulting images are more highly resolved and are therefore useful to determine intracellular distribution and uptake kinetics.

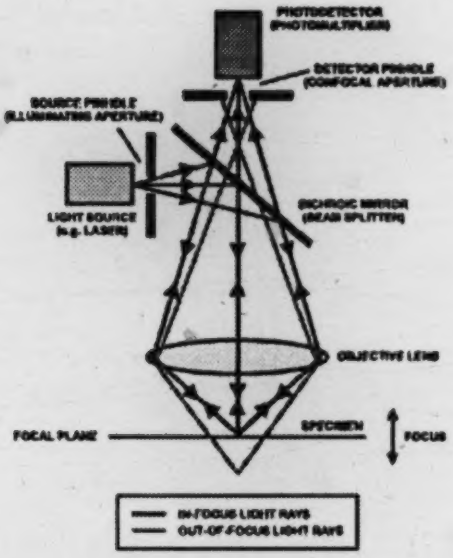

Fig. 1.2.2 Simplified Optics of a CLSM (Ladic, 1999)

1.3. Chemistry of Fluorescent Derivatives of β-Cyclodextrin and a Guest Drug

1.3.1. Fluorescent Dyes

Detection of fluorescence is a powerful analytical technique in biological studies. This method enables the researcher to detect particular components of complex biomolecular assemblies, including living cells, proteins and other biological samples by using fluorescent probes (Haugland *et al.* 1996). One of the attractive advantages of this method is extreme sensitivity. The detection limits are often one to three orders of magnitude lower than those encountered in absorption spectroscopy. Typical detection limits are in the parts per billion range (Skoog *et al.* 1998). Selectivity is another advantage of fluorescence method. Each fluorophore has a unique fluorescence spectrum. The fluorescent probes can selectively be targeted to different biomolecules. For example, fluorescent probes can selectively bind to a receptor, nucleic acid, membrane and different organelles, etc.

4-Chloro-7-nitrobenzofurazan (NBD-Cl, Fig. 1.3.1) is a fluorescence derivatization reagent for amines (Ghosh *et al.* 1968). This reagent can also react with thiols and alcohols and the resulting derivatives have shorter absorption and emission wavelengths than amine derivatives (Birkett *et al.* 1970). NBD-Cl reacts easily with secondary amines and is capable of derivatizing proline and hydroxyproline (Imai *et al.* 1981). NBD-Cl is mostly used as derivatization reagent for chromatographic analysis of amino acids and other low molecular weight amines. For absorption and fluorescence emission spectra, quantum yields of NBD-amine derivatives are mainly dependent on solvent (Lancet *et al.* 1977). The fluorescence intensity of the NBD-amines is much stronger in apolar solvents (Ghosh *et al* 1968). The quantum yield of NBD-amines decreases with increasing

polarity of its environment, thus, the fluorescence quantum yield of NBD-amines in water is low. The absorption and emission wavelengths of NBD-amine derivatives in methanol are around 465 nm and 535 nm, respectively.

Rhodamine B isothiocyanate (Fig. 1.3.1) is a long-wavelength dye. Isothiocyanate form thioureas upon reaction with amine. The absorption and emission wavelengths of Rhodamine B isothiocyanate (in methanol) are around 540 nm and 625 nm, respectively (Haugland, 1996).

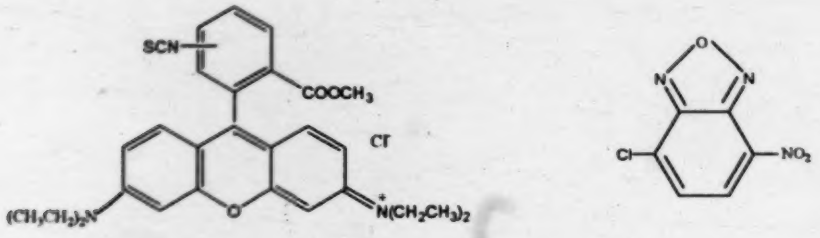

(a) (b)

Fig.1.3.1 Structure of (a) Rhodamine B Isothiocyanate (b) NBD-Cl

1.3.2. Applications of NBD Derivatives

Two fluorescent derivatives of glucose labeled with NBD have been reported. One derivative, 6-(*N*-(7-nitrobenz-2-oxa-1,3-diazol-4-yl)amino)-6-deoxyglucose (6-NBDG, excitation wavelength: 472 nm, emission wavelength: 547 nm in water), was used to assess glucose uptake activity of several cell lines. 6-NBDG was used to study the hexose transport system of human red blood cells. This derivative entered cells via the glucose permease pathway. D-glucose inhibited 6-NBDG uptake in human erythrocytes (Speizer

et al. 1985). Cloherty *et al.* (1995) designed a protocol to determine whether or not 6-NBDG transport in erythrocytes was diffusion-limited. The 6-NBDG content of erythrocytes was measured by fluorescence spectroscopy after 6-NBDG was extracted from cells with 3% perchloric acid. Their results suggested that the uptake of 6-NBDG in erythrocytes was not diffusion-limited because the transport rate of 6-NBDG was not affected by the medium viscosity. The uptake of 6-NBDG by BJAB cells, an EBV-negative B lymphocyte cell line, was studied by flow cytometry (Rauchman *et al.* 1992). The results obtained showed that Glut-2 (one member of a family of Na^+-independent glucose transporters) transfectants enhanced uptake of 6-NBDG. The modification at the C-6 position, however, should inhibit phosphorylation, thus, the generation of glucose-6-phosphate after uptake. A second NBD glucose derivative, 2-(*N*-(7-nitrobenz-2-oxa-1,3-diazol-4-yl)amino)-2-deoxyglucose (2-NBDG, excitation wavelength: 475 nm, emission wavelength: 550 nm in water), was synthesized to allow phosphorylation to occur at C-6 in cells. The uptake activity of 2-NBDG in *Escherichia coli* was assessed by measuring the fluorescence intensity with a spectrofluorometer (Yoshioka *et al.*1996). This kinetic study showed that the uptake of 2-NBDG in *Escherichia coli* cells was inhibited by D-glucose. The localization of 2-NBDG taken up by *Escherichia coli* cells was investigated by fractionating cells into periplasm, membrane and cytoplasm fractions after treatment with 50 μM 2-NBDG. Each fraction was applied on a silica gel sheet and developed with 17:3 acetonitrile:water. A fluorescent spot that had R_f value different from the 2-NBDG was found in the cytoplasm. This result suggested that the new compound was the fluorescent analog of a glucose metabolite, possibly the phosphorylated C-6 derivative (Yoshioka *et al.* 1996).

NBD derivatives were also used to study cell uptake by CLSM. An NBD derivative, 12-(*N*-methyl)-*N*-[(7-nitrobenz-2-oxa-1,3-diaxol-4-yl)amino]octacecanoic acid (12-NBD stearate) was used to visualize and characterize the uptake in single rat hepatocytes (Elsing *et al.* 1995). This intracellular kinetic study showed that fluorescence intensity in the cytoplasm increased linearly within the first 60s, representing unidirectional cellular influx. The extracellular 12-NBD stearate also could enter the nucleus of the rat hepatocytes (Gorski *et al.* 1996). The fluorescence intensity increased faster in the cytoplasm than in the nucleus, however, the rate of 12-NBD stearate uptake in the nucleus increased linearly. A fluorescent conjugate of octreotide (an octapeptide with activity similar to that of somatostatin), 4-nitrobenzo-2-oxa-1,3-diaxol (NBD)-octreotide, was used to study the transport across monolayers of cerebrovascular endothelial cells by CLSM (Jaehde *et al.* 1994). The CLSM images obtained suggested that octreotide transport across the endothelial monolayer occurred primarily via the paracellular route. From the information above, NBD derivatives are suitable to study transport of fluorescent compounds by CLSM.

1.3.3. Fluorescent Cyclodextrin Derivatives

Several detection methods have been employed to detect CyDs, and detection systems, such as refractive index detectors (Koizumi *et al.* 1985), pulsed amperometric detectors (Kubota *et al.* 1992), evaporative light scattering detectors (Caron *et al.* 1997) and fluorescence detectors have been investigated.

Generally, the fluorescence method utilizes the ability of CyDs in forming non-covalent complexes with a fluorescent dye, followed by detection of fluorescence

(Kinsland *et al.* 1984). Two HPLC methods with detection based on inclusion complex formation were developed. One of them involved negative-colorimetric detection after post-column complexation with phenolphthalein (Makela *et al.* 1987). A second HPLC method was based on fluorescence enhancement of a fluorophore (1-naphthol) added to the mobile phase containing CyDs (Reeuwijk *et al.* 1993; Grosse *et al.* 1997).

Fluorescent-labeled CyDs that are currently available include fluorescein labeled β-CyD (Wang *et al.* 1993), dansyl labeled CyD (Ikeda *et al.* 1996; Ueno *et al.* 1990; Nakamura *et al.* 1995), pyrene labeled γ-CyD (Ueno *et al.* 1989; Ueno *et al.* 1990), *p*-(Dimethylamino)benzoyl (DMAB) labeled CyD (Hamasaki *et al.* 1993) and a dansyl labeled CyD dimer (Nakamura *et al.* 1995). The major interest in these fluorescent CyD derivatives was the application to molecular recognition, where complexation of a guest compound could be detected by spectroscopic changes (Kuwabara *et al.* 1994). Most of the fluorescent derivatives of CyDs are mono-modified at C-6 position by the desired fluorophore. CyD hosts usually form intramolecular complexes by including the attached chromophore moiety into their hydrophobic cavities (Kuwabara *et al.* 1994). Upon addition of guest molecules (e.g. 1-adamantanol), displacement of the chromophore from inside of the CyD cavity results in dramatic environmental change from a hydrophobic environment to a polar one. The fluorescence intensity of these fluorescent moieties is sensitive to microenvironmental changes, being stronger in a hydrophobic environment than in a hydrophilic environment. The environmental change can induce remarkable changes in fluorescence spectra of reduction of fluorescence intensity (Hamasaki *et al.* 1993). Based on this phenomenon, fluorescent derivatives of CyDs can be used as a host-guest sensory system for detecting guest compounds which can form inclusion complexes

with CyDs. For example, dansyl labeled β-CyDs exhibited remarkable recognition, showing high sensitivities for ursodeoxycholic acid and chenodeoxycholic acid because the fluorescence intensities decreased dramatically after the addition of these two guest compounds, respectively (Ueno *et al.* 1990).

2. Hypothesis and Objectives

Based on the previous discussion, the following hypotheses were established for the current work:

- CyDs are taken up intracellularly by living cells.
- CLSM is a suitable technique to visualize intracellular uptake and distribution of CyD and their complexes if they are labeled with fluorescent tags.

To test these hypotheses, a number of specific experimental objectives were identified:

- To synthesize mono-labeled fluorescent derivatives of CyDs and a fluorescently labeled guest drug.
- To determine the intracellular uptake of CyDs and their inclusion complexes by CLSM. Specific parameters to be examined include:
    - Effect of temperature on intracellular uptake CyDs
    - Effect of serum proteins on intracellular uptake of CyDs
    - Intracellular uptake kinetics and distribution of CyDs

3. Experimental

3.1. General Materials and Methods

4-Chloro-7-nitrobenzofurazan and adamantanamine hydrochloride were purchased from Lancaster Synthesis Ltd. β-Cyclodextrin, sodium azide, and rhodamine B isothiocyanate (a mixture of isomers) were purchased from Aldrich Co. Preparative C18 bulk packing material (50-105 μm) was purchased from Waters Co. Lipoprotein (from bovine plasma) was purchased from Sigma Co.

A Vortex Genie™ (Scientific Industries, Inc., USA) was used for mixing small samples. An autoflow CO_2 water-jacketed incubator (NUAIRE™ US, USA) was used for normal cell cultures. All fluorescence spectra were obtained using a SPEC FluoroMax® spectrofluorometer (SPEC Industries Inc. USA). A Labconco freeze dryer 3 was used for lyophilization. ^1H NMR spectra were recorded either on a Bruker AM-300 (Dr. Somayaji) or a 500 MHz Varian VXR-500 NMR (Dr. Diakur). The synthesized compounds were characterized by the electrospray mass spectrometry (ES-MS) on a VG Trio-2000 quadrupole mass spectrometer (Fisons, UK). A confocal laser-scanning microscope (CLSM, LEICA MICROSYSTEMS HEIBEIBERG GMBH, Germany) was used for cell uptake experiments.

The hepatoblastoma cell line HepG2 and skin melanoma cell line SK-MEL-24 were gifts from Faculty of Medicine and Dr. Miller's laboratory, respectively. RPMI-1640 (for SK-MEL-24 cell line) medium and MEM (for HepG2 cell line) medium were obtained from the GIBCO BRL Co. Corning® 35 mm/tissue culture dishes (Corning Glass Works, N.Y. USA) were used for cell-uptake experiments using Confocal Laser Scanning Microscopy, and 75 mL cell culture flasks (Corning Costar) were used for the normal cell

culture experiments. Phosphate buffered saline (PBS, pH 7.4) was prepared for rinsing monolayer cells and mounting the cover slip on the microscope slide. This buffer consists of 0.23 g NaH_2PO_4 (anhydrous; 1.9 mM), 1.15 g $NaHPO_4$ (anhydrous; 8.1 mM), 9.00 g NaCl (154 mM) and 1000 mL H_2O (Current Protocols in Immunology).

3.2. Synthesis of Fluorescent Labeled β-Cyclodextrin

Mono-6-deoxy-6-(*p*-toluenesulfonyl)-β-cyclodextrin (β-CyDOTs, 1). Compound **1** was synthesized according to the procedure of Petter *et al.* (1990). β-CyD (6.0 g, 5.3 mmol) was suspended in water (50 mL). NaOH (0.66 g, 16.4 mmol) was dissolved in water (2 mL) and added dropwise over 6 min to the CyD suspension. The suspension became homogeneous and slightly yellowish. *p*-Toluensulfonyl chloride (1.0 g, 5.3 mmol) in acetonitrile (3 mL) was added dropwise over 8 min. A white precipitate formed immediately. The reaction mixture was stirred for 2 h at 23^0C, and then the white precipitate was removed by suction filtration. The filtrate was stored in the refrigerator overnight at 4^0C. A second crop was recovered by suction filtration to provide 0.72 g of **1** as a white solid (11% yield, mw: 1289). ^{1}H NMR (300 MHz, DMSO-d_6) δ 7.74 (d, J = 8.0 Hz, 2H, aromatic), 7.42 (d, J = 8.0 Hz, 2H, aromatic), 5.87-5.58 (m, 14H), 4.82 (br s, 4H), 4.76 (br m, 3H), 4.55-4.13 (m, 6H), 3.74-3.43 (m, 28H), 3.42-3.18 (m, overlaps with HOD), 2.42 (s, 3H).

Crude mono-6-deoxy-6-azido-β-cyclodextrin (β-CyDN_3, 2). Compound **2** was synthesized according to the procedure of Petter *et al.* (1990). Dried β-CyDOTs **1** (536 mg, 0.42 mmol), KI (10 mg, 0.06 mmol) and NaN_3 (270 mg, 4.2 mmol) were dissolved in

dry N, N-dimethylformamide (DMF, 2.5 mL), and the reaction mixture was stirred at 80 ^{0}C for 48 h. The reaction mixture was then cooled to room temperature, and Amberlite MB-3 resin (2 g) was added to remove the salts. After the solution became clear, the reaction mixture was filtered and the resin was rinsed with DMF. Acetone (100 mL) was added to the combined filtrate and the solution was stirred for 0.5 h. The white precipitate was collected by filtration and dried overnight to give 662 mg of crude **2**.

Per-*O*-acetyl-mono-6-deoxy-6-azido-β-cyclodextrin (3) In order to obtain pure **2**, the mixture obtained above was subsequently acetylated according to the procedure published by Tekeo *et al.* (1989). Crude β-CyDN$_3$ **2** (467 mg, 0.40mmol) in acetic anhydride (12 mL) and pyridine (25 mL) was stirred for 72 h at room temperature. The mixture was then coevaporated with toluene to give a brown foam. The product was purified by silica gel column chromatography using 6:4 hexane-acetone as eluent to give 369 mg (46%) of **3** as a white solid: R_f 0.11 (3:2 hexane-acetone); ^{1}H NMR (300 MHz, $CDCl_3$) δ 5.30-5.08 (m, 7H), 5.07-4.90 (m, 7H), 4.78-4.65 (m, 7H), 4.55-4.40 (m, 7H), 4.25-3.94 (m, 14H), 3.74-3.54 (m, 7H), 2.10-1.90 (m, 60H, $COCH_3$).

Mono-6-deoxy-6-azido-β-cyclodextrin (β-CyDN$_3$, 2) from (3). To a solution of compound **3** (350 mg, 0.17 mmol) in methanol (10 mL) was added methanolic sodium methoxide (1 mmol/mL, 0.52 mL) and the reaction was stirred for 72 h at room temperature. During this time a white precipitate had formed. The reaction mixture was neutralized with acetic acid (12 mmol) and the solvents were removed. The resulting residue was purified by silica gel column chromatography using 8:2:2 isopropanol-

ammonium hydroxide-water as eluent to give pure β-CyDN$_3$ **2** (189 mg, 0.16 mmol) in 94 % yield. R_f 0.16 (8:2:2 isopopanol-amonnium hydroxide-water).

Mono-6-deoxy-6-amino--β-cyclodextrin (β-CyDNH$_2$, 4). β-CyDN$_3$ **2** (185 mg, 0.16 mmol) was dissolved in 1:1 water-DMF (4 mL) and triphenylphosphine (183 mg, 0.69 mmol) was added to the solution. THF (2 mL) and methanol (2mL) were then added to dissolve the precipitated triphenylphosphine. The reaction mixture was stirred for 0.5 h at room temperature. During this time, a precipitate again formed, and methanol (1.5 mL) was added to dissolve the precipitate. After 1 h, ammonium hydroxide (28%, 2 mL) was added and the reaction was stirred for 2 h. During this time, additional methanol (1 mL) was added to dissolve the precipitate. After 2 h, ammonia hydroxide (28 %, 3 mL) was added and the reaction was stirred overnight. The solvents were evaporated, and the residue was purified by silica gel column chromatography using 7:2:2 isopropanol-ammonium hydroxide-water as eluent to give 165 mg (91%) of compound **4** as a white solid: R_f 0.11 (8:2:2 isopopanol-water-ammonium hydroxide); ^{1}H NMR (500 MHz, D_2O) δ 5.18-5.10 (m, 7H, H1), 4.0 (t, 7H, H3), 3.98-3.88 (m, 31H, H6, H5), 3.7 (dd, 7H, H2), 3.62 (t, 6H, H4), 3.54 (t, 1H, H4), 3.30 (bd, 1H, H6), 3.06 (dd, 1H, H6); ES-MS in positive ionization mode, calcd *m/z* 1134.01, found *m/z* 1135.7.

4-(*N*-mono-6-deoxy-6-amino-β-cyclodextrin)-7-nitrobenzofuran (NBD-β-CyD, 5). Compound **5** was synthesized according to the procedure of Yoshioka (Yoshioka *et al.* 1996). β-CyDNH$_2$ **4** (15 mg, 13.2 μmol), NBD-Cl (7.9 mg, 39.7 μmol) and $NaHCO_3$ (15 mg, 0.18 mmol) were dissolved in 2:1 water-methanol (1.5 mL). The reaction

mixture was stirred in the dark at room temperature for 15 hours. The solvents were removed and the dark brown residue was purified by C18 reverse phase column chromatography using methanol-water as eluent for gradient elution. The desired product 5 (8 mg) was obtained in 47% yield as a pale yellow solid. R_f 0.27 (7:2:2 isopopanol-water-ammonium hydroxide); ^{1}H NMR (500 MHz, D_2O) δ 8.5 (br s, 1H, aromatic), 6.6 (br s, 1H, aromatic), 5.26 (d, 1H, H1 CyD), 5.18 (d, 2H, H1 CyD), 5.17 (d, 2H, H1 CyD), 5.11 (br s, 1H, H1 CyD), 5.03 (br s, 1H, H1 CyD), 4.29-3.57 (m, 42H); ES-MS in positive ionization mode: In water sodium adduct, calcd *m/z* 1319.08, found *m/z* 1320.6; In 0.05 % aqueous trifluoroacetic acid (TFA), calcd *m/z* 1297.10, found *m/z* 1298.6.

3.3. Study of NBD-β-CyD and its Amantidine Complexes by Fluorescence Spectrofluorometry

NBD-β-CyD and its amantidine complexes were prepared as 0.2 mg/mL aqueous solutions, respectively. Each sample was prepared in triplicate. Emission and excitation spectra of these samples were obtained and are shown in section 4.2.

3.4. Stability of NBD-β-CyD in MEM and RPMI-1640 Media

NBD-β-CyD (2 mg) was added to each of two Corning^R 35 mm/tissue culture dishes that contained 2 mL of RPMI-1640 and MEM medium, respectively. After vortexing, the samples were placed into an incubator at 37^{0}C. Samples were withdrawn and checked by TLC at 10, 15, 30, 45, 60, 75, 90, 105, 120, 135, 150 min. The eluting solvent was 7:2:2 isopropanol- ammonium hydroxide-water.

3.5. Fluorescent Labeled Amantidine

4-(1-*N*-adamantanamino)-7-nitrobenzofuran (NBD-amantidine 6). 1-Adamantanamine hydrochloride (94.3 mg, 0.50 mmol), 4-chloro-7-nitrobenzofurazan (NBD-Cl, 100 mg, 0.50 mmol) and potassium carbonate (200 mg, 1.45 mmol) were dissolved in methanol (3 mL), and the reaction mixture was stirred in the dark for 24 h. The methanol was evaporated and the residue was dissolved in chloroform (50 mL) and washed with water (50 mL, 3 times). The organic solution was evaporated, and the residue was purified by silica gel column chromatography using 6:1 hexane-acetone as eluent to give **6** (27 mg) in 17% yield as an orange solid after lyophilization. R_f 0.71 (1:1 hexane-ethyl acetate); ^{1}H NMR (500 MHz, $CDCl_3$) δ 8.4 (d, 1H, J_d = 8.8 Hz, aromatic), 6.4 (d, 1H, J_d = 8.8 Hz, aromatic), 6.15 (br s, 1H, NH), 2.2 (br s, 3H, adamantane γ-protons), 2.15 (br s, 6H, adamantane α-protons), 1.8 (m, 6H, adamantane β-protons).

Preparation of inclusion complexes

Two methods were explored in an attempt to prepare inclusion complexes of NBD-amantidine with β-CyD. Method one: NBD-amantidine **6** (5.0 mg, 0.016 mmol) and β-CyD (18.2 mg, 0.016 mmol) were added to water (2 mL) and the mixture was stirred in the dark at 60^{0}C for 4 h. Method two: NBD-amamtidine **6** (5.0 mg, 0.016 mmol) was dissolved in methanol (2 mL). β-CyD (18.2 mg, 0.016 mmol) was dissolved in water (2 mL). These two solutions were mixed together and stirred for 4 h. The methanol was evaporated. In both cases, a majority of the NBD-containing solid did not dissolve in water.

NBD-labeled glycine (7). Glycine (10 mg, 0.13 mmol), NBD-Cl (50 mg, 0.25 mmol) and $NaHCO_3$ (33 mg, 0.40 mmol) were dissolved in 2:1 water-methanol (3 mL) and the mixture was stirred in the dark at room temperature for 48 h. After removing the solvents, the reaction mixture was purified by C18 reverse phase column chromatography using water-methanol as eluent. The gradient elution profile was varied from 100% water to 9:1 water-methanol. The product that was obtained was unstable and decomposed to another fluorescent compound within 3-6 h, therefore, was unsuitable for further use.

Rhodamine B isothiocyanate labeled amantidine (8). Three methods were used in an attempt to prepare this material. Method 1: Rhodamine B isothiocyanate (mixture of isomers, 5 mg, 9.3 μmol), 1-adamantanamine hydrochloride (3.5 mg, 18.7 μmol) and $NaHCO_3$ (3.14 mg, 37.4 μmol) were dissolved in methanol (1 mL) and stirred in the dark at room temperature for 24 h. The reaction was checked by TLC using 9:1 chloroform-methanol. Method 2: Rhodamine B isothiocyanate (5 mg, 9.3 μmol) and 1-adamantanamine hydrochloride (3.5 mg, 18.7 μmol) were dissolved in pyridine (1 mL) and stirred in the dark at room temperature for 48 h. Method 3: Rhodamine B isothiocyanate (5 mg, 9.3 μmol) and 1-adamantanamine hydrochloride (3.5 mg, 18.7 μmol) were dissolved in 7:3 methanol-triethylamine (1 mL) and stirred in the dark at room temperature for 48 h. All three methods gave complex mixture.

Rhodamine B isothiocyanate labeled glycine (9). Rhodamine B isothiocyanate (mixture of isomers, 5 mg, 9.3 μmol) and glycine (5 mg, 66.7 μmol) were dissolved in sodium bicarbonate buffer (1 mL, pH 9.0) and stirred in the dark at room temperature for

48 h. The reaction mixture was purified by C18 reverse phase column chromatography using methanol-water as the mobile phase. The gradient elution profile was varied from 100% water to 1:1 water-methanol.

All of the methods used in an attempt to prepare the materials of Rhodamine B isothiocyanate labeled compounds gave complex mixtures because the starting material of Rhodamine B Isothiocyanate was a mixture of isomers. Several byproducts were observed by TLC in the reaction mixture. The purification was not successful and the reaction conditions still need to be optimized.

3.6. Intracellular Uptake of NBD-β-CyD and its Amantidine Inclusion Complexes

Culture of HepG2 and SK-MEL-24 cell lines in flasks. HepG2 and SK-MEL-24 cells were maintained in MEM and RPMI-1640 medium, respectively. Both media contained 10% (v/v) fetal bovine serum (FBS), 1% penicillin/streptomycin (v/v). The cells were grown in 75 mL flasks in an atmosphere of 5% CO_2 and 100% relative humidity, and passaged every 4 days. Confluence was reached within 4-5 days after passage.

The conditions of confocal laser scanning microscopy. The confocal laser scanning microscope system comprised of an argon-krypton laser with major emission lines of 488, 568 and 647 nm. The multiuser/multitasking image analysis software (Leica Lasertechnik GmbH, Heidelberg) was run on a Motorola 68030 CPU workstation, using the OS-9 operating system. All physical parameters related to fluorescence illumination and detection were kept constant in the study. The parameters were as follows: 512 x 512

pixel image, 100/1.32 oil-immersion objective lens, KP 510 short-pass excitation filter, TK 488 beam-splitter; the emission was detected using photomultiplier 2 (PMT 2), LP 515 barrier long-pass filter, photomultiplier gain 752 V, pinhole 75, offset –34.

Sample preparation. Two days prior to the experiment, trypsinized HepG2 and SK-MEL-24 cells (2 mL) were plated in 3 cm petri dishes and grown as a monolayer culture. Solutions of either NBD-β-CyD (0.03 mg/mL) or its amantidine complex (0.03 mg/mL) in different media were prepared. Prior to initiation of the experiment, the 3 cm petri dishes containing the cells were rinsed gently 3 times with PBS (pH=7.4), then medium containing NBD-β-CyD (1 mL) were added to the petri dishes. The incubations were performed in the dark at different temperatures and time intervals. After incubation, the medium was removed, and the petri dishes were gently rinsed 3 times with PBS. A glass coverslip was directly mounted on the surface of the monolayer culture using a small amount of 1:1 PBS-glycerol. Control cultures were prepared identically and the samples and controls were studied by CLSM.

Intracellular uptake experiments. HepG2 and SK-MEL-24 cells were used for the intracellular uptake tests of NBD-β-CyD and its amantidine complex. Each experiment was performed in triplicate, and at least three randomly chosen images were taken from each petri dish. The images were stored on an optical disk for further analysis of fluorescence intensity within regions of interest. For cytoplasm, over fifteen measurements were obtained from the images while for mitochondria, twenty to thirty

measurements were obtained from the images. The number of measurements obtained was dependent on the quality of the image.

1. Temperature dependency: The compounds and their complexes were dissolved in normal media (with FBS), then added to petri dishes containing monolayer cells. After incubating at near 0^0C and 37^0C for 30 min, the samples were studied by CLSM as described previously.

2. Serum protein dependency: The compounds and their complexes were dissolved in normal medium with FBS and medium without FBS, respectively, then added to the petri dishes containing monolayer cells. After incubating at 37^0C for 30 min, the samples were studied by CLSM as described previously.

3. Kinetics study in FBS medium: The compounds and their complexes were dissolved in medium with FBS, then added to the petri dishes containing monolayer cells. After incubating at 37^0C for 0.5, 2, 5, 15, 30, 60 min, the samples were studied by CLSM as described previously.

Kinetics study in the medium without FBS: The compounds and their complexes were dissolved in medium without FBS (containing 0.1% lipoprotein w/v), then added to petri dishes containing monolayer cells. After incubating at 37^0C for 0.5, 2, 5, 15, 30, 60 min, the samples were studied by CLSM as described previously.

Note: In the kinetics study, samples of the same compound in different medium were studied on the same day.

3.7. Data statistical analysis. The profiles of intracellular uptake tests were analyzed with "SigmaPlot" (Version 3.0). Significance of differences between experiments were calculated by Student's t test in Sigma Plot using two-tailed distributions and either a two-sample equal variance (homoscedastic) or a two-sample unequal variance (heteroscedastic) method. In all cases, statistical significance was calculated at the 95% confidence level ($p < 0.05$).

4. Results and Discussion

4.1. Synthesis of Fluorescent Labeled β-CyD

As mentioned previously, the permeation of CyDs across biological membranes, especially cell membranes, is of interest in the application of CyDs as potential drug carriers. In order to use CLSM to investigate the permeation pathways of CyDs across the biological membrane, a fluorescent derivative of CyD was synthesized (Scheme 4.1). The synthesis of 4-(*N*-mono-6-deoxy-6-amino-β-cyclodextrin)-7-nitrobenzofuran **5** (NBD-β-CyD) was initiated by the reaction of β-CyD with one equivalent of *p*-toluensulfonyl chloride in aqueous sodium hydroxide solution (Petter *et al.* 1990). The reaction was stirred at room temperature for 2 h, and then kept at 4^0C overnight. The solid was collected by filtration to give compound **1** (β-CyDOTs) in 11% yield. Compound **1** then was converted to compound **2** (β-$CyDN_3$) by reacting with 10 equivalents of sodium azide in dry *N,N*-dimethylformamide (DMF) containing a catalytic amount of potassium iodide. The resulting crude compound **2** was subsequently acetylated in pyridine-acetic anhydride to provide the totally protected CyD derivative **3**, which was purified by column chromatography over silica gel. Compound **2** strongly interacted with silica gel due to the polar hydroxyl groups, and could not be efficiently purified by silica gel. Compound **3** was deacylated in methanolic sodium methoxide solution to give pure β-$CyDN_3$ **2** in 94% yield. Pure compound **2** was then converted to compound **4** (β-$CyDNH_2$) by reacting with triphenylphosphine (4 equivalents), followed by hydrolysis (Staudinger reaction). The final compound **5** (NBD-β-CyD, yield 47%) was synthesized by reaction of compound **4** with NBD-Cl in the $NaHCO_3$ solution (Yoshioka *et al.* 1996). Column chromatography over silica gel using 7:2:2 isopropanol-water-ammonium

hydroxide was only partially successful because a fluorescent byproduct could not be totally separated from NBD-β-CyD. More efficient separation was achieved on C18 reverse phase column chromatography using gradient elution (methanol-water as solvent). This novel fluorescent derivative of β-CyD was used to study cell uptake using CLSM.

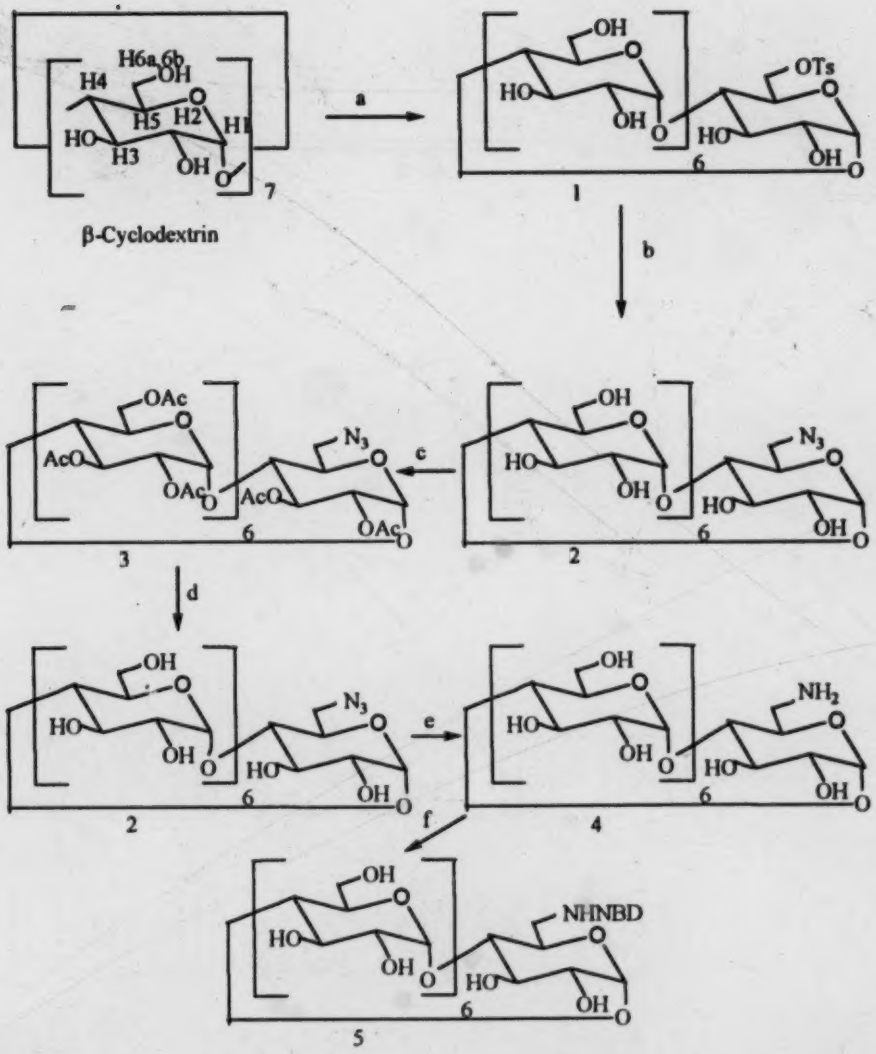

Scheme 4.1 a) NaOH/TsCl, b) KI/NaN_3/DMF, c) Py/Ac_2O, d) NaOMe/MeOH, e) NH_4OH/$(C_6H_5)_3P$/MeOH/H_2O, f) NBD-Cl/$NaHCO_3$/H_2O/MeOH.

4.2. Study of NBD-β-CyD and its Amantidine Complex by Spectrofluorometry

This experiment was designed to compare the fluorescence spectra of NBD-β-CyD to its amantidine inclusion complex. Ikeda *et al.* (1996) reported that some fluorescent CyD derivatives form self inclusion complexes. These authors synthesized a novel fluorescent CyD derivative by insertion of a leucine residue between CyD and the dansyl residue. The leucine, as a connecting arm, was flexible enough to allow the dansyl residue to penetrate deeply into the CyD cavity and form an intramolecular complex. The fluorescence intensity was affected by complex formation with other guest molecules. Both NBD-β-CyD and an inclusion complex between compound **5** (NBD-β-CyD) and amantidine were characterized by fluorescence spectrometry with the hope that there would be a notable difference between the complex and compound **5** alone. It was anticipated that NBD-β-CyD could not form a self-inclusion complex due to the length of spaces and the rigidity of the fluorophore, however, it was not known at the outset if an intermolecular complex could be formed. The covalent bond between β-CyD and the NBD residue is direct and therefore, the NBD residue was not expected to be included into the cavity of NBD-β-CyD in an intramolecular fashion. Little influence would therefore be expected on the fluorescence intensities of NBD-β-CyD, when forming a complex with other guest molecules. The fluorescence spectra of NBD-β-CyD and its amantidine complex are shown in Figure 4.2.1 and Fig. 4.2.2 and the fluorescence intensities are shown in Table 4.2. The maximum emission wavelength of NBD-β-CyD and its amantidine complex was at around 544 nm. The maximum excitation wavelengths were at 307 nm and 313 nm, respectively.

Table 4.2 The fluorescence intensities of NBD-β-CyD and its complex in water

(λ_{Ex} = 406 nm, 0.2 mg/mL)

Compound	Fluorescent intensity (n=3,cps)
NBD-β-CyD	$(3.46 \pm 0.06) \times 10^{6}$ [a]
NBD-β-CyD/amantidine complex	$(3.44 \pm 0.08) \times 10^{6}$

Value = mean ± SEM, [a] no significant difference of fluorescence intensities from amantidine complex ($p>0.05$)

From the data shown in Table 4.2, the fluorescent intensity of NBD-β-CyD showed no significant difference from that of its amantidine complex under the experimental conditions of this CLSM study. Both compound **5** (NBD-β-CyD) and its amantidine complex display the same profile, and no reduction of intensity was found for the latter. The variation of fluorescence intensity contributed by formation of the intramolecular and intermolecular complexes can therefore be disregarded.

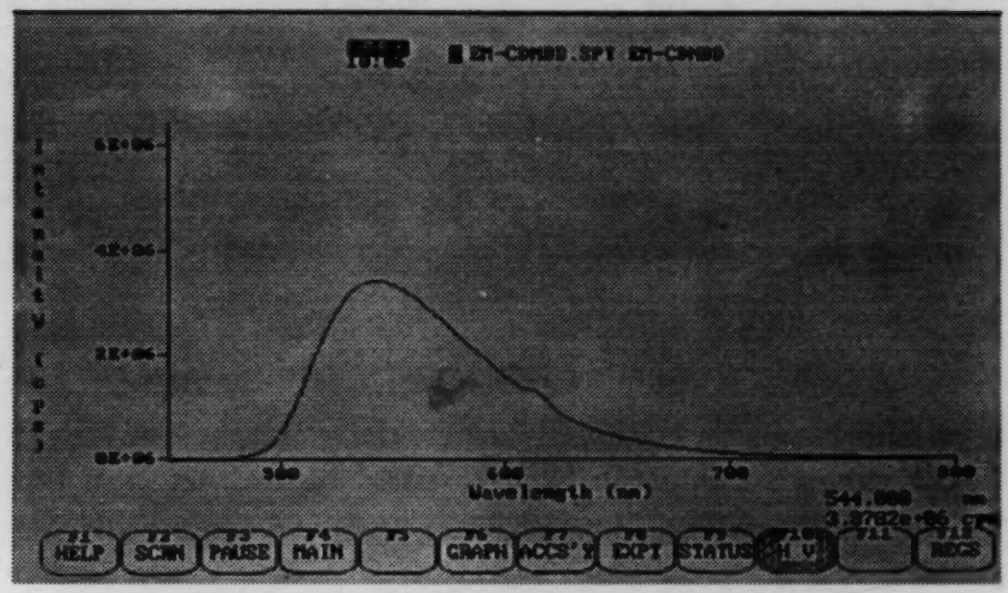

(a)

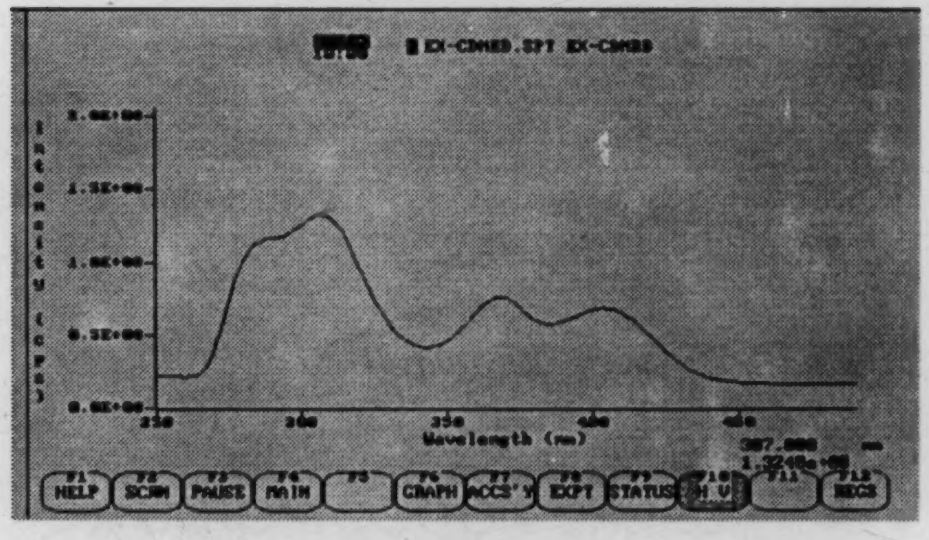

(b)

Fig. 4.2.1 Fluorescence spectra of NBD-β-CyD a) emission spectrum
b) excitation spectrum (0.2mg/mL)

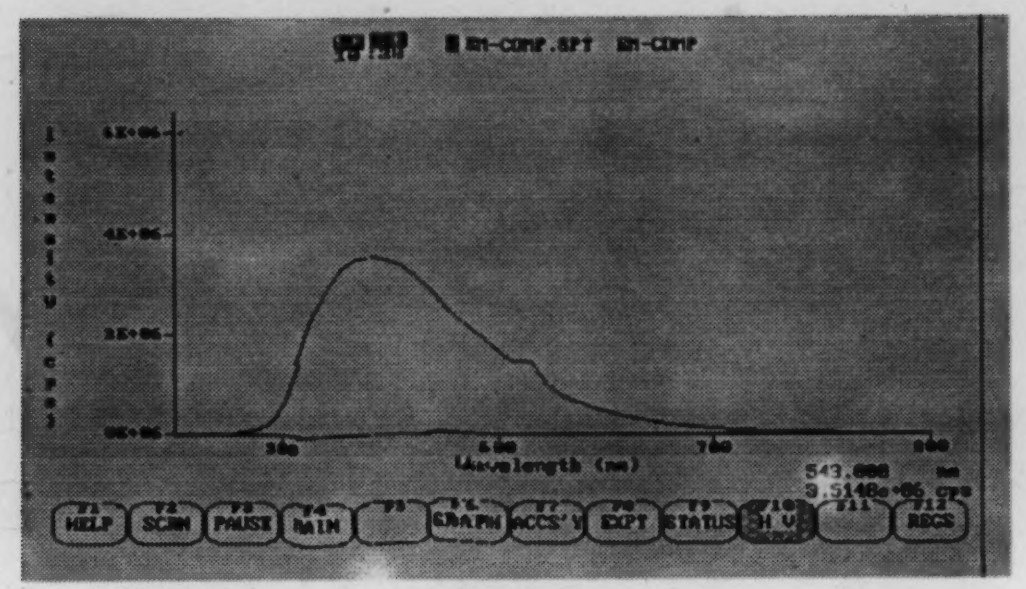

(a)

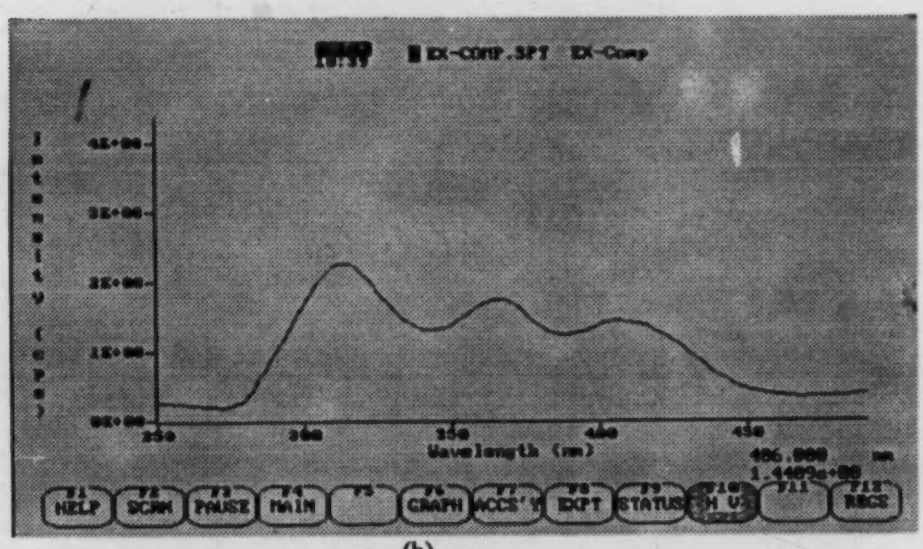

(b)

Fig. 4.2.2 Fluorescence spectra of NBD-β-CyD complex with amantidine
a) emission spectrum b) excitation spectrum (0.2 mg/mL)

4.3. Stability of NBD-β-CyD in MEM and RPMI-1640 Media

The stability of the NBD-β-CyD **5** was an important factor influencing decisions with respect to the experimental design of intracellular uptake and detection by CLSM. During CLSM imaging, the compound should be stable in the medium without any degradation, as fluorescent decomposition products of NBD-β-CyD **5** could lead to incorrect interpretations. If fluorescent decomposition products formed during the incubation period with the cells, the intracellular uptake of both NBD-β-CyD **5** and fluorescent decomposition products could not be differentiated. Our first task was to test, by TLC, the stability of NBD-β-CyD **5** in culture media. NBD-β-CyD **5** was visualized on TLC by long-wavelength light and could also be detected by charring with 5 % methanolic sulfuric acid. NBD-β-CyD (1 mg/mL) was dissolved in both types of culture media described in the experimental section, and incubated at 37^0C. An aliquot was withdrawn and checked at different time intervals (10, 15, 30, 45, 60, 75, 90, 105, 120, 135, 150 min) by TLC, using 7:2:2 isopropanol-water-ammonium hydroxide as the solvent system. Within 1 h, only one fluorescent spot was present (R_f = 0.27), which could also be charred by 5% methanolic sulfuric acid and corresponded to pure NBD-β-CyD **5**. This result indicated that NBD-β-CyD **5** was stable for at least 1 h. In aliquots withdrawn after the first hour, a very faint second fluorescent spot began to appear (R_f = 0.94) which did not char, therefore did not contain carbohydrate. Within the second hour, the fluorescence intensity of this second spot was increased with increasing incubation times. After 2 h, a third spot at $R_f \approx 0.2$ was visible after charring. At 150 min, the intensity of the third spot after charring was ≈25% of the intensity of first spot in the same aliquot. This indicated that the second fluorescence byproduct contained the NBD

residue and the third spot was a β-CyD residue. The conclusion of this experiment was that NBD-β-CyD was stable in both culture media for at least 1 h, but began to slowly degrade after that time.

4.4. Fluorescent Labeled Amantidine (NBD-Amantidine, 6)

The fact that NBD-β-CyD 5 could be taken up by cells led us to postulate that it should be possible to study the intracellular uptake of both the host and guest in a CyD complex if each component contained a fluorescent label. As mentioned in the previous chapter, amantidine readily forms an inclusion complex with β-CyD. In order to study the efficiency of β-CyD/guest systems in the delivery of drug molecules across the membrane, the synthesis of a fluorescent derivative of amantidine was attempted. An inclusion complex with β-CyD could be used in studying intracellular uptake by CLSM. The route of synthesis is shown in Scheme 4.4.

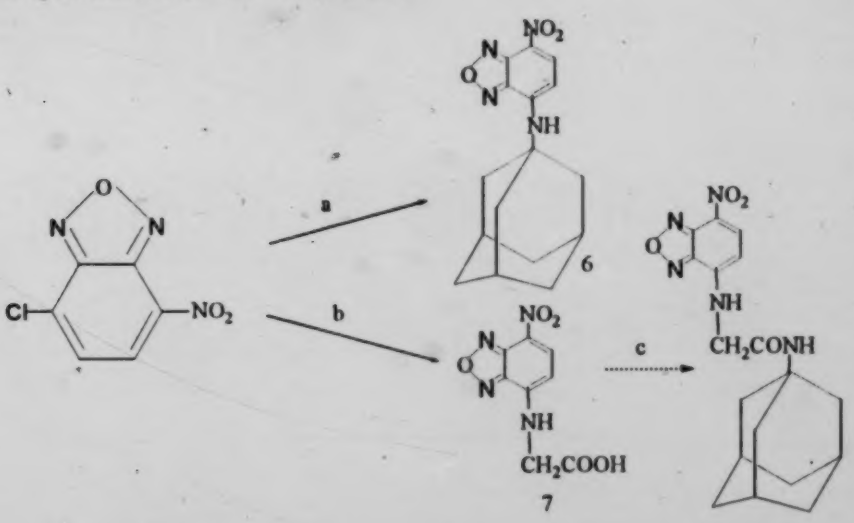

Scheme 4.4 a) NBD-Cl/MeOH/$NaHCO_3$, b) glycine/MeOH/$NaHCO_3$, c) amantidine/DCC

NBD-amantidine **6** was synthesized by reacting adamantanamine hydrochloride with one equivalent of 4-chloro-7-nitrobenzofuruzan in methanol containing potassium carbonate. This reaction gave compound **6** in 17% yield. Two methods were explored to prepare the NBD-amantidine inclusion complex with β-CyD. In both cases, the resulting complexes were not soluble in water or culture medium. An aqueous soluble complex could not be prepared with compound **6.** A second approach, the synthesis of compound **7** was attempted. Glycine would be introduced between amantidine and the NBD residue. The first step was to prepare NBD-labeled glycine **7** (Scheme 4.4). Unfortunately, the NBD-labeled glycine was unstable, therefore it was unsuitable for further use. Compound **7** decomposed within 3-6 h and gave two fluorescent compounds: One was compound **7**, and the other was fluorescent byproduct. The mixture was checked by TLC (65:35:2 chloroform-methanol-water), and the R_f values of **7** and the unknown derivative in this solvent system were 0.5 and 0.6, respectively. Further exploration of providing an NBD-labeled amantidine derivative was abandoned, however, in the future, it might be feasible to prepare a fluorescently labeled guest compound for dual label studies with NBD-admantidine **7**. Instead, focus was shifted to the preparation of a Rhodamine B labeled guest (amantidine).

4.5. Rhodamine B Labeled Amantidine (8, 9)

The preparation of a Rhodamine B derivative of adamantanamine was explored in order to differentiate the signal from NBD-β-CyD **5** by CLSM's dual channel sequential scanning in cell uptake studies. Three approaches to conjugate a fluorescent group to amantidine skeleton were attempted (Scheme 4.5). Each reaction employed a different

base, namely pyridine, sodium bicarbonate, and triethylamine. In each case, a complex mixture was obtained. It is possible that the reaction was inefficient for steric reasons, thus, a short linking arm (glycine) was introduced. In the first step, glycine was conjugated to Rhodomine B via the thiourea linkage. Because of the mixture of isomers of the fluorescent dye, several byproducts were obtained after reaction, and purification of the desired product became challenging. Preliminary results indicate that conjugation does proceed, however, this reaction still needs to be further investigated. Work in this area was abandoned for the time being.

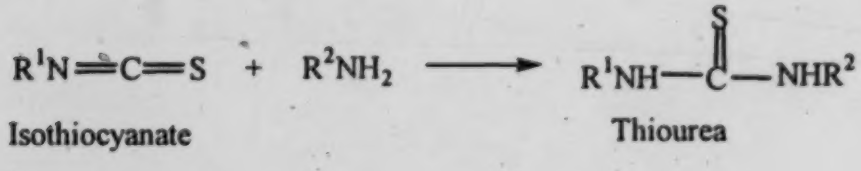

Scheme 4.5 Reaction of a primary amine with an isothiocyanate

4.6. Intracellular Uptake of NBD-β-CyD and its Amantidine Inclusion Complex

4.6.1. Intracellular Distribution of NBD-β-CyD

The inherent fluorescence of NBD-β-CyD permitted direct observation of its intracellular uptake and distribution by confocal laser scanning microscopy. In order to test the intracellular uptake of NBD-β-CyD, two cell lines were selected. The HepG2 cell line was isolated from a liver biopsy with primary hepatoblastoma and hepatocellular carcinoma, with no evidence of the hepatitis B viral genome in the cells (Knowles *et al.* 1980). SK-MEL-24 cell line, a second cell line, was isolated from human melanomas (Guldberg *et al.* 1997).

The intracellular uptake of both NBD-β-CyD and its amantidine inclusion complex was studied. Even though a dual labeled complex was not currently obtained, it is possible that intracellular uptake of a complex and the host alone are dramatically different. The intracellular distribution of NBD-β-CyD and its amantidine inclusion complex is shown in Fig. 4.6.1 and Fig. 4.6.2. There was no observable difference between NBD-β-CyD and its amantidine inclusion complex, and the intracellular distribution was the same in both cell lines (Fig.4.6.2). Absence of nuclear stain in both cell lines indicated that no NBD-β-CyD entered the nuclei of either cell line within the limits of detection of CLSM. The cytoplasm was diffusely and granularly stained by the fluorescent derivative. Uptake of NBD-β-CyD was most prominent in mitochondria, represented by brightly elongated oval and round foci spread within the cytoplasm. The fluorescence intensity of labeled mitochondria was 3-4 times higher than that of the cytoplasm of the cells. Mitochondria occupy a substantial fraction of the cytoplasm in all eucaryotic cells. For example, each liver cell contains 1000-2000 mitochondria, which in total occupy nearly a fifth of the cell volume (Alberts *et al.* 1989). Mitochondrial electron transport-linked reactions provide 95% of the body's energy needs, and utilize over 90% of the available cellular oxygen (Chaudry, 1983). Oxidation of foodstuffs is first used to create an electrochemical proton gradient across the mitochondrial membrane. Positively charged molecules can be electrophoretically distributed into the mitochondrial matrix based on the high negative transmembrane potential of mitochondria (Johnson *et al.* 1980; Grouselle *et al.* 1990). From the structure of NBD-β-CyD, the secondary amine group is easily protonated leading to a positively charged compound. The intensity of this single positively charged ion is low because of the *p*-NO_2 group which is an electron

withdrawing group. The areas selected to integrate fluorescence intensity are shown in Fig. 4.6.1. The fluorescence intensity integrated by CLSM is the mean of intensity of the selected area (relative fluorescence intensity, unit). The net relative fluorescence intensity was obtained from subtracting the fluorescence intensity of control samples that were identically prepared as the other samples.

Fig. 4.6.1 Selected areas for semi-quantification of fluorescence intensity (SK-MEL-24 with NBD-β-CyD incubated 30 min in RPMI-1640 medium)

a b

Fig. 4.6.2 Confocal microscopic images of NBD-β-CyD in a) HepG2 cells in monolayer culture b) SK-MEL-24 cells in monolayer culture

4.6.2. Effect of Temperature on the Intracellular Uptake

The cell membrane encloses a cell, defining the cell's extent and maintaining a substantial difference between its contents and the environment. It is therefore a highly selective filter to control the entry of substances into cells and the exit of waste products. The common structure of cell membranes includes a lipid-protein bilayer held together by non-covalent interactions. The cell membrane is highly impermeable to most polar molecules, and therefore, hydrophilic molecules cross the cell membranes with difficulty. Small water-soluble molecules are usually transported across the cell membranes by specialized transmembrane proteins. For the transport of macromolecules such as proteins, polynucleotides, and polysaccharides across cell membranes, the mechanisms are different from the transport of small molecules, which is mediated by specific transport proteins. The transport of macromolecules and larger particles involves endocytosis and exocytosis. NBD-β-CyD is a highly hydrophilic compound, which is expected to have a low solubility in cell membranes. It is postulated that endocytosis is a possible transport mechanism for NBD-β-CyD and its amantidine complex.

It is possible to determine whether the intracellular uptake of NBD-β-CyD occurs via a specific receptor by studying the influence of temperature on intracellular uptake (Ostlund *et al.* 1996). Cooling is accepted as a practical way of lowering a cell's metabolism to demonstrate the mechanism of passive diffusion into cells. Energy dependent processes such as active transport can not occur near 0^0C (ice bath) because the carrier proteins that are responsible for active transport are tightly coupled to a source of metabolic energy, such as adenosine triphosphate (ATP) hydrolysis, etc (Larsen. *et al.* 1988). In the case of NBD-β-CyD and its amantidine complex, a clear temperature-

dependence was found (Fig. 4.6.3 and Fig. 4.6.4). NBD-β-CyD and its amantidine complex were incubated with both cell lines at 37^{0}C or near 0^{0}C (ice bath) for 30 min in medium containing FBS. The intracellular distribution of NBD-β-CyD at the two different temperatures was found to be similar. Fluorescence accumulated in the cytoplasm and mitochondria, but the fluorescence intensities were clearly temperature-dependent. When NBD-β-CyD and its amantidine complex were incubated with both cell lines, the fluorescence intensities in the mitochondria and cytoplasm at 37^{0}C were significantly ($p<0.01$) higher than near 0^{0}C (ice bath). For the HepG2 cell line, the fluorescence intensities of labeled mitochondria and cytoplasm at 37^{0}C were 4.2 and 1.3 times higher than near 0^{0}C (ice bath), respectively. The fluorescence intensities of mitochondria and cytoplasm in the presence of the amantidine complex at 37^{0}C were 4.6 and 1.5 times higher than near 0^{0}C (ice bath), respectively. For SK-MEL-24 cell line, the fluorescence intensities of mitochondria and cytoplasm in the presence of NBD-β-CyD at 37^{0}C were 8.0 and 3.5 times higher than near 0^{0}C (ice bath), respectively. For the complex, the fluorescence intensities of mitochondria and cytoplasm were 21.8 and 3.0 times higher than near 0^{0}C (ice bath), respectively. These data show that the intracellular uptake of NBD-β-CyD is strongly temperature–dependent, and indicate that NBD-β-CyD does not interact with either cell line via a specific transport carrier. It is therefore postulated that NBD-β-CyD is taken up by cells via endocytosis. When the incubation was near 0^{0}C (ice bath), a small amount of fluorescent derivative crossed the cell membranes and accumulated in mitochondria and cytoplasm, indicating that some passive diffusion of NBD-β-CyD occurred.

From Fig. 4.6.3 and 4.6.4, fluorescence intensities were different between both cell lines in mitochondria and cytoplasm under the same experimental conditions. The fluorescence intensities of mitochondria especially in the SK-MEL-24 cell line were significantly higher than in the HepG2 cell line in the approximate range of 50-85 units. It is difficult to conclude that different uptake mechanisms are present in these two cell lines, but the uptake amount of NBD-β-CyD was different in these two cell lines, especially the uptake by their mitochondria.

Fluorescence intensities differed between NBD-β-CyD and its amantidine complex in mitochondria and cytoplasm respectively under similar experimental conditions and concentrations. The average fluorescence intensities of NBD-β-CyD alone were about 7 units higher than that of the complex in mitochondria in the HepG2 cell line. The result changed when the SK-MEL-24 cell line was tested. The average fluorescence intensities of NBD-β-CyD alone were about 31 units lower than that of the complex in mitochondria. In both cell lines, the average fluorescence intensities in cytoplasm were marginally different between NBD-β-CyD and its amantidine complex (Fig. 4.6.3 and Fig. 4.6.4). The origin of this difference between NBD-β-CyD and its amantidine complex remains to be determined. The free drug (amantidine), NBD-β-CyD and the complex are in equilibrium in solution. The components of the medium, especially albumin, cholesterol and lipoproteins (as mentioned in the previous chapter) can also form complexes with NBD-β-CyD. When NBD-β-CyD and its amantidine complex are incubated with cells, the fluorescent substances accumulating in cells could include free NBD-β-CyD, amantidine complex and protein complexes with NBD-β-CyD. The behavior of intracellular uptake of NBD-β-CyD and its amantidine complex via

endocytosis was also not clear from these experiments. A dual fluorescence approach with a different label on each component of the complex would provide a means to test the intracellular uptake of the inclusion complexes in the future, however, it was not possible to synthesize a suitable fluorescent derivative of amantidine as part of this work at this time.

Several factors influencing the results should be considered, including cell growth conditions of the same cell line on the different days or in different culture flasks, sample handling, CLSM conditions and effects on fluorescence yield (e.g. pH, ionic strength, etc). Although all the parameters of CLSM were constant, the semi-quantitative nature of CLSM should also be considered. The area selected to integrate fluorescence intensity is crucial. The area of the mitochondria is small, and therefore the standard deviation of the mean of the fluorescence intensity was higher than for cytoplasm. The other organelles (e.g. mitochondria, etc) in the cytoplasm will influence the relative fluorescence intensity of cytoplasm integrated by CLSM.

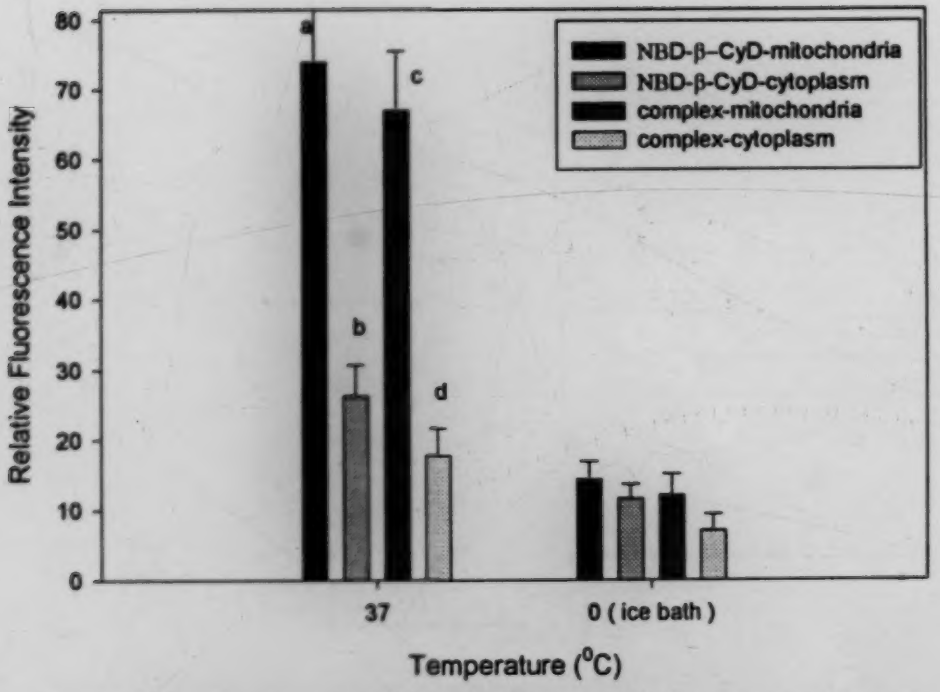

Fig. 4.6.3 Temperature-dependence of intracellular fluorescence intensity after incubation with NBD-β-CyD and NBD-β-CyD/amantidine complex (HepG2, 30 min in normal medium)
[a, b, c, d] Significance of differences from cell uptake near 0°C ($p<0.01$)

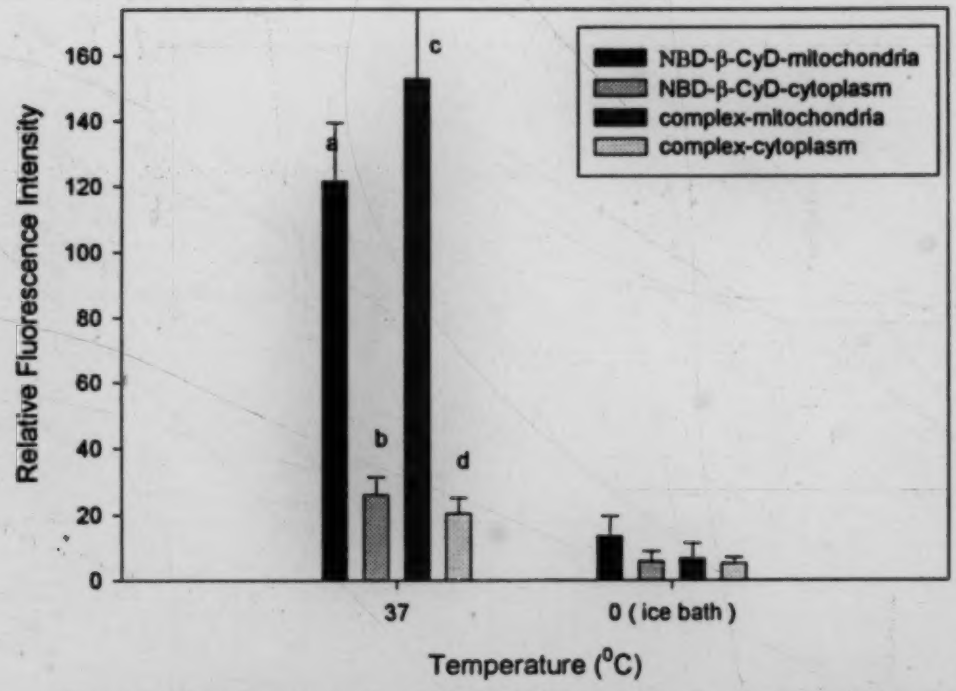

Fig. 4.6.4 Temperature-dependence of intracellular fluorescence intensity after incubation with NBD-β-CyD and NBD-β–CyD/amantidine complex (SKMEL-24, 30 min in normal medium)
[a, b, c, d] Significance of differences from cell uptake near 0^0C ($p<0.01$)

4.6.3. Effect of Serum Proteins on Intracellular Uptake

As mentioned previously, CyDs can form inclusion complexes with cholesterol in the cell membrane. CyDs can also form complexes with accessible hydrophobic regions in lipoproteins and consequently precipitate them. The following experiment was designed to test the effect of proteins in FBS on the intracellular uptake of NBD-β-CyD. NBD-β-CyD and its amantidine complex were added to the medium with or without FBS, and incubated with each cell line for 30 min at 37 ^{0}C.

The results obtained showed that the intracellular distribution of NBD-β-CyD was independent of the presence or absence of FBS in the medium. The fluorescent derivatives accumulated in the mitochondria and cytoplasm as before. Fig. 4.6.5 shows that when the fluorescent substances were incubated with the HepG2 cell line the average fluorescence intensities of NBD-β-CyD and its complex incubated in the two types of media varied from 56 to 74 units for stained mitochondria and from 18 to 26 units for stained cytoplasm. Fig. 4.6.6 shows that the average fluorescence intensities of NBD-β-CyD and its amantidine complex incubated in the two types of media varied from 121 to 161 for stained mitochondria and from 20 to 36 units for stained cytoplasm, when fluorescent substances were incubated with SK-MEL-24 cell line. From the results of the t-test shown in Fig. 4.6.5 and 4.6.6, the values of the average fluorescence intensities accumulated in mitochondria and cytoplasm of NBD-β-CyD alone have significant differences ($p<0.01$) between both media in both cell lines. For the complex, only the average fluorescence intensities accumulated in cytoplasm in SK-MEL-24 cells have significant differences ($p<0.01$) between both media. The average fluorescence intensities accumulated in mitochondria in both cell lines have no significant difference between

both media. For the HepG2 cell line, the fluorescence intensities of NBD-β-CyD and its amantidine complex accumulated in mitochondria were 74 and 67 units in medium with FBS, respectively, 56 and 73 units in medium without FBS, respectively. For the SK-MEL-24 cell line, the fluorescence intensities of NBD-β-CyD and its amantidine complex accumulated in mitochondria were 122 and 153 units in medium with FBS, respectively, 161 and 148 units in medium without FBS, respectively. There appears to be only a slight difference in the fluorescence intensities accumulated in mitochondria and cytoplasm. The intensity ranges of each sample should be considered as equal when the factors influencing the experimental results mentioned previously are considered. The difference of average fluorescence intensity in same cell line was only marginally different. The conclusion from these experiments is that serum proteins only marginally influence the intracellular uptake in mitochondria and cytoplasm. Therefore one cannot conclude that proteins in FBS have a significant effect on the intracellular uptake of NBD-β-CyD and its amantidine complex. The data indicate that proteins including albumin and lipoprotein did not play an important role in the process of intracellular uptake of NBD-β-CyD and its amantidine complex.

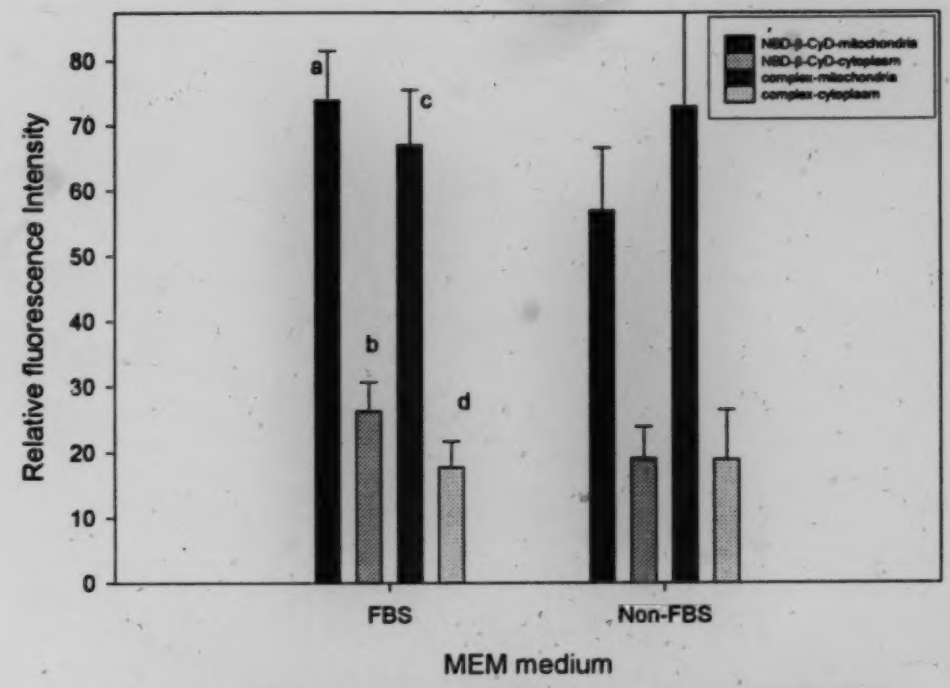

Fig. 4.6.5 Effect of serum proteins on cell uptake of intracellular fluorescence intensity after incubation with NBD-β-CyD and NBD-β-CyD/amantidine complex (HepG2, 30 min)
[a, b] significant difference from medium without FBS ($p<0.01$)
[c, d] no significant difference from medium without FBS ($p_c = 0.0649$, $p_d = 0.5729$)

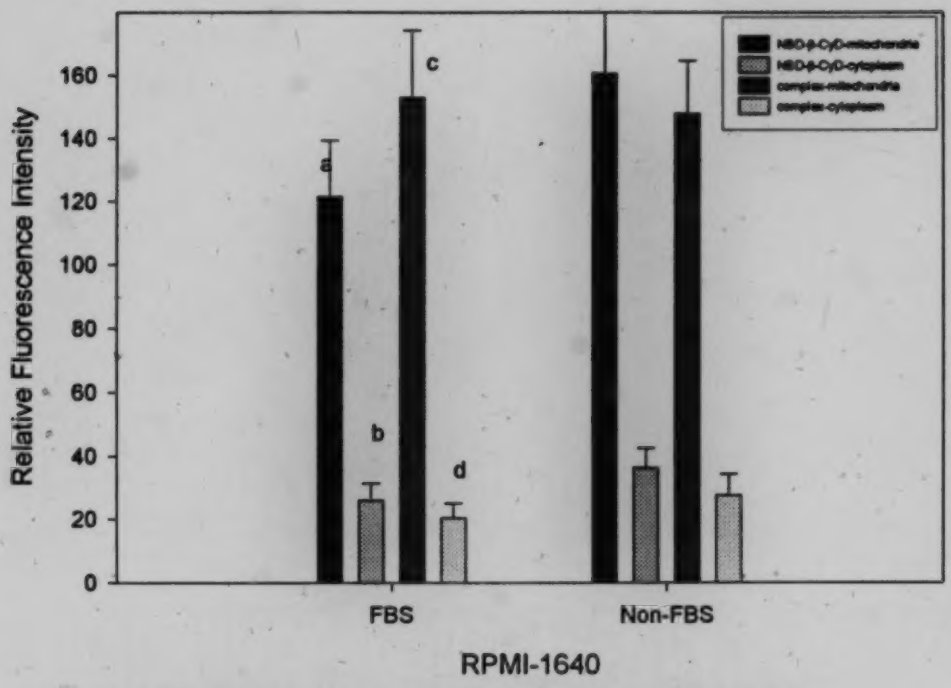

Fig. 4.6.6 Effect of serum proteins on cell uptake of intracellular fluorescence intensity after incubation with NBD-β-CyD and NBD-β-CyD/amantidine complex (SK-MEL-24, 30 min)
[a, b, d] significant difference from medium without FBS ($p<0.01$)
[c] no dignificant difference from medium without FBS ($p_c = 0.4053$)

4.6.4. Intracellular Uptake Kinetics Study

The intracellular uptake kinetics of NBD-β-CyD and its amantidine complex in HepG2 and SK-MEL-24 cell lines was studied by semi-quantitative CLSM. This technique involves integration of the fluorescence intensity of selected regions stained by fluorescence. The experiments were performed in two different media: one containing FBS and the other containing lipoprotein alone. The lipoprotein used in the experiments was obtained from bovine plasma, and contained 90.8% high density lipoprotein (HDL) along with 8.1% low density lipoprotein (LDL). High density lipoproteins, as physiological cholesterol acceptors, can induce the efflux of cholesterol from cells (Kilsdonk *et al*. 1995). Cholesterol is an integral membrane component, thus the efflux of cholesterol results in enhanced fluidity and permeability of the cell membrane and therefore affects cell membrane function. Mammalian cell cholesterol is derived by receptor-mediated uptake of low-density lipoproteins. From the information above, lipoproteins may potentially affect the intracellular uptake of NBD-β-CyD and its amantidine complex.

From the results obtained the intracellular distribution was found to be the same as the previous experiments in both cell lines when cells were incubated with NBD-β-CyD and its amantidine complex which were dissolved in different media (one medium with FBS, the other medium with lipoprotein alone). The intracellular distribution was found to be localized primarily in mitochondria and cytoplasm, and no nuclear uptake was observed within the limits of detection of CLSM. The efflux of cholesterol would be a result when the cells were in a medium containing a high concentration of HDL (0.1 % w/v). Figure 4.6.7 - 4.6.10 show the uptake kinetics as determined by CLSM. The

profiles in four figures show that the linear uptake phase occurs between 5 min to 60 min. The regression fitting data are shown in Table 4.6.1.

Table 4.6.1 The regression data of kinetic studies of intracellular fluorescence intensity after incubation with NBD-β-CyD and NBD-β-CyD/amantidine complex

	Equations	R^2	Line (name)
Fig. 4.6.7 (HepG2, mitochondria)	Y =1.74 x + 38.67	0.9969	NBD-β-CyD-FBS
	Y = 1.27x + 36.10	0.9695	NBD-β-CyD-lipoprotein
	Y = 1.51x + 90.81	0.9641	Complex-FBS
	Y = 1.71x + 67.75	0.9602	Complex-lipoprotein
Fig. 4.6.8 (HepG2, cytoplasm)	Y = 0.58x + 4.39	0.9874	NBD-β-CyD-FBS
	Y = 0.46x + 2.30	0.9652	NBD-β-CyD-lipoprotein
	Y = 0.62x + 11.18	0.9361	Complex-FBS
	Y = 0.53x + 8.02	0.9214	Complex-lipoprotein
Fig. 4.6.9 (SK-MEL-24, mitochondria)	Y = 1.77x +55.52	0.9141	NBD-β-CyD-FBS
	Y = 1.56x + 31.95	0.9746	NBD-β-CyD-lipoprotein
	Y = 1.81x + 105.43	0.5769	Complex-FBS
	Y = 2.17x + 61.33	0.8533	Complex-lipoprotein
Fig. 4.6.10 (SK-MEL-24, cytoplasm)	Y = 0.72x +1.17	0.9535	NBD-β-CyD-FBS
	Y = 0.53x + 2.84	0.9764	NBD-β-CyD-lipoprotein
	Y = 0.59x + 18.74	0.8724	Complex-FBS
	Y = 0.69x + 9.46	0.9019	Complex-lipoprotein

An intracellular uptake test for the same preparation (NBD-β-CyD or its amantidine complex) in both types of medium was performed on the same day using the cells from the same source. Each figure shows the uptake profile in mitochondria or cytoplasm in each cell lin, which provides a means to determine differences between the influence of lipoproteins and FBS in the intracellular uptake of NBD-β-CyD and its amantidine complex. The various subcellular organelles demonstrated their unique uptake kinetic profiles. Fluorescence accumulation in mitochondria increased rapidly within the first 5 min, and then gradually increased during the next 45 min. The accumulation of fluorescence in cytoplasm increased gradually over the entire experimental time (1 h).

The profiles of the uptake kinetics in four figures indicate similar trends. Due to the high standard deviation for each time point, especially for mitochondria in both cell lines, one cannot conclude with certainty that there are significant differences between medium containing lipoproteins alone and containing FBS. The profiles in the four figures show that the intracellular uptake in mitochondria and cytoplasm was only marginally different between the medium containing lipoprotein and the medium containing FBS when considering the standard deviation. There are two possibilities for this slight difference. One possibility is that the function of the cell membranes was altered by the efflux of cholesterol induced by the presence of HDL, and the uptake of the fluorescent derivative was therefore decreased. The other possibility was that the intracellular uptake was decreased by precipitation of NBD-β-CyD by lipoproteins.

The data indicate that the amount of intracellular uptake for the amantidine complex was slightly higher than NBD-β-CyD alone when they were incubated with monolayer cells. However, for the relatively higher standard deviation, this difference is not statistically significant. From the results in previous sections, no significant difference in uptake between NBD-β-CyD and its amantidine complex was found when the experiment was finished on the same day. From the results obtained one cannot conclude that the intracellular uptake kinetics of NBD-β-CyD differs significantly from its amantidine complex.

The complex can dissociate to free drug and NBD-β-CyD, and free NBD-β-CyD can form complexes with proteins in the medium, thus leading to indistinguishable results. Only NBD-β-CyD can give fluorescence signal. The intracellular uptake behavior of NBD-β-CyD and its complexes with amantidine or proteins is not clear. It was not

possible to identify differences in the intracellular uptake of NBD-β-CyD and its amantidine complex under the experimental conditions employed. To solve this problem, a fluorescently labeled guest is required. A dual-labeled complex will give more information regarding the relative distribution of NBD-β-CyD and its amantidine complex.

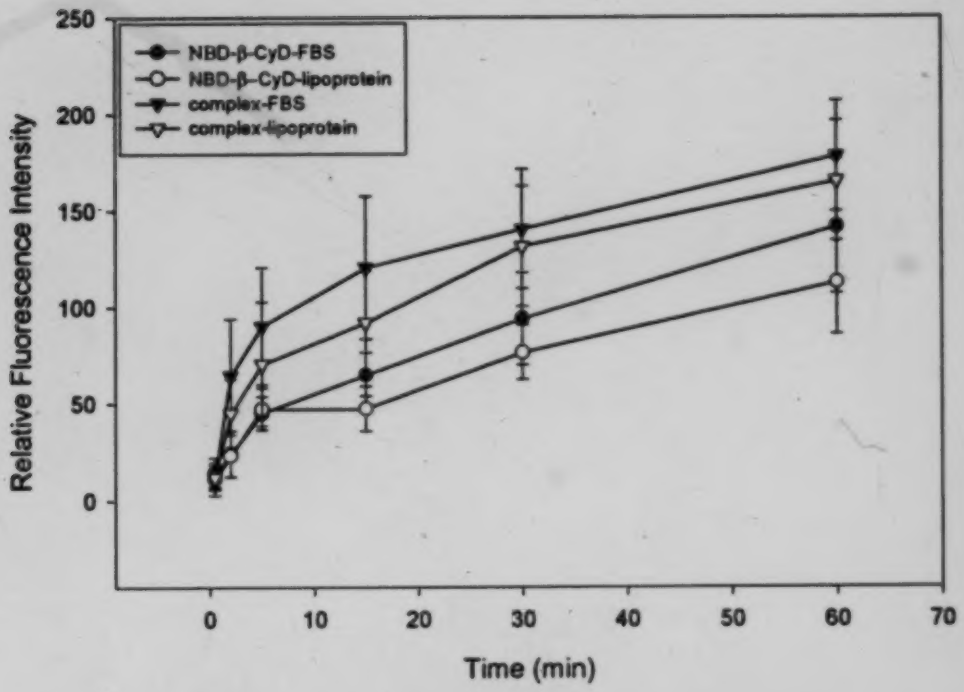

Fig. 4.6.7 Kinetics study of cell uptake of intracellular fluorescence intensity after incubation with NBD-β-CyD and NBD-β-CyD/amantidine complex (HepG2, Fluorescence in mitochondria)

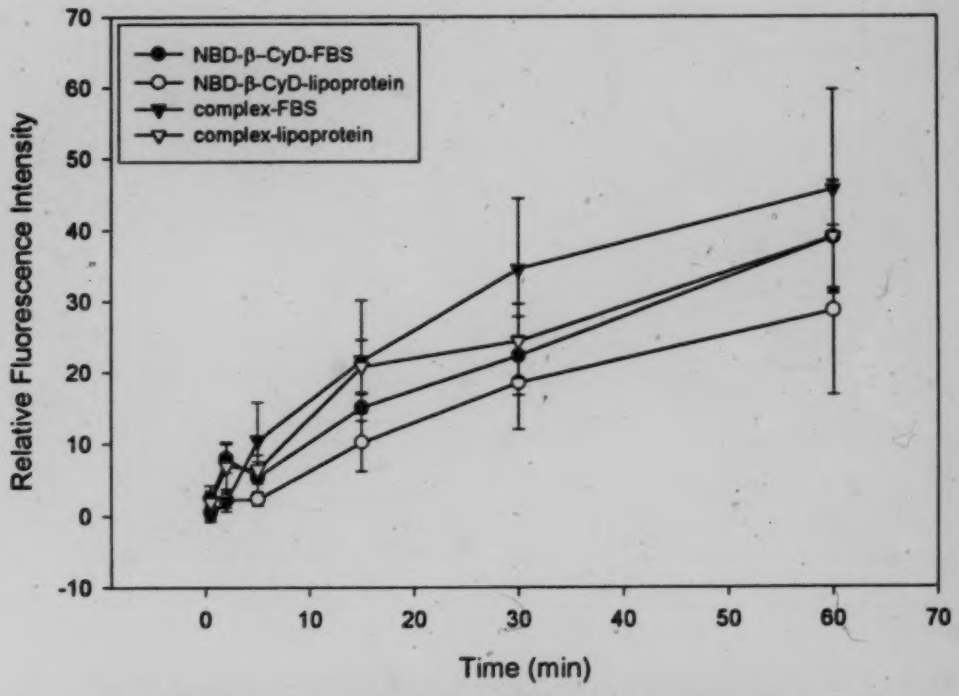

Fig. 4.6.8 Kinetics study of cell uptake of intracellular fluorescence intensity after incubation with NBD-β-CyD and NBD-β-CyD/amantidine complex (HepG2, Fluorescence in cytoplasm)

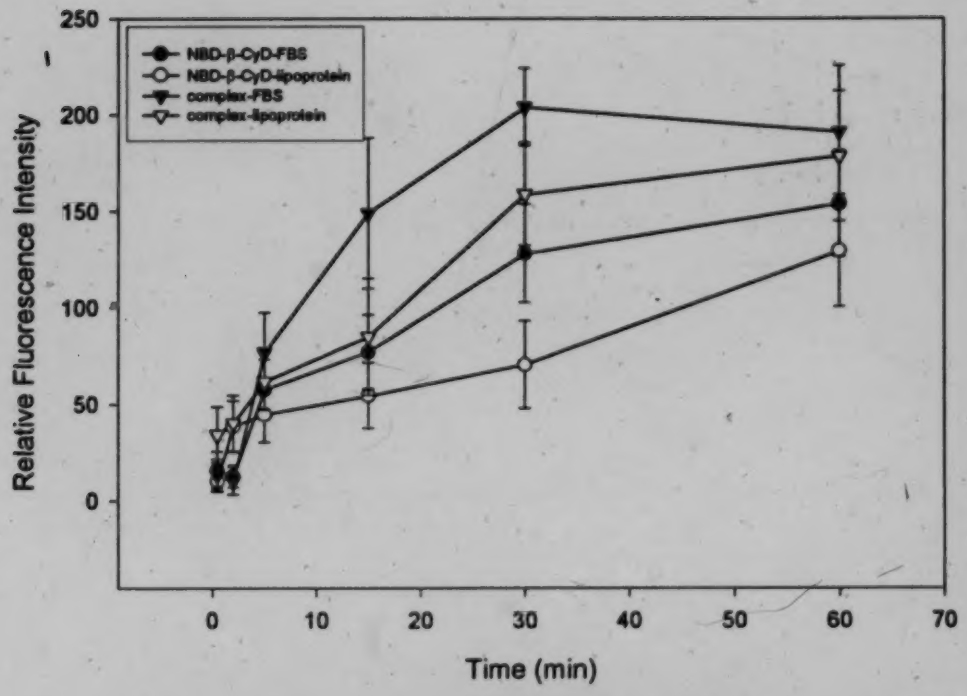

Fig. 4.6.9 Kinetics study of cell uptake of intracellular fluorescence intensity after incubation with NBD-β-CyD and NBD-β-CyD/amantidine complex (SK-MEL-24, Fluorescence in mitochondria)

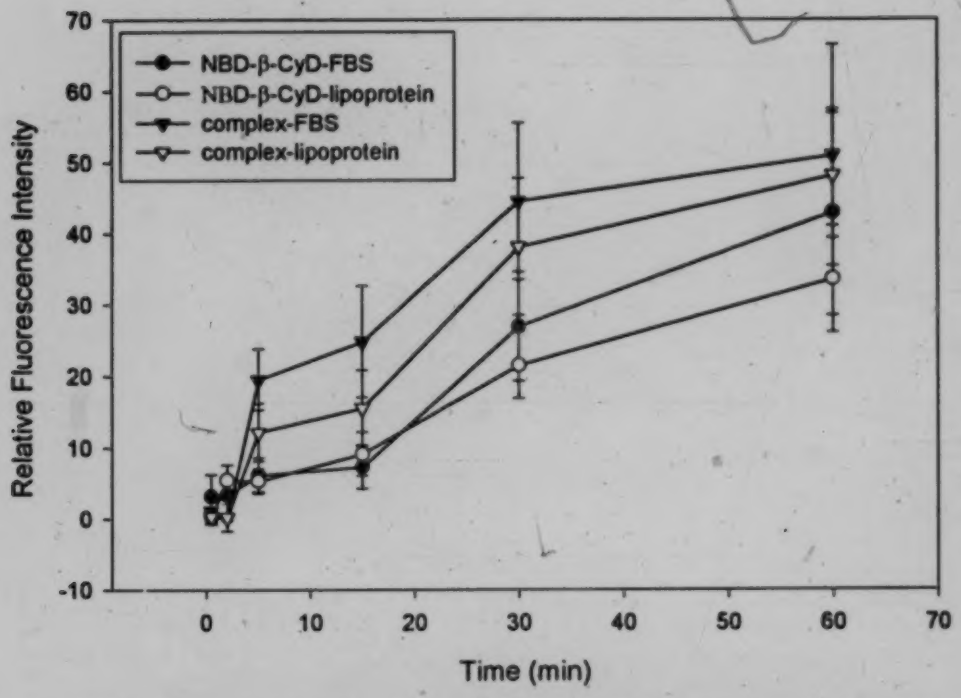

Fig. 4.6.10 Kinetics study of cell uptake of intracellular fluorescence intensity after incubation with NBD-β-CyD and NBD-β-CyD/amantidine complex(SK-MEL-24, Fluorescence in cytoplasm)

5. Conclusion and Future Work

Confocal laser scanning microscopy is a powerful tool that can be employed to visualize and detect the permeation of fluorescently labeled compounds across cell membranes. Intracellular uptake kinetics can be observed using CLSM to detect and quantify the area of interest in the individual cell, such as mitochondria, lysosome, cytoplasm, etc. The results obtained from CLSM provide spatial information, but is only semi-quantitative.

4-Chloro-7-nitrobenzofurazan (NBD-Cl) is a suitable fluorescence derivatization reagent for the amine groups and also is a reasonable candidate for intracellular uptake studies using CLSM. Mono-NBD labeled β-CyD (NBD-β-CyD) gives a fluorescence signal strong enough to be visualized and detected by CLSM. Although there is a potential for fluorescence quenching, no problems in this regard were found when the experiment is finished relatively quickly (within 1 h).

The novel compound, NBD-β-CyD was found to be useful for study of intracellular uptake in the two cell lines used in this study (HepG2 and SK-MEL-24). The experimental data showed that NBD-β-CyD was taken up by the two cell lines, indicating that the β-CyD may also be taken up by these two cell lines. Intracellular distribution was demonstrated in mitochondria and cytoplasm and no nuclear uptake was observed. The intracellular uptake of NBD-β-CyD and its amantidine complex showed a clear temperature-dependence, and thus, passive diffusion occurred near 0^0C (ice bath). No significant effect of serum proteins on intracellular uptake of NBD-β-CyD and its amantidine complex was found. From the kinetics study, the linear phase of intracellular uptake was between 5 – 60 min in mitochondria and cytoplasm. One cannot conclude that

there are significant differences of intracellular uptake when NBD-β-CyD and its amantidine complex were incubated with cells in the medium containing FBS or medium containing lipoproteins alone.

Comparing the results of intracellular uptake of NBD-β-CyD to its amantidine complex, it is difficult to determine the significant difference between them. A fluorescently labeled guest compound (amantidine) will be required to resolve this issue. A dual-labeled complex will give more useful information on intracellular uptake using the feature of dual channel scanning of CLSM, since the intracellular uptake of a dual-labeled complex can be differentiated by CLSM. The results obtained from these experiments will provide more accurate information than detecting the single labeled complex.

Before CyDs can be applied as drug carriers in the pharmaceutical field, their delivery mechanisms should be thoroughly studied. The work in this project represents a preliminary stage in the elucidation delivery mechanisms of CyDs and some progress has been made towards elucidating the delivery with CyDs as drug carriers. The phenomenon of the intracellular uptake of CyDs and their inclusion complexes has been studied by CLSM. Further studies on the delivery mechanisms of CyDs and their inclusion complexes across cell membranes need to be studied intensively.

Chapter 3

ELECTROSPRAY MASS SPECTROMETRY STUDIES OF NITRO-FUNCTIONALIZED DRUGS AND CYCLODEXTRIN-DRUG COMPLEXES

1. Introduction

1.1. Background

Mass spectrometry (MS) has recently become more popular as an analytical technique because of the rapid development of the instruments themselves, the introduction of powerful computer controlled systems, and computer-aided interpretation of data (Clench *et al.* 1992). Generally, a mass spectrometer can be divided into three basic components: the inlet, the ion source and the mass analyzer. In order to minimize the collision between air molecules and ions formed in the ion source, the analyzer is always under vacuum. The inlet and ion source (the means of delivering the sample) are combined together in many modern instruments (VG Trio-200 User Guide).

Several types of ionization sources are available for mass spectrometers, including electron ionization (EI), chemical ionization (CI), direct chemical ionization (DCI) and field ionization (FI). In all types of mass spectrometers, sample ions have to be in the vapor phase to pass through the mass analyzer. For involatile and thermally labile compounds, gas phase ions can not be easily produced without applying heat. Although direct interface between GC and MS is straightforward, major problems were encountered during interfacing mass spectrometry with liquid chromatography because of the limitations in ionization technology. Most of the samples suitable for separation by liquid chromatography are involatile or thermally labile or both. New techniques

involving ionization and the inlet systems now allow MS to be coupled directly to liquid chromatography. One technique called "LC-MS" is now used to inject a sample solution directly into a mass spectrometer. LC-MS can be applied to intact proteins, involatile and thermally labile compounds. Several types of LC-MS exist, including thermospray (TSP), plasmaspray (PSP), electrospray (ES) and dynamic FAB (dy-FAB) (Clench *et al.* 1992). ES is of particular interest to characterizing host/guest complexes.

1.2. Electrospray Mass

Electrospray mass spectrometry (ES-MS) was originally pioneered in the 1980s and its applications have rapidly expanded since then. ES-MS can be applied to analyze high-molecular-weight compounds including proteins, nucleotides, and synthetic polymers. ES-MS has three features that differ from those of other mass-spectrometric techniques: (i) multiply charged ions of high molecular-weight compounds can be analyzed, (ii) since analyte ions are already present in solution prior to introduction to the mass spectrometer, the ES-MS can be coupled with many types of separation techniques such as liquid chromatography including HPLC, and electrophoresis, and (iii) ES-MS technique is a mild, soft ionization technique. This technique can measure protonated (or deprotonated) molecular ions of polar, non-volatile, high molecular mass and themolabile compounds. The study of the non-covalent interactions between molecules becomes possible because ES-MS is a soft ionization technique (Cole *et al.* 1997; Abian, 1999). Part of the objective of this project was to study non-covalent CyD complexes by ES-MS.

1.3. The Overall Mechanism of the Ionization Process of ES-MS

Ion production in ES-MS involves three major steps: (i) charged droplets at the end of a capillary tip are produced by high electronic potentials (Fig. 1.3 a), (ii) solvent evaporation from the surface of the charged droplets is accomplished by a drying gas and heat, and leads to the formation of smaller droplets (Fig. 1.3 b), and (iii) ions are emitted from the surface of the resulting highly charged small droplet when the Coulombic repulsion exceeds the surface tension of the droplet (VG ORGANIC Back to Basics).

ES-MS affords ion transfer of a wide variety of ions dissolved in a wide variety of solvents. These ions can be generated by proton transfer (positive ion formation) or abstraction (negative ion formation). Ions include singly and multiply charged inorganic ions (Li^+, Na^+, Ca^{2+} etc.), anions of inorganic and organic acids (NO_3^-, SO_4^-, etc.), singly and multiply protonated organic bases (amines, peptides, etc.) and singly and multiply deprotonated organic acids or organophosphates (nucleic acids, etc.). Almost any polar solvent can be used, including protic solvents like water, methanol and ethanol or aprotic solvents like acetonitrile, acetone and dimethylsulfoxide (Kebarle *et al.* 1997). ES-MS is currently the softest MS technique available. The gas-phase ions detected by the mass analyzer are most likely the same as in the solution.

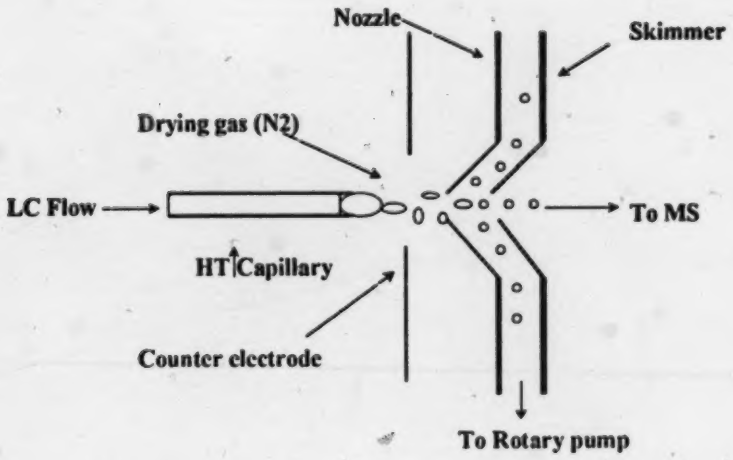

(a)

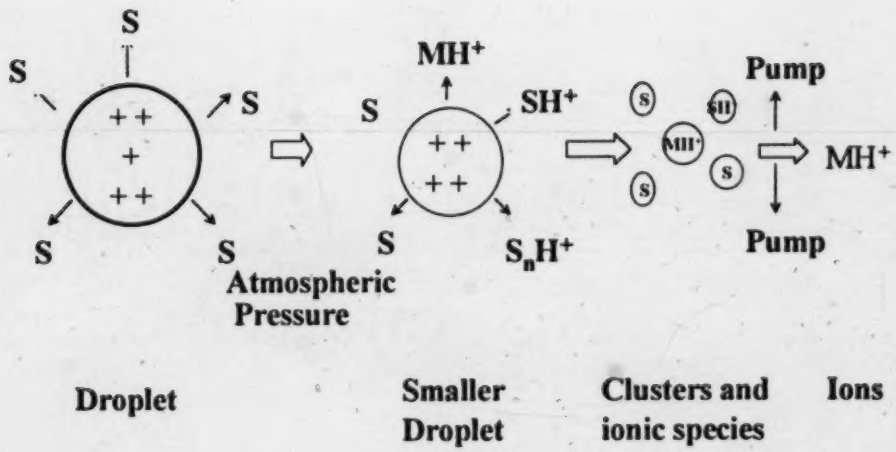

(b)

Figure 1.3 (a) Schematic diagram of an electrospray inlet/ion source (b) Ion formation (S: solvent, SH^+: solvent ion, S_nH^+: solvent cluster ion, MH^+: sample ion, VG ORGANIC Back to Basics)

1.4. Applications of ES-MS

ES-MS of peptides and proteins. ES-MS is an important tool for the analysis of proteins and peptides. Combined, ES-MS and matrix-assisted laser desorption/ionization (MALDI) spectrometry can be used to detect nearly all proteins (Roepstorff, 1992). Several aspects of protein structure, especially primary structure, can be directly studied by ES-MS. The information obtained includes molecular-weight, sequence, metal-binding stoichiometry, and subunit stoichiometry of the quaternary structure (Loo *et al.* 1997; Burlingame, 1996; Meyer *et al.* 1993; Ashton *et al.* 1994).

ES-MS of nucleic acids and their constituents. Nucleic acids and their constituents were at one time a considerable challenge for analysis by mass spectrometry because of their polarity and thermal lability (Crain, 1997). The introduction of ES-MS and MALDI made possible the analysis of oligonucleotides and intact nucleic acids. The separation and analysis of nucleosides is important in the biochemistry. These compounds play the important roles in cell metabolism, hormonal control and genetic activity. Typically, analysis of these compounds involves the use of conventional liquid chromatography combined with UV detection. The information provided by UV detection is based upon column retention time by comparison to a standard. This information alone is not enough because it lacks accurate chemical information. ES-MS can be coupled with liquid chromatography and is a powerful tool suitable for analysis of the nucleic acids. This technique alone provides additional qualitative information by indicating the analyte's molecular weight with its retention time (Banks *et al.* 1994).

ES-MS of drug metabolism and pharmacokinetics. Drug metabolism occurs when a drug is biotransformed into its metabolites, which are chemically different from the parent drugs. A new drug with enhanced pharmacological activities can be usefully developed when the impact of drug metabolism is understood. Therefore, both parent drugs and their metabolites in the body should be characterized and quantified after administration (Poon *et al.* 1997). Several methods of measuring the concentrations of drugs and drug metabolites in tissues and blood over a period of time are available, such as GC-MS, LC-UV, LC with radioactivity detection, and radioimmunoassay. LC-UV and LC-radioactivity are not specific, and analytes should possess UV chromophores or radioactivity, respectively. The technique of combining ES-MS with liquid chromatography has several advantages over other methods including reliability, structural specificity for many compounds, and minimal sample handling. LC-MS has become one of the more powerful methods for studying drug metabolism and pharmacokinetics (Poon *et al.* 1997; Henion *et al.* 1993; Williams *et al.* 1999).

ES-MS of carbohydrates and lipids. As a structural analysis technique, ES-MS is useful to study the structure of carbohydrate and lipids because processes such as desalting a sample, adding organic solvents and applying heat to evaporate solvents do not affect the mass analysis of carbohydrates and lipids. Carbohydrates and lipids include oligosaccharides and their simple glycosides, neutral as well as acidic glycosphingolipids (gangliosides, phospholipids etc.) (Ohashi, 1997).

ES-MS of non-covalent binding (host-guest) complexes. In general, host-guest interactions involve the establishment of multiple non-covalent bonds between a large and geometrically concave organic molecule (the host) and a simpler organic or inorganic molecule or ion (guest). Several analytical techniques for the detection of non-covalent complexes are available including UV, HPLC, capillary electrophoresis, NMR spectroscopy, and mass spectrometry. Mass spectrometry, especially Fast Atom Bombardment (FAB) and Electrospray have become important investigative tools for studying host-guest molecular complexes because of their soft ionization process (Vincenti *et al.* 1995). Direct application of MS in studying non-covalent interactions in proteins has recently been reviewed (Smith *et al.* 1994).

Several research groups have carried out work on the analysis of CyD complexes. The inclusion complexes of β-CyD with three amino acids (Gly, Phe and Trp) as ions in the gas phase were detectable by ES-MS (Sun *et al.* 1998). Ionspray mass (IS-MS) which is a pneumatically assisted ES-MS, was also used to detect inclusion complexes of the parent CyDs and their derivatives such as DM-β-CyD, HP-β-CyD, etc. with different prodrugs such as ephedrin, terfernadine, *etc* (Selva *et al.* 1995; Walker *et al.* 1998; Bakhtiar *et al.* 1997). The conclusion from these studies was that the gaseous protonated 1:1 inclusion complex of CyDs with guest molecules transferred by ES-MS from solutions to the mass analyzer should be at host-guest associations. In the above cases, ammonium acetate buffer was used to ensure that the complexes were protonated due to lack of readily ionizable groups in CyDs for positive ionization mode of detection. It was shown that free CyDs, which were detected as protonated species, were present, indicating that the complex and the free components were in equilibrium in the matrix

solution. From the information obtained, ES-MS has become a powerful tool for non-covalent complex analysis. For our work two CyD host-guest complexes were prepared: β-CyD with amantidine and NBD-β-CyD, described previously, with amantidine in order to test whether the ES-MS is suitable for detecting these non-covalent complexes. In the future, this technique could be applied for microanalysis of CyDs and their complexes in biological matrices.

1.5. Investigation of Nitro-Functionalized Drugs Using ES-MS

Nitro-functionalized drugs. Some research groups had studied nitro-functionalized compounds using mass spectrometry. 2,4-Dinitroimidazole (*m/z* 158) was detected using electron ionization mass spectrometry and the compound was characterized by the presence of a parent molecular ion at *m/z* 158 along with other primary product ions oringinating from nitro substituents such as $NO_2^{\cdot}$ (m/z 46), $NO^{\cdot}$ (m/z 30), etc. The formation of the $NO_2^{\cdot}$ ion involves a primary fragmentation pathway involved in C-NO_2 bond cleavage (Minier *et al.* 1996). Tandem mass spectrometry has been employed to detect the nitro-functionalized compounds such as nitro-substituted polynuclear aromatic hydrocarbons (nitro-PAH). These nitro compounds were identified by their molecular ions and the presence of the $NO_2^{\cdot}$ (m/z 46) ions (Henderson *et al.* 1982; Vincenti *et al.* 1996). Recently, ES-MS was applied to analyze the nitro-functionalized derivative of tyrosine (Bordini *et al.* 1999). Tyrosine can react with peroxynitrite ($ONOO^{-}$) which transforms it into 3-nitrotyrosine. The NO_2 group is introduced on the aromatic ring. The resulting 3-nitrotyrosine gave strong signal when detected by ES-MS, however, this amino acid possesses two ionizable groups. During our work, we found that ions of

certain nitro-functionalized compounds without carboxy- or amino-substituents could also readily be detected by ES-MS. In order to further investigate this application of ES-MS, a group of compounds (Fig. 4.1.1) was selected for ES-MS analysis. A common structural feature is that they all possess a nitro functional group. Within this group of compounds, IAZA, flutamide, and hydroxyflutamide were of particular interest in our laboratory.

Flutamide, a non-steroidal fluorine-containing nitrophenyl propamide, is used for its antiandrogen effects in prostate cancer chemotherapy. It acts as a prodrug that is rapidly metabolized to 2-hydroxyflutamide, which is its active metabolite. The pharmacokinetic profile of these two drugs has been previously studied in our laboratory using HPLC with UV detection (Zuo *et al.* 1996; Zuo, 1998).

Iodoazomycin arabinoside (IAZA) has been developed as a hypoxia imaging agent in our group (Mannan *et al.* 1991). It is a sugar-coupled 2-nitroimidazole and is a promising bioreductive probe for quantifying hypoxia as it is selectively trapped in hypoxic cells. Tissue hypoxia is caused by many disease conditions including cancer, diabetes, and cardiac insufficiencies. It is advantageous to develop a non-invasive diagnostic imaging agent, such as radioiodinated IAZA (^{123}I-IAZA), which could distinguish viable but hypoxic tissue from dead tissue. The pharmacokinetic profile of IAZA has recently been studied using an extremely sensitive high-performance liquid chromatography assay of the radiolabelled parent drug (Stypinski *et al.* 1998). To complement the sensitive radioassay, ES-MS was applied for the analysis of IAZA as this technique would potentially assist in both the chemical characterization and quantification of this hypoxia agent for *in vivo* work.

After becoming familiar with collection of ES-MS data of these selected drug compounds, the experience gained in this regard was then applied to more complex applications. The interest would then be shifted to the study of the non-covalent complexes, such as the CyD host/guest system.

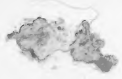

2. Hypothesis and Objectives

Based on the above information, the following hypotheses were established:

- Cyclodextrin (CyD) can be detected in the form of a charged host-guest complex.
- Electrospray mass spectrometry (ES-MS) can be used for studying these non-covalent charged molecular complexes in solution.

The first objective was to familiarize ourselves with the application of ES-MS in difficult single molecule circumstances. The objective of this project was to develop a method of analyzing cyclodextrin/guest complexes. The method should be able to detect and characterize such drugs and complexes at low level.

3. Experimental

3.1. General Materials and Methods

Adamantanamine hydrochloride was purchased from Lancaster Synthesis Ltd. β-Cyclodextrin, nifedipine, 4-nitroimidaxole, medronidaxole, 5-nitro-8-hydroxyquinoline, chloramphenicol, sodium azide, sodium iodide and cesium iodide were purchased from Aldrich Co. 2-Hydroxyflutamide was a gift from Schering Plough (NJ, USA). HPLC grade distilled water and acetonitrile used for the Electrospray Mass Spectrometry (ES-MS) study were purchased from Fisher Scientific Co. IAZA was synthesized by Dr. Piyush Kumar. 4-(*N*-mono-6-deoxy-6-amino-β-cyclodextrin)-7-nitrobenzofuran (NBD-β-CyD) was synthesized as described earlier (Chapter 2, Section 3.2). Disposable Waters™ SepPak cartridges (C18, Classic, Short body) were purchased from Waters Co. Horse heart myoglobin was purchased from Sigma Co.

A Vortex Genie™ (Scientific Industries, Inc., USA) was used for mixing small samples. Centrifugations were performed in an IEC HN-SII centrifuge (DAMON/IEC DIVISION, USA). A Dubnoff Metabolic Shaking Incubator (Precision Scientific Co., USA) was used to incubate compounds with plasma at 37^0C.

A Labconco Freeze Dryer 3 was used for lyophylization. ES-MS studies were performed on either a VG Trio-2000 quadrupole ES-MS (Data were acquired using MassLynx (version 2.0) software.) or a Micromass ZabSpec Hybrid Sector-TOF ES-MS (Data were acquired using the OPUS software package on a Digital Alpha station with the VMS operating system in Deptartment of Chemistry).

Male Sprague-Dawley rats (250-350 g) purchased from the University of Alberta Animal Services Facility were used for obtaining blood samples. All animal studies were

handled in accordance with Guidelines of the Canadian Council on Animal Care, with review and approval of the experimental protocols by the University of Alberta Health Sciences Animal Welfare Committee.

3.2. ES-MS Studies of Nitro-Functionalized Compounds

Calibration

Two calibration standards were used for the calibration of the electrospray mass spectrometer in the negative ionization mode: (1) a sugar mixture was prepared by dissolving corn syrup (1 mg) in 0.5 mL, maltose (1 mg) in 5 mL, raffinose (1 mg) in 12 mL, and maltotetraose (1mg) in 12 mL 50% aqueous acetonitrile, and then combining equal volumes of these four solutions (VG Trio-200 user guide); (2) a sodium iodide solution was prepared by dissolving sodium iodide at 2 μg/μL in 50:50 isopropanol-water, and adding cesium iodide to a concentration 0.05 μg/μL (VG Trio-200 user guide).

One calibration standard was used for the calibration of the electrospray mass spectrometer in the positive ionization mode: horse heart myoglobin, consisting of 10 μL of a solution of approximately 20 pmol/μL of horse heart myoglobin in 50% aqueous acetonitrile with 1% formic acid added (VG Trio-200 user guide).

The Parameters of mass spectrometry

Sample introduction into the electrospray ionization (ESI) source was accomplished by direct injection. The injection volume was 10 μL, and the delivery solvent was 1:1 water-acetonitrile at a flow-rate of 10-30 μL/min. The source parameters consisted of a

temperature of 79^{0}C, a cone voltage of 35-45 V, a capillary potential 3.55 kV, a nebulizer nitrogen flow-rate of 20 L/h and a nitrogen bath gas flow-rate of 300 L/h.

ES-MS of nitro-functionalized compounds

Nifedipine, 4-nitroimidaxole, IAZA, flutamide, hydroxyflutamide, medronidaxole, 5-nitro-8-hydroxyquinoline, chloramphenicol base, 2-methyl-5-nitroimidazole, 2-hydroxy-5-nitrobenzaldehyde, 3-nitro-1,2,3-triazole, 2 (*p*-nitrophenyl)ethyl *O*-(β-*D*-galactopyranosyl)-(1→4)-β-D-glucopyranoside (JD1-199L, from Dr. Diakur) and 5-bromo-3-nitro-1,2,4-triazole were dissolved in 1:1 water-acetonitrile (0.2-0.5 mg/mL). After vortex mixing, each sample was analyzed by ES-MS in either positive ionization mode or negative ionization mode under the conditions described previously. The results and spectra are discussed in section 4.1.

ES-MS detection limit for four nitro-functionalized drugs

Each of the four drugs (IAZA, flutamide, hydroxyflutamide and nifedipine) were dissolved in the mobile phase (1:1 water-acetonitrile), then serially diluted and the samples were detected by ES-MS in the negative ionization mode. The injection volume was 10 μL. The spectra and limit of detection (LOD) are discussed in section 4.2.

To confirm the results for IAZA, an independent analysis was carried out on the more powerful ZabSpec mass spectrometer in the Department of Chemistry. Three concentrations in 1:1 water:acetonitrile (10 μg/mL, 1 μg/mL, and 0.1 μg/mL) and two concentrations in plasma (10 μg/mL, 0.1 μg/mL) were selected for detection by ES-MS in both the positive and negative ionization modes.

Rat blood samples were obtained by heart puncture and collected in heparinized tubes. The blood was centrifuged at 8000 rpm for 15 min, and the obrained plasma was used for the following experiments. Plasma was stored at -20^0C until use.

Samples of IAZA in plasma were prepared as follows: IAZA from stock solution in saline was mixed *in vitro* with rat plasma (total volume 500 μL), then shaken over 1 h in the Dubnoff Metabolic Shaking Incubator at 37^0C. SepPak cartridges were conditioned with methanol (4 mL), then washed with HPLC grade water (5 mL). The samples were loaded onto the cartridges and eluted first with water (4 mL), to wash out the majority of contaminants, followed by methanol (3 mL) to elute the partly purified analyte. The methanol fractions were collected, evaporated to dryness, and then reconstituted with the mobile phase (1:1 water-acetonitrile) (Stypinski *et al.* 1998).

3.3. Characterization of β-Cyclodextrin Complexes with ES-MS

Preparation of inclusion complexes

Amantidine (3.0 mg, 15.9 μmol) and β-cyclodextrin (18 mg, 15.9 μmol) were dissolved in HPLC grade water (2 mL). After stirring and equilibration for 4 hours at room temperature, the water was removed by lyophilization. Amantidine (2.9 mg, 15.4 μmol) and NBD-β-CyD (20 mg, 15.4 μmol) were dissolved in 1.5 mL HPLC grade water. After stirring and equilibration for 4 hours at room temperature, the water was removed by lyophilization.

Sample preparation and detection by ES-MS

Amantidine inclusion complexes with NBD-β-CyD (1 mg/mL) and with β-CyD (5 mg/mL, 2.5 mg/mL, 1.25mg/mL and 0.625 mg/mL) were prepared in aqueous solution. Each sample (10 μL) was introduced into ES-MS by direct injection in the positive ionization mode. The delivery solvent was HPLC grade water (Section 4.3), and the source parameters were those described previously. The amantidine β-CyD inclusion complex (5 mg/mL) was also analyzed at different cone voltages (5,15, 50, 60, 70 V) (Section 4.3).

4. Results and Discussion

4.1. ES-MS Studies of Nitro-Functionalized Drugs

Thirteen nitro-functionalized compounds (Figure 4.1.1) were selected to be analyzed by ES-MS. Analysis was carried out in either the positive or negative ionization mode. The delivery solvent was 1:1 water-acetonitrile and conditions are described in the Experimental Section (Section 3.2). The molecular ions were detected in either the positive or negative ionization mode as their corresponding $[M+H]^+$ and $[M-H]^-$ ions, respectively. The results are summarized in Table 4.1.1. Several compounds, such as 5-nitro-8-hydroxyquinoline, metronidazole, 2-methyl-5-nitroimidazole could be detected in both ionization modes. Certain compounds, such as flutamide and hydroxyflutamide, could be detected only in the negative ionization mode. As mentioned previously, ES-MS requires that analyte ions are present in solution before they are transferred to the gas phase. The mechanism of the ionization processes of these compounds in both ionization modes was not clear. The following discussion suggests a possible ionization mechanism for the one of the compounds, iodoazomycin arabinoside.

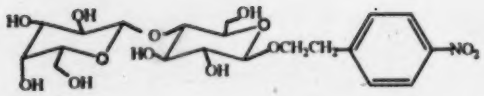

1. JD1-199L

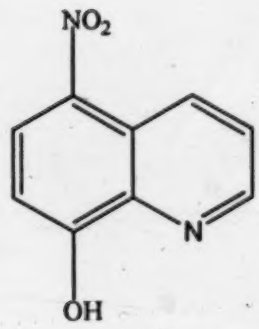

2. 5-nitro-8-hydroxyquinoline

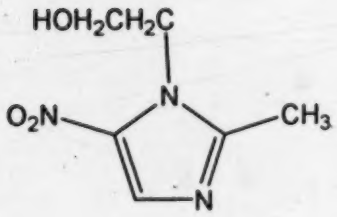

3. Metronidazole

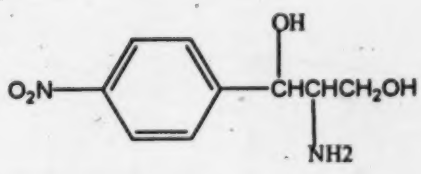

4. Chloramphenicol Base

Figure 4.1.1 Structures of nitro-functionalized compounds (part I)

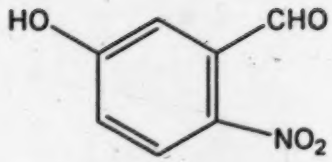

5. 5-hydroxy-2-nitrobenzaldehyde

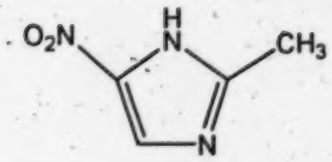

6. 2-methyl-5-nitroimidazole

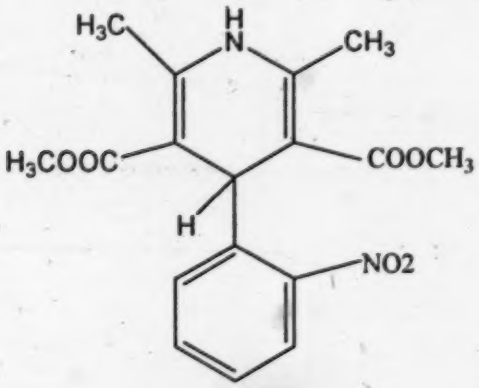

7. Nifedipine

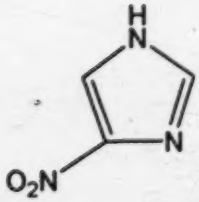

8. 4-nitroimidazole

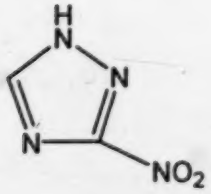

9. 3-nitro-1,2,4 triazole

Figure 4.1.1 Structures of nitro-functionalized compounds (part II)

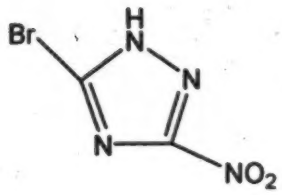

10. 5-bromo-3-nitro-1,2,4 triazole

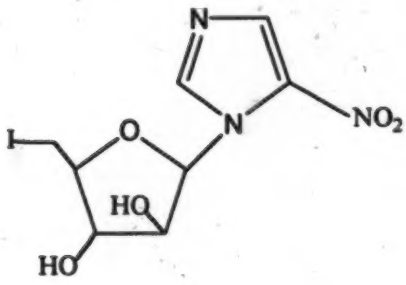

11. Iodoazomycin arabinoside (IAZA)

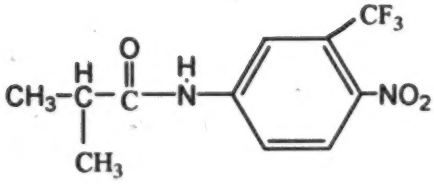

12. Flutamide

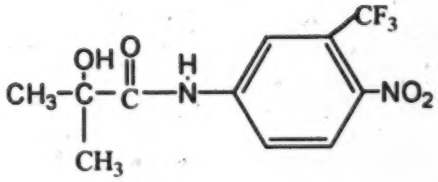

13. Hydroxyflutamide

Figure 4.1.1 Structures of nitro-functionalized compounds (part III)

Table 4.1.1 ES-MS spectra (either positive (ES^+) or negative (ES^-) ionization mode) of the thirteen compounds in Figure 4.1.1

COMPOUNDS	FORMULA	M.W.	Signals in ES^- $[M-H]^-$	Signals in ES^+ $[M+H]^+$
1. JD1-199L	$C_{20}H_{29}O_{13}N$	491.45	490.4	
2. 5-nitro-8-hydroxyquinoline	$C_9H_6N_2O_3$	190.16	189.1	191.1
3. Metronidazole	$C_6H_9N_3O_3$	171.16	170.1	172.1
4. Chloramphenicol Base	$C_9H_{12}N_2O_4$	212.21	211.2	213.2
5. 5-hydroxy-2-nitrobenzaldehyde	$C_7H_5NO_4$	167.12	166.1	
6. 2-methyl-5-nitroimidazole	$C_4H_5N_3O_2$	127.10	126.1	128.2
7. Nifedipine	$C_{17}H_{18}N_2O_6$	346.34	345.1	347.2
8. 4-nitroimidazole	$C_3H_3N_3O_2$	113.08	113.0	114.5
9. 3-nitro-1,2,4 triazole	$C_2H_2N_4O_2$	114.06	113.1	
10. 5-bromo-3-nitro-1,2,4 triazole	$C_2HN_4O_2Br$	192.96	191.0&193.0	
11. IAZA	$C_8H_{10}N_3O_5I$	354.97	353.9	355.9
12. Flutamide	$C_{11}H_{11}F_3N_2O_4$	276.22	275.1	
13. Hydroxyflutamide	$C_{11}H_{11}F_3N_2O_3$	292.21	291.2	

Figure 4.1.3 shows the spectra obtained for IAZA in solution (1:1 acetonitrile-water) in both ionization modes, which was characterized by two peaks at m/z 355.9 and 377.9 in the positive ionization mode due to $[M+H]^+$ and $[M+Na]^+$ ions, respectively. The peak at m/z 710.9 is possibly due to the formation of a dimer $[M(M+H)^+]$ (cald *m/z* 710.8). IAZA was also characterized by a peak at m/z 353.9 in the negative ionization mode due to $[M-H]^-$ ions. The possible ionization mechanism of IAZA in both ionization modes is shown in Figure 4.1.2.

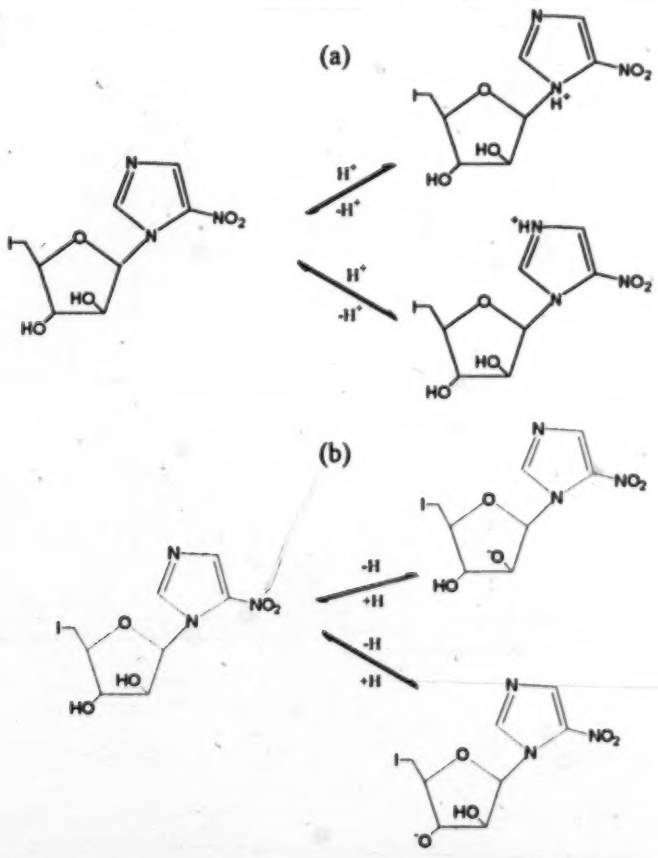

Figure 4.1.2 Possible ionization mechanisms for IAZA (a) IAZA in positive ionization mode (b) IAZA in negative ionization mode.

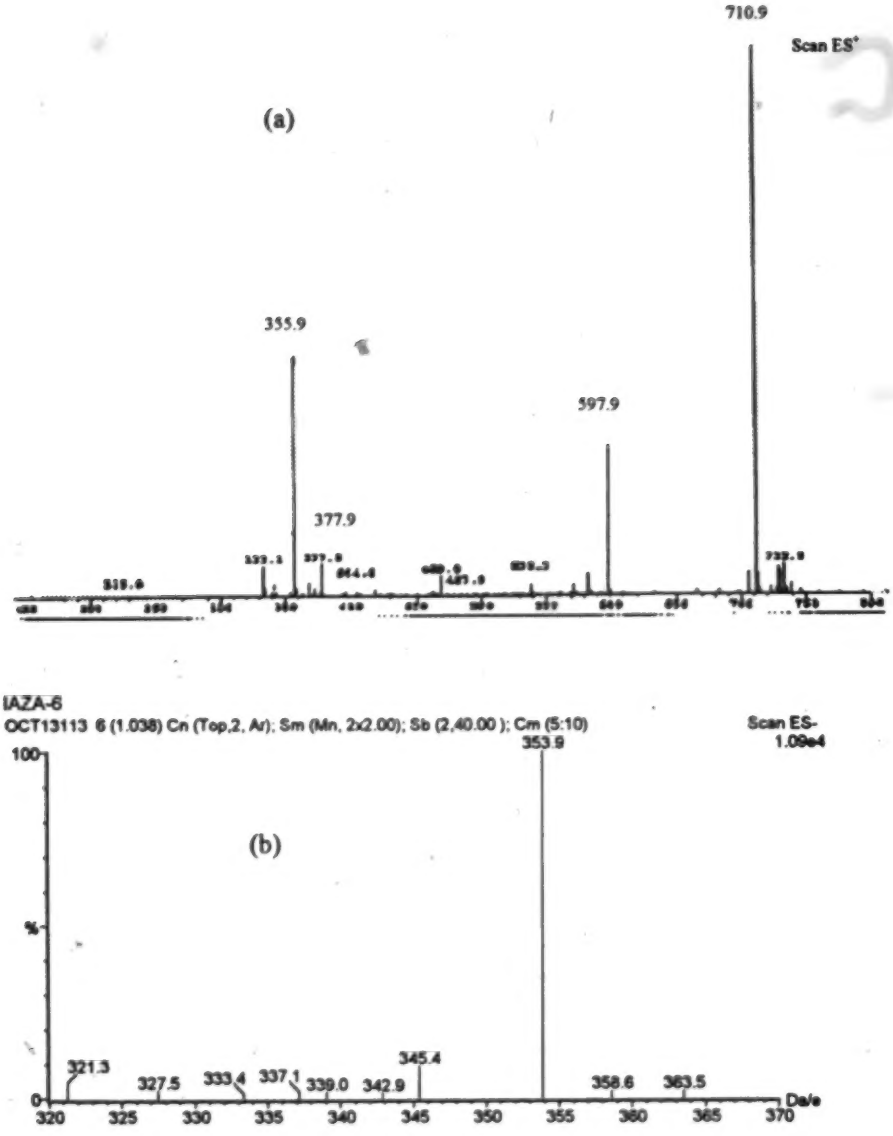

Figure 4.1.3 The spectra of IAZA a) in positive ionization mode b) in negative ionization mode

4.2. ES-MS Detection Limits of Four Nitro-Functionalized Drugs

After initial experience with ES-MS was gained from the detection of nitro-functionalized compounds, this project focused on four drugs, flutamide, hydroxyflutamide, nifedipine, and iodoazomycin arabinoside (IAZA), which were of interest to our laboratory. The limit of detection of these four drugs by ES-MS in the negative mode is shown in Table 4.2.1. Figure 4.2.1 shows the spectra of serially diluted IAZA (1.95, 3.9, 7.8, 15.6, 31.2 μg/mL) and two spectra of these spectra are shown in Fig. 4.2.1.

Table 4.2.1 Limit of detection (LOD) in ES-MS negative ionization mode

IAZA (M.W. 354.9)	Hydroxyflutamide (M.W. 292.21)	Flutamide (M.W. 276.22)	Nifedipine (M.W. 346.34)
1.95 μg/mL	0.095 μg/mL	2.5 μg/mL	1.5 μg/mL

The conventional analytical method applied to the analysis of flutamide, hydroxyflutamide and nifedipine is high performance liquid chromatography with UV detection (Grundy, 1996; Zuo, 1998), and the limits of detection for these three compounds were found to be around 5 ng/mL. The diagnostic agent, radioiodinated IAZA (I^*- IAZA) is normally administered in a small dose (0.1-10 mg/patient), and the amount present in blood is not easily analyzed by the standard HPLC method. Thus, a very specific assay based on an extraction protocol followed by HPLC analysis with a

gamma counter as a detector was developed. The addition of non-radiolabelled IAZA to the blood containing radiolabelled IAZA was applied as an internal standard. The assay allowed both identification of the HPLC peak of IAZA by UV detection, and highly sensitive quantification by gamma counting of the UV peak. The limit of detection of radiolabelled IAZA was found to be 7.46 pg/mL (Stypinski *et al.* 1998). Although the limit of detection using this specific procedure was much lower than that using ES-MS, the technique of ES-MS would potentially allow for both chemical characterization and quantification of the analytes.

The first experiment was to determine whether IAZA was detectable in plasma by ES-MS. IAZA was dissolved in saline solution and then mixed with rat plasma *in vitro*. Samples of IAZA at several concentrations were incubated with rat plasma, then extracted and analyzed by ES-MS using 1:1 acetonitrile-water as the mobile phase. All the samples were detected by ES-MS in the positive ionization mode. The limit of detection of clean samples where IAZA was dissolved in mobile phase was found to be 0.1 μg/mL when samples were analyzed in the Department of Chemistry. IAZA in plasma could be detected at a level of around 1μg/mL. Consequently, ES-MS can potentially be applied to analysis of IAZA *in vivo*.

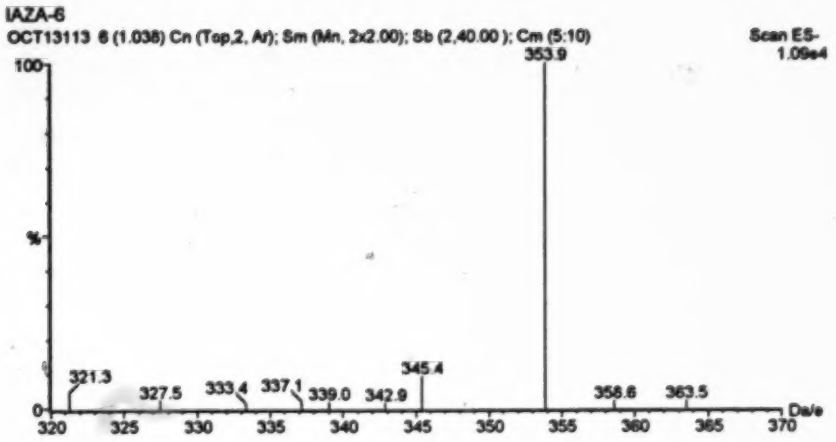

(a)

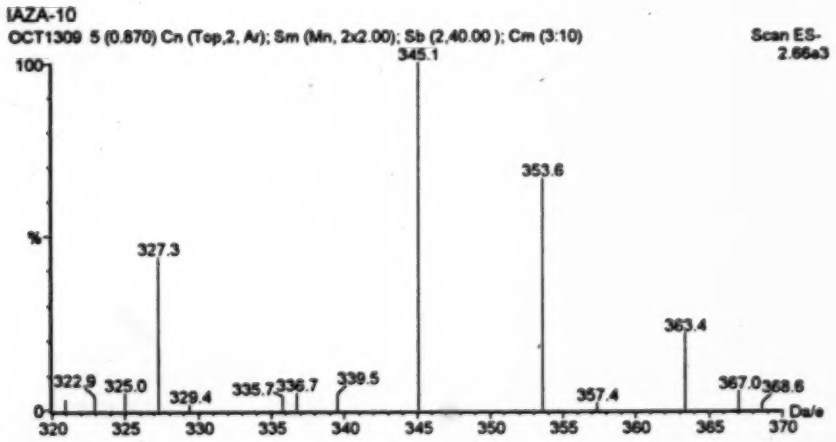

(b)

Fig. 4.2.1 The spectra of serial dilution of IAZA in the negative ionization mode a) 31.2 µg/mL (*m/z*: 353.9) b) 1.95 µg/mL (*m/z*: 353.6)

4.3. Characterization of β-CyD Complexes using ES-MS

Inclusion complexes, between β-CyD (mw 1135) and the fluorescent derivative NBD-β-CyD (mw 1297.10) as hosts, and adamantanamine hydrochloride as the guest (MW 187.71) were prepared in a 1:1 molar ratio. Both complexes were detected by ES-MS in the positive ionization mode. Ammonium acetate buffer was used to ensure that such complexes are protonated due to the lack of a readily ionizable group in the CyDs (Sun *et al.* 1998). In the current work, pure water was selected as the mobile phase because of the effect of additional agents (e.g. methanol, acetonitrile, etc) on complex stability. The complex between β-CyD and amantidine was characterized by a peak at the correct MW (calculated *m/z* 1287.25, found *m/z* 1288.2) (Fig. 4.3.1). The peak at m/z 152.6 was due to guest ions [adamantane+NH_3^+] (Scheme 4.3 a). The complex between NBD-β-CyD and amantidine was also characterized by a peak at the correct MW (calcd *m/z* 1449.36, found *m/z* 1450.2) (Fig. 4.3.1).

As the process of complex formation is an equilibrium, three major factors can influence the equilibrium when the complexes are detected by ES-MS: dilution (Szejtli, 1994), competing agent and high cone voltage (Bakhtiar *et al.* 1997).

In aqueous solution, the slightly apolar cavity of CyD is occupied by water molecules which are energetically unfavored (polar-apolar interaction) and therefore, can be readily replaced by appropriate "guest molecules", which are less polar than water (Szejtli, 1994). After the complexes are dissolved in water, an equilibrium is established between the dissociated and associated species, as expressed by the binding constant K_a (Equation 4.3).

$$CyD + D \rightleftharpoons CyD.D$$

$$K_{1:1} = \frac{[CyD]}{[CyD][D]}$$

Equation 4.3. Equilibrium of Complex

Dilution affects the equilibrium of complex formation/dissociation. The ratio of complex to free drug becomes lower at low concentration (Figure 4.3.2) because CyD and free drug (amantidine) have difficulty "meeting" together in an aqueous solution when both of them are present in a low concentration.

Each drug has a specific binding constant ($K_{1:1}$) with CyD, thus, various compounds will compete with each other when they are present in the same solution containing CyD. In the experiments performed to characterize the two complexes, the solvent used was pure water because an organic solvent would have caused the dissociation of the complexes before the samples were introduced into ES-MS analyzer. This factor of competing agent can influence the equilibrium of the complex in solution.

In order to detect a non-covalent complex such as a CyD/guest complex, the amount of internal energy transferred to the complex during ionization must be low enough to prevent dissociation. When increasing the cone voltage of ES-MS, more internal energy will be transferred to the molecular complex, causing more fragmentation and dissociation of the non-covalent complex (Bruins, 1997; Bakhtiar *et al.* 1997). In the ES-MS experiments, an attempt was made to detect the complex at a higher cone voltage, but the results could not confirm the effect of this third factor that high cone voltage causes

the dissociation of the non-covalent complex (Bakhtiar *et al.* 1997). However, at higher cone voltage, more information about structure could be obtained (Figure 4.3.3). The cone voltage normally used was 35V. When the cone voltage was increased to 70V, more fragments were produced than at 35V. A fragment peak was found at *m/z* 135.8 which possibly results from the loss of NH_3.

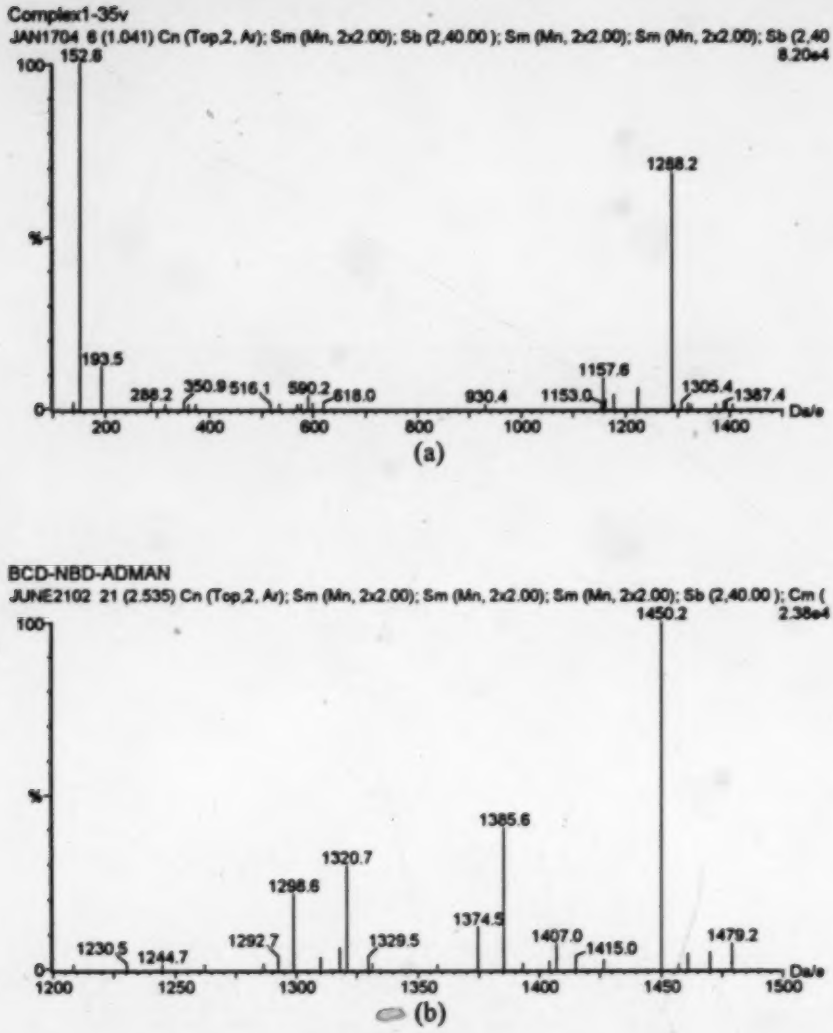

Fig. 4.3.1 The spectra of two complexes a) complex between β-CyD and amantidine (5 mg/mL) b) NBD-β-CyD with amantidine (1 mg/mL)

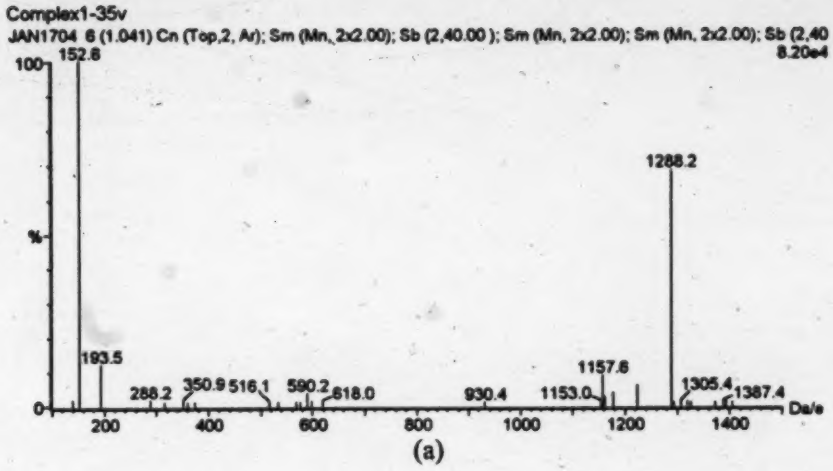

(a)

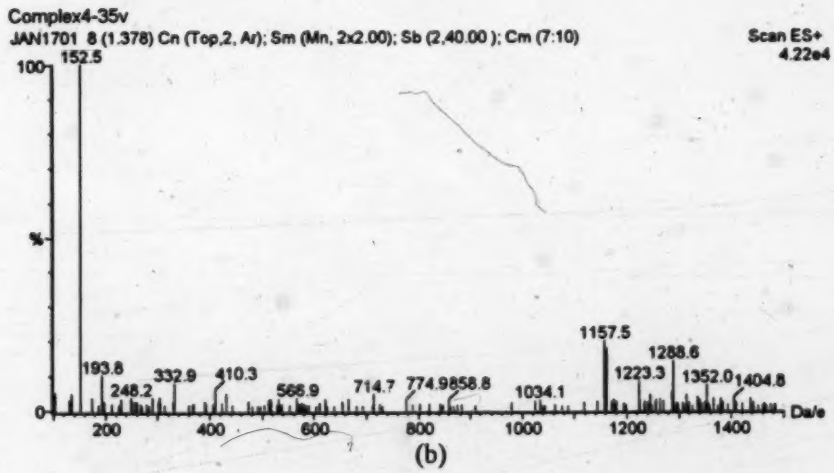

(b)

Fig. 4.3.2 The effect of dilution on the formation of CyD/amantidine Complex a) 5 mg/mL b) 0.625 mg/mL

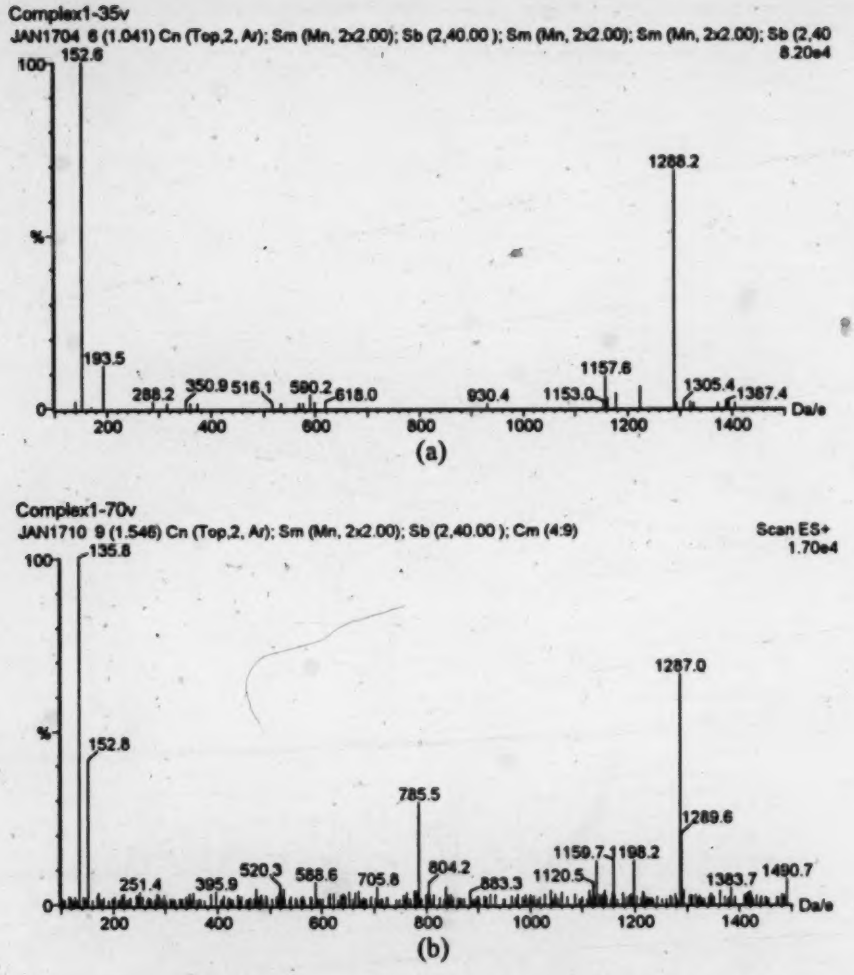

Fig. 4.3.3 The effect of high cone voltage on the formation of CyD/amantidine complex a) cone voltage 35 V b) cone voltage 70 V

5. Conclusions

Some compounds in this study were detected by ES-MS in either the positive or negative ionization mode, and others could be detected only by negative ionization. Very good signals in ES-MS were observed in most cases. The sensitivity of these compounds is generally higher in the negative ionization mode than in the positive ionization mode on the Fisons ES-MS used. The common feature of these compounds is that they all possess the nitro group. The complexation of β-CD with a charged molecule (amantidine) can give a good signal in ES-MS$^+$. Three factors can change the equilibrium of the process of forming a non-covalent host-guest complex: dilution, competing agent and high cone voltage in ES-MS. These preliminary experiments did not provide enough evidence to confirm the third factor (high cone voltage in ES-MS causes the dissociation of the non-covalent complexes). The results of the preliminary experiments however, do indicate that ES-MS can be used to analyze CyD/guest complexes.

In order to apply ES-MS to study non-covalent complexes, the experimental conditions must be optimized to prevent the dissociation of drug complexes during the process of analysis. In future, this technique can potentially be applied to study more drug complex models *in vivo*.

Chapter 4

GENERAL DISCCUSSION AND CONCLUSIONS

It is recognized that prior to the application of CyDs as drug carriers in *vivo*, the pharmacokinetics, metabolism and toxicity of CyDs should be thoroughly understood. The first project focused on the permeation pathways of CyD and its amantidine complex across cell membranes using CLSM. The requirements for using the CLSM are to synthesize the fluorescent derivatives of CyD and amantidine. Only the fluorescent derivative (NBD-β-CyD) of β-CyD, which was labeled with NBD, was successfully synthesized in the current work. The results show that NBD-β-CyD is suitable for intracellular uptake studies using CLSM. The conclusion of the intracellular uptake study using CLSM is that the endocytoic uptake of NBD-β-CyD does exist. The intracellular uptake shows a clear temperature-dependence. There are no significant effects of proteins such as albumin, lipoproteins, etc on the intracellular uptake. Under the experimental conditions employed, no significant difference of intracellular uptake between NBD-β-CyD and its amantidine complex was observed.

In order to apply ES-MS for the study of non-covalent complexes of CyD, a group of compounds was selected for analysis by ES-MS along with CyD host-guest complexes. These nitro-functionalized compounds were readily detected in either positive ionization mode or negative ionization mode by ES-MS and may be suitable guests for detection of the corresponding complexes. Four of these compounds of interest in our laboratory were studied in greater detail by ES-MS and compared to their conventional methods such as HPLC, radiometry, etc. ES-MS can be used to chemically characterize and quantify of

these compounds and therefore, ES-MS can potentially be applied for the analysis of these compounds *in vivo*. Also, some preliminary experiments show that ES-MS is suitable for detecting CyD/complexes with amantidine, and this technique can potentially be employed as a general technique to analysis the complex in biological matrices.

REFERENCES

Abian, J. The coupling of gas and liquid chromatography with mass spectrometry. *J. Mass Spectrom.* 34, 157-168, 1999.

Alberts, B., Bray, D., Lewis, J., Raff, M., Roberts, K. and Watson, J. D. Molecular biology of the cell. Garland Publishing Press: New York & London, 2nd Ed. 1989.

Anderson, G. H., Robbins, F. M., Domingues, F. J., Moores, R. G. and Long, C. L. The utilization of scharfinger dextrins by the rat. *Toxicol. Appl. Pharmacol.* 5, 257, 1963.

Ashton, D. S., Beddell, C. R., Green, B. N. and Oliver, R. W. Rapid validation of molecular structures of biological samples by electrospray-mass spectrometry. *FEBS Lett.* 342, 1-6, 1994.

Atger, V. M., Moya, M. de la l., Stoudt, G. W., Rodrigueza, W. V., Phillips, M. C. and Rothblat, G. H. Cyclodextrins as catalysts for the removal of cholesterol from macrophage foam cells. *J. Clin. Invest.* 99, 773-780, 1997.

Bakhtiar, R., Hop, C. E. C. A. and Walker, R. B. Effect of cyclodextrins on the hydrolysis of an oxazolidine prodrug of (1*R*, 2*S*)-(-)-ephedrine-*cis*-2-(4-methoxyphenyl)-3,4-dimethyl-5-phenyloxazolidine. *Rapid Commun. Mass Spectrom.* 11, 598-602, 1997.

Banks, F. J. and Shen, S. J. Whitehouse, C. M. and Fenn, J. B. Ultrasonically assisted electrospray ionization for LC/MS determination of nucleosides from a transfer RNA Digest. *Anal. Chem.* 66, 406-414, 1994.

Bender, H. Cyclodextrin-Glucanotransferase von *Klebsiella pneumoniae*: 2. Bedeutung des enzymes fur den metabolismus der cyclodextrin bei *Klebsiella pneumoniae* M5a1. *Arch. Microbiol.* 113, 49-66, 1977.

Birkett, D. J., Price, N. C., Radda, G. K. and Salmon, A. G. The reactivity of SH groups with fluorogenic reagent. *FEBS Lett.* 6, 346-348, 1970.

Bordini, E. and Hamdan, M. Investigation of some covalent and noncovalent complexes by Matrix-assisted Laser Desorption/Ionization Time-of-Flight and Electrospray Mass Spectrometry. *Rapid Commun. Mass Spectrom.* 13, 1143-1151, 1999.

Bruins, A. P. ESI source design and dynamic range considerations. *Electrospray ionization mass spectrometry: fundamentals, instrumentation, and applications*. Ed: Cole, R. B. John Wiley & Sons Press: New York, 107-136, 1997.

Burlingame, A. L. Characterization of protein glycosylation by mass spectrometry. *Current Opinion in Biotechnology*, 7, 4-10, 1996.

Caron, I., Elfakir, C. and Dreux, M. Advantages of evaporative light scattering detection for the purity control of commercial cyclodextrins. *J. Liq. Chrom. & Rel. Technol.* 20, 1015-1035, 1997.

Chaudry, I. H. Cellular mechanisms in shock and ischemia and their correction. *Am. J. Physiol.* 245, R117-34, 1983.

Chio, Y. H. and Toyoda, Y. Cyclodextrin removes cholesterol from mouse sperm and induces capacitation in a protein-free medium. *Biol. Reprod.* 59, 1328-1333, 1998.

Clench, M. R. A comparison of thermospray, plasmaspray, electrospray and dynamic FAB. *VG Monographs in Mass Spectrometry*, 3, VG Instruments, 1992.

Cloherty, E. K., Sultzman, L. A., Zottola, R. J. and Carruthers, A. Net sugar transport is a multistep process. Evidence for cytosolic sugar binding sites in erythrocytes. *Biochem.* 34, 15395-15406, 1995.

Cole, R. B. Preface. *Electrospray ionization mass spectrometry: fundamentals, instrumentation, and applications*. Ed: Cole, R. B. John Wiley & Sons Press: New York, 1997.

Cramer, F. Cyclodextrin- a paradigmatic model. *Int. Symp. On Cyclodextrins*, Budapest, 3-14, 1981.

Crain, P. F. Electrospray ionization mass spectrometry of nucleic acids and their constituents. *Electrospray ionization mass spectrometry: fundamentals, instrumentation, and applications*. Ed: Cole, R. B. John Wiley & Sons Press: New York, 421-457, 1997.

Diakur J., Zuo Z. and Wiebe L. I. Synthesis and drug complexation studies with β-cyclodextrins fluorinated on the primary face. *J. Carbohydr. Chem.* 18, 209-223, 1999.

Eftink, M. R., Andy, M. L., Bystrom, k., Perlmutter, H. D. and Kristol, D. S. Cyclodextrin inclusion complexes: Studies of the variation in the size of acyclic guests. *J. Am. Chem. Soc.* 111, 6765-6772, 1989.

Elsing, C., Winn-Borner, U. and Stremmel, W. Confocal analysis of hepatocellular long-chain fatty acid. *Am. J. Physiol.* 269, G842-851, 1995.

Feederle, R., Pajatsch, M., Kremmer, E. and Bock, A. Metabolism of cyclodextrins *by Klebsiella oxytoca* M5a1: purification and characterization of a cytoplasmically located cyclodextrinase. *Arch. Microbiol.*165, 206-212, 1996.

Fiedler, G., Pajatsch, M. and Bock, A. Genetics of novel starch utilisation pathway present in *Klebsiella oxytoca*. *J. Mol. Biol.* 256, 279-291, 1996.

Flaschel, E., Landert, J. P. and Renken, A. Process development for the production of α-cyclodextrin. *I. Int. Symp. On Cyclodextrins*, Budapest, 41-49, 1981.

Flourie, B., Molis, C., Achour, L, Dupas, H., Hatat, C. and Rambaud, J. C. Fate of β-Cyclodextrin in the human intestine. *J. Nutr.* 123, 676-680, 1993.

Frijlink H. W., Visser, J., Hefting, N. R., Oosting, R., Meijer, D. K. and Lerk, C. F. The pharmacokinetics of beta-cyclodextrin and hydroxypropyl-beta-cyclodextrin in the rat. *Pharm. Res.* 7, 1248-1252, 1990.

Gergely V., Sebestyen, G. and Virag, S. Toxicity studies of beta-cyclodextrin. *I. Int. Symp. On Cyclodextrins*, Budapest, 109-113,1981.

Gerloczy, A., Fonagy, A., Keresztes, P., Perlaky, L., Szejtli, J. and Arzneim, F. Absorption, distribution, excretion and metabolism of orally administered ^{14}C-β-cyclodextrin in rat. *Drug. Res.* 35, 1042-1047, 1985.

Ghosh, P. B. and Whitehouse, M. W. 7-chloro-4-nitrobenzo-2-oxa-1,3-diazole: a new fluorogenic reagent for amino acids and other amines. *Biochem. J.* 108, 155-156, 1968.

Gorski, J., Elsing, C., Bucki, R., Zendzian-Piotrowska, M. and Stremmel, W. The plasma borne free fatty acids rapidly enter the hepatocellular nuclei. *Life Sci.* 59, 2209-2215, 1996.

Grossse, P. Y., Bressolle, F., Vago, P. and Pinguet, F. Tumor cell membrane as a potential target for methyl-β-cyclodextrin. *Anticancer Res.* 18, 379-384, 1998.

Grosse, P. Y., Pinguet, F., Joulia, J. M., Astre, C. and Bressolle, F. High-performance liquid chromatographic assay for methyl-β-cyclodextrin in plasma and cell lysate. *J. Chromatogr. B*, 694, 219-226, 1997.

Grouselle, M., Tueux, O., Dabadie, P., Georgescaud, D. and Mazat, J. P. Effect of local anaesthetics on mitochondrial membrane potential in living cells. *Biochem. J.* 271, 269-272, 1990.

Grundy, J. S. Thesis: Factors affecting nifedipine bioavailability. Edmonton, Alberta, Canada: Ph.D. Thesis, University of Alberta, 1996.

Guldberg, P., Straten, P. T., Brick, A., Ahrenkiel, V., Kirkin, A. F. and Zeuthen, J. Disruption of the *MMAC1/PTEN* gene by deletion or mutation is a frequent event in malignant melanoma. *Cancer Res.* 57, 3660-3663, 1997.

Hamasaki, K. Ikeda, H., Nakamura, A., Ueno, A., Toda, F., Suzuki, I. and Osa, T. Fluorescent sensors of molecular recognition. Modified cyclodextrins capable of exhibiting guest-responsive twisted intramolecular charge transfer fluorescence *J. Am. Chem. Soc.* 115, 5035-5040, 1993.

Henderson, T. R., Royer, R. E. and Clark, C. R. MS/MS analysis of diesel emissions and Fuels treated with NO_2^+. *J. Appl. Toxicol.* 2, 231-237, 1982.

Henion, J., Wachs, T. and Mordehai, A. Recent developments in electrospray mass spectrometry including implementation on an ion trap. *J. Pharm. Biomed. Anal.* 11, 1049-1061, 1993.

Hirayama, F., Yamamoto, M. and Uekama, K. Acid-catalyzed hydrolysis of maltosyl-beta-cyclodextrin. *J. Pharm. Sci.* 81, 913-916, 1992.

Huagland, R. P., Spence, M. T. Z. and Johnson, L. D. Handbook of fluorescent probes and research chemicals. Molecular Probes Press: Eugene, Or. 6th Ed. 1996.

Ikeda, H., Nakamura, M., Ise, N., Oguma, N., Nakamura, A., Ikeda, T., Toda, F. and Ueno, A. Fluorescent cyclodextrins for molecule sensing: Fluorescent properties, NMR characterization, and inclusion phenomena of *N*-dansylleucine-modified cyclodextrins. *J. Am. Chem. Soc.* 118, 10980-10988, 1996.

Imai, K. and Watanabe, Y. Fluorimetric determination of secondary amino acids by 7-fluoro-4-nitrobenzo-2-oxa-1,3-diazole. *Anal. Chim. Acta.* 130, 377-383, 1981.

Irie, T., Fukunaga, K. and Pitha, J. Hydroxypropylcyclodextrins in parenteral use. I: Lipid dissolution and effects on lipid transfers in vitro. *J. Pharm. Sci.* 81, 521-523,1992.

Irie, T., Fukunaga, K., Garwood, M. K., Carpenter, T. O. and Pitha, J. Hydroxypropylcyclodextrins in parenteral use. II: Effects on transport and disposition of lipids in rabbit and humans. *J. Pharm. Sci.* 81, 524-528, 1992.

Irie, T., Otagiri, M., Sunada, M., Uekama, K., Ohtani, Y., Yamada, Y. and Sugiyama, Y. Cyclodextrins-induced hemolysis and shape change of human erythrocytes *in vitro*. *J. Pharmacobio-Dynamics*, 5, 741-744, 1982.

Irie, T. and Uekama, K. Pharmaceutical application of cyclodextrin. III. Toxicological issues and safety evaluation. *J. Pharm. Sci.* 86, 147-162, 1997.

Jaehde, U., Masereeuw, R., De Boer, A. G., Fricker, G., Nagelkerke, J. F., Vonderscher, J. and Breimer, D. D. Quantification and visualization of the transport of octreotide, a somatostatin analogue, across monolayers of cerebrovascular endothelial cells. *Pharm. Res.* 11, 442-448, 1994.

Jaffe, D. B. Confocal laser scanning microscopy. http://glu.ls.utsa.edu/CLSM, 1999.

Johnson, L. V., Walsh, M. L. and Chen, L. B. Localization of mitochondria in living cells with rhodamine 123. *Proc. Natl. Acad. Sci.* 77, 990-994, 1980.

Jones, S. P., Grant, D. J. W., Hadgraft, J. and Parr, G. D. *Acta Pharm. Technol.* 1984, 30, 213-223. Cited in Szejtli, J. Medicinal applications of cyclodextrins. *Med. Res. Rev.* 14, 353-386, 1984.

Kebarle, P. and Ho, Y. On the mechanism of elctrospray mass spectrometry, *Electrospray ionization mass spectrometry: fundamentals, instrumentation, and applications*. Ed: Cole, R, B. John Wiley & Sons Press: New York, 3-63, 1997.

Kilsdonk, E. P. C., Yancey, P. G., Stoudt, G. W., Bangerter, F. W., Johnson, W. J., Phillips, M. C. and Rothblat, G. H. Cellular cholesterol efflux mediated by cyclodextrins. *J. Biol. Chem.* 270, 17250-17256, 1995.

Kinsland, L. N. and Wiechelman, K. J. Use of β-cyclodextrin fluorophore complexes to improve the efficiency of fluorescent label incorporation into proteins. *J. Biochem. Biophys. Methods*. 9, 81-83, 1984.

Knowles, B. B., Howe, C. C. and Aden, D. P. Human hepatocellular carcinoma cell lines secrete the major plasma proteins and hepatitis B surface antigen. *Science*, 209, 497-499, 1980.

Koizumi, K., Kubota, Y., Okada, Y. and Utamura, T. Microanalysis of β-cyclodextrin in plasma by high-performance liquid chromatography. *J. Chromatogr.* 341, 31-41, 1985.

Kubota, Y., Fukuda, M., Ohtsuji, K. and Koizumi, K. Microanalysis of β-cyclodextrin and glucosyl-β-cyclodextrin in human plasma by high-performance liquid chromatography with pulsed amperometric detection. *Anal. Biochem.* 201, 99-102, 1992.

Kubota, Y., Fukuda, M., Muroguchi, M. and Koizumi, K. Absorption, Distribution and Excretion of β-cyclodextrin and glucosyl-β-cyclodextrin in rats. *Biol. Pharm. Bull.* 19, 1068-1072, 1996.

Kuwabara, T., Nakamura, A., Ueno, A. and Toda, F. Inclusion complexes and guest-induced color changes of pH-indicator-modified β-cyclodextins. *J. Phys. Chem.* 98, 6297-6303, 1994.

Ladic, L. 3-D confocal microscopy. http://www.cs.ubc.ca/spider/ladic/overview.html, 1999.

Lancet, D. and Pecht, I. Spectroscopic and immunochemical studies with nitrobenzoxadiazolealanine, a fluorescent dinitrophenyl analogue. *Biochem.* 16, 5150-5157, 1977.

Larsen, T., Solberg, S., Johansen, R. and Jorgensen, L. Effect of cooling on the intracellular concentrations of Na^+, K^+ and Cl^- in cultured human endothelial cells. *Scand. J. Clin. Lab. Invest.* 48, 565-571, 1988.

Loftsson, T. and Brewster, M. E. Pharmaceutical application of cyclodextrins. 1. Drug solubilization and stabilization. *Pharm. Sci.* 85, 1017-1169, 1996.

Loo, J. A., and Loo, R. O. Electrospray Ionization mass spectrometry of peptides and proteins, *Electrospray ionization mass spectrometry: fundamentals, instrumentation, and applications*. Ed: Cole, R. B. John Wiley & Sons Press: New York, 385-419, 1997.

Makela, M., Korpela, T. and Laakso, S. Colorimetric determination of β-cyclodextrin: two assay modifications base on molecular complexation of phenolphthalein. *J. Biochem. Biophys. Methods*. 14, 85-92,1987.

Mannan, R. H., Somayaji, V. V., Lee, H., Mercer, J. R., Chapman, J. D. and Wiebe, L. I. Radioiodinated 1-(5-iodo-5-deoxy-beta-D-arabinofuranosyl)-2-nitroimidazole (iodoazomycin arabinoside: IAZA): a novel marker of tissue hypoxia. *J. Nucl. Med.* 32, 1764-1770, 1991.

Marques, H. M. C., Hadgraft, J. Kellaway, I. W. and Taylor, G. Studies of cyclodextrin inclusion complexes. III. The pulmonary absorption of Beta-, Dm-beta- and HP-beta-cyclodextrin in rabbits. *Int. J. Pharm.* 77, 297-302, 1991.

Masson, M., Loftsson, T., Masson, G. and Stefansson, E. Cyclodextrins as permeation enhancers: some theoretical evaluations and in vitro testing. *J. Control. Release.* 59, 107-118, 1999.

Matsubara, K., Abe, K., Irie, T. and Uekama, K. Improvement of nasal bioavailability of luteinizing hormone-releasing hormone agonist, buserelin, by cyclodextrin derivatives in rats. *J. Pharm. Sci.* 84, 1295-1300, 1995.

Marttin, E., Verhoef, C. J., Cullander, C., Romeijn, S. G., Nagelkerke, J. F. and Merkus, F. W. H. M. Confocal Laser Scanning Microscopic visualization of the transport of dextrans after nasal administration to rats: Effects of absorption enhancers. *Pharm. Res.* 4, 631-637, 1997.

Marttin, E., Verhoef, J. C., Spies, F., Van der Meulan, J., Nagelkerke, J. F., Koerten, H. K. and Merkus, F. W. H. M. The effect of methylated beta-cyclodextrins on the tight junctions of the rat nasal respiratory epithelium: electron microscopic and confocal laser scanning microscopic visualization studies. *J. Control. Release*. 57, 205-213, 1999.

Meyer, H. E., Eisermann, B., Heber, M., Hoffmann-Posorske, E., Korte, H., Weigt, C., Wegner, A., Hutton, T., Donella-Deana, A., and Perich, J. W. Strategies for nonradioactive methods in the localization of phosphorylated amino acids in proteins. *FASEB. J.* 7, 776-782, 1993.

Miller, G. G., Brown K., Moore, R. B., Diwu, Z. J., Liu, J., Huang, L., Lown, W. J., Begg, D. A., Chlumecky, V., Tulip, J. and McPhee, M. S. Uptake kinetics and intracellular localization of hypocrellin photosensitizers for photodynamic therapy: a confocal microscopy study. *Photochem. Photobiol.* 61, 632-638, 1995.

Miller, G. G., Brown, K., Ballangrud, A. M., Barajas, O., Xiao, Z., Tulip, J., Lown, W. J., Leithoff, J. M., Allalunis-turner, J. M., Mehta, R. D. and Moor, R. B. Preclinical assessment of hypocrellin B and hypocrellin B derivatives as sensitizers for photodynamic therapy of cancer: Progress update. *Photochem. Photobiol.* 65, 714-722, 1997.

Minier, L. and Behrens, R. Mass spectra of 2,4-dinitroimidazole and its isotopomers using simultaneous thermogravimetric modulated beam mass spectrometry. *J. Mass Spectrom.* 31, 25-30, 1996.

Miyazawa, I., Ueda, H., Nagase, H., Endo, T., Kobayashi, S. and Nagai, T. Physicochemical properties and inclusion complex formation of delta-cyclodextrin. *Eur. J. Pharm. Sci.* 3, 153-162, 1995.

Nakamura, M., Ikeda, A., Ise, N., Ikeda, T., Ikeda, H., Toda, F. and Ueno, A. Densyl-modified β-cyclodextrin with a monensin residues as a hydrophobic, metal responsive cap. *J. Chem. Soc., Chem. Commun.* 721-722, 1995.

Nakamaru, M., Ikeda, T., Nakamura, A., Ikeda, H., Ueno, A. and Toda, F. Remarkable molecular recognition of dansyl-modified cyclodextrin dimer. *Chem. Lett.* 343-344, 1995.

Nashijo, J. and Nagai, M. Inclusion complex of 8-anilinonaphtalens-1-sulfonate with β-cyclodextrin. *J. Pharm. Sci.* 80, 153-156, 1991.

Neufeld, E. B., Cooney, A. M., Pitha J., Dawidowicz, E. A., Dwyer, N. K., Pentchev, P. G. and Blanchette-Mackie, E. J. Intracellular trafficking of cholesterol monitored with a cyclodextrin. *J. Biol. Chem.* 271, 21604-21613, 1996.

Ohashi, Y. Electrospray ionization mass spectrometry of carbohydrates and lipids, *Electrospray ionization mass spectrometry: fundamentals, instrumentation, and applications*. Ed: Cole, R. B. John Wiley & Sons Press: New York, 459-498, 1997.

Ohtani, Y., Irie, T., Uekama, K., Fukunaga, K. and Pitha, J. Differential effects of alpha-, beta-, and gama-cyclodextrins on human erythrocytes. *Eur. J. Biochem.* 186, 17 –22, 1989.

Orstan, A. and Ross, J. B. A. Investigation of the β-cyclodextrin-indole inclusion complex by absorption and fluorescence spectroscopies. *J. Phys. Chem.* 91, 2735-2745, 1987.

Ostlund, R. E., Seemayer, R. Jr., Gupta, S., Kimmel, R., Ostlund, E. L. and Sherman, W. R. A stereospecific *myo*-Inositol/*D-chiro*-Inositol transporter in HepG2 liver cells. *J. Biol. Chem.* 271, 10073-10078, 1996.

Pajatsch, M., Gerhart, M., Peist, R., Horlacher, R., Boos, W. and Bock, A. The periplasmic cyclodextrin binding protein CymE from *Klebsiella oxytoca* and its role in maltodextrin and cyclodextrin transport. *J. Bacteriol.* 180, 2630-2635, 1998.

Petter, R. C., Salek, J. S., Sikorski, C. T., Kumaravel, G. and Lin, F. T. Cooperative binding by aggregated mono-6-(alkylamino)-β-cyclodextrins. *J. Am. Chem. Soc.* 112, 3860-3868, 1990.

Poon, G. K. Drug Metabolism and Pharmacokinetics, *Electrospray ionization mass spectrometry: fundamentals, instrumentation, and applications*. Ed: Cole, R. B. John Wiley & Sons Press: New York, 499-525, 1997.

Rajewski, A. R. and Stella, V. J. Pharmaceutical applications of cyclodextrins. 2. *In Vivo* drug delivery. *J. Pharm. Sci.* 85, 1142-1169, 1996.

Rasmusson, B. J., Flanagan, T. D., Turco, S. J., Epand, R. M. and Petersen, N. O. Fusion of Sendai virus and individual host cells and inhibition of fusion by lipophosphoglycan measured with image correlation spectroscopy. *Biochim. Biophys. Acta.* 1404, 338-352, 1998.

Rauchman, M. I., Wasserman, J. C., Cohen, D. M., Perkins, D. L., Hebert, S. C., Milford, E. and Gullans, S. R. Expression of GLUT-2 cDNA in human B lymphocytes: analysis of glucose transport using flow cytometry. *Biochim. Biophys. Acta.* 1111, 231-238, 1992.

Reeuwijk, H. J. E. M., Irth, H. and Tjaden, U. R. Liquid chromatographic determination of β-cyclodextrin derivatives based on fluorescence enhancement after inclusion complexation. *J. Chromatogr.* 614, 95-101, 1993.

Rodal, S. K., Skretting, G., Garred, O., Vilhardt, F., Deurs, B. V. and Sandvig, K. Extraction of cholesterol with methyl-β-cyclodextrin perturbs formation of clathrin-coated endocytic vesicles. *Mol. Biol. Cell.* 10, 961-974, 1999.

Roepstorff, P. Characterization of proteins by mass spectrometry. *Analyst*, 117, 299-303, 1992.

Saenger, W. Cyclodextrin inclusion compounds in research and industry. *Angew. Chem. Int. Ed. Engl.* 19, 344-362, 1980.

Selva, A. and Casetta, B. Study of the salts with organic hydroxy acids of the terfenadine β-cyclodextrins inclusion complex in solution by ionspray mass spectrometry. *J. Mass Spectrom.* 30, 219-220, 1995.

Skoog, D. A., Holler, F. J. and Nieman, T. A. Principles of instrumental analysis. Harcourt Brace & Company Press: Orlando, Fl. 5th Ed. 1998.

Smith, D. L. and Zhang, Z. Probing noncovalent structural features of proteins by mass spectrometry. *Mass Spectrom. Rev.* 13, 411-29, 1994.

Smith, L. C., Pownall, H. J. and Gotto Jr., A. M. The plasma lipoproteins: Structure and metabolism. *Ann. Rev. Biochem.* 47, 751-777, 1978.

Speizer, L., Haugland, R. and Kutchai, H. Asymmetric transport of a fluorescent glucose analogue by human erythrocytes. *Biochim. Biophys. Acta.* 815, 75-84, 1985.

Straighten, C. E. "Cyclodextrin based drug delivery system." In Pharmaceutical Manufacturing International Ed. Barber Ms, Sterling Press: London, 1990.

Stypinski, D., Wiebe L. I. and Mercer J. R. A rapid and simple assay to determine the blood and urine concentrations of 1-(5-[$^{123/125}$I]iodo-5-deoxyarabinofuranosyl)-2-nitroimidazole, a hypoxic cell marker. *J. Pharm. Biomed. Anal.* 16, 1067-1073, 1998.

Sun, W.X., Cui, M., Liu, S. Y., Song, F. R. and Elkin, Y. N. Electrospray ionization mass spectrometry of cyclodextrin complexes with amino acids in incubated solutions and in eluates of Gel Permeation Chromatography. *Rapid Commun. Mass Spectrom.* 12, 2016-2022, 1998.

Szejtli, J., Gerloczy, A. and Fonagy, A. Intestinal absorption of ^{14}C-labelled β-cyclodextrin in rats. *Arzneim. – Forsch/Drug Res.* 30, 808-810, 1980.

Szejtli, J. Cyclodextrins: A new group of industrial basic materials. *Die Nahrung*, 29, 911-924, 1985.

Szejtli, J. *Cyclodextrin Technology*. Ed: Davies, J. E. D. Kluwer Academic Press: Dordrecht, The Netherlands, 1988.

Szejtli, J. Medicinal applications of cyclodextrins. *Med. Res. Rev.* 14, 353-386, 1994.

Tabushi, I., Kiyosuke, Y., Sugiomoto, T. and Yamamura, K. Approach to the aspects of driving force of inclusion by α-cyclodextrin. *J. Am. Chem. Soc.* 100, 916-919, 1978.

Tekeo, K., Mitoh, H. and Uemura, K. Selective chemical modification of cyclomalto-oligosaccharides *via tert*-butyldimethylsilylation, *Carbohydr. Res.* 187, 203-221, 1989.

Tong, W. Q., Lach, J. L., Chin, T. F. and Guillory, J. K. Structural effects on the binding of amine drugs with the diphenylmethyl functionality to cyclodextrins. I. A microcalorimetric study. *Pharm. Res.* 8, 951-957, 1991.

Ueno, A., Suzuki, I. and Osa, T. Association dimers, excimers, and inclusion complexes of pyrene-appended γ-cyclodextrins. *J. Am. Chem. Soc.* 111, 6391-6397, 1989.

Ueno, A., Minato, S., Suzuki, I., Fukushima, M., Ohkubo, M., Osa, T., Hamada, F. and Murai, K. Host-guest sensory system of densyl-modified β-cyclodextrin for detecting steroidal compounds by dansyl fluorescence. *Chem. Lett.* 605-608, 1990.

Ueno, A., Suzuki, I. and Osa, T. Host-guest sensory systems for detecting organic compounds by pyrene excimer fluorescence. *Anal. Chem.* 62, 2461-2466, 1990.

VG Back to Basics manual: Electrospray Ionisation (and APCI). VG ORGANIC, Fisons Instruments.

VG Trio-2000, Users Guide. VG Biotech, Fisons Instruments.

Vincenti, M. Host-Guest chemistry in the Mass Spectrometry. *J. Mass Spectrom.* 30, 925-939, 1995.

Vincenti, M., Minero, C., Pelizzetti, E., Fontana, M. and De Maria, R. Sub-parts-per-billion determination of nitro-substituted polynuclear aromatic hydrocarbons in airborne particulate matter and soil by electron capture-tandem mass spectrometry. *J. Am. Soc. Mass Spectrom.* 7, 1255-1265, 1996.

Walker, R. B., Dholakia, V. N., Brasfield, K. L. and Bakhtiar, R. Effect of hydroxypropyl-β-cyclodextrin on the central stimulant activity of (-)-Ephedrine and an oxazolidine prodrug in rats. *Gen. Pharmac.* 30, 725-731, 1998.

Wang, Y., Ikeda, T. Ueno, A. and Fujio, T. Fluorescein modified β-cyclodextrin as a charge-changeable receptor. *Tetrahedron Lett.* 34, 4971-4974, 1993.

Wenz, G. Cyclodextrins as building blocks for supramolecular structures and functional units. *Angew. Chem. Int. Ed. Engl.* 33, 803-822, 1994.

Williams, T. M., Kind, A. J., Houghton, E. and Hill, W. D. Electrospray collision-induced dissociation of testosterone and testosterone hydroxy analogs. *J. Mass Spectrom.* 34, 206-216, 1999.

Yoshioka, K., Takahashi, H., Homma, T., Saito, M., Oh, K., Nemoto, Y. and Matsuoka, H. A novel fluorescent derivative of glucose applicable to the assessment of glucose uptake activity of *Escherichia coli*. *Biochim. Biophys. Acta*. 1289, 5-9, 1996.

Zuo, Z., Kwon, G. and Wiebe, L. I. Solubilization of flutamide by hydroxypropyl-β-cyclodextrin. *Pharm. Res.* 13, S-259, 1996.

Zuo, Z. Solubilization & PK of flutamide with HPβCD. Edmonton, Alberta, Canada: Ph.D. Thesis, University of Alberta, 1998.